Stress-Induced Regulation of ATF3 Expression in Kidney Tubules *in vitro* and *in vivo*

Dissertation

zur
Erlangung der naturwissenschaftlichen Doktorwürde
(Dr.sc.nat.)

vorgelegt der
Mathematisch-naturwissenschaftlichen Fakultät
der
Universität Zürich

von
Tina Dauwalder
von
Beatenberg BE

Promotionskomitee

Prof. Dr. François Verrey
Prof. Dr. Johannes Loffing
Prof. Dr. Sabine Werner

Zürich, 2011

Contents

1 Summary

The mineralocorticoid hormone aldosterone is a key player in blood pressure control by the kidney where it induces the transcription of a number of genes in its target tubules. The aim of this work was to characterize the role that the potentially aldosterone-induced activating transcription factor 3 (ATF3) plays in the kidney, specifically in the aldosterone sensitive tubule segments, including the connecting tubule (CNT) and the cortical collecting duct (CCD). To study the role of ATF3 in principal cells, the main cell type responding to aldosterone in the CNT/CCD, mouse cortical collecting duct mpkCCD$_{Cl14}$, cells were transduced with two lentiviral constructs, allowing Doxycycline-inducible overexpression of ATF3. Epithelia formed by these cell lines and also by another cell line, mCCD$_{Cl6}$ were analyzed for their transepithelial ion transport characteristics in an Ussing chamber set-up, but did not provide conclusive results regarding a functional role of ATF3 expression. Further investigations showed that the previously observed induction of ATF3 was rather mediated by stress than by aldosterone, both *in vivo* in mouse kidney and *in vitro* in cultured kidney epithelial cell lines. Specifically, we observed *in vitro* in mCCD$_{Cl6}$ cells 1 h after a medium change an upregulation of ATF3 mRNA independent of aldosterone which was also observed at the protein level. Analysis of signalling pathways potentially mediating this upregulation of ATF3 upon medium change led to the identification of a rapid increase in phosphorylation of three different mitogen activated protein kinases (MAPK) JNK/SAPK1, ERK1/2 and p38. Interestingly, this effect appeared to be dependent on a low CO_2 partial pressure of the replacement medium. *in vivo*, we showed that an intra-peritoneal injection of a physiological saline solution in mice induces an upregulation of ATF3 mRNA in the kidney as opposed to other organs like brain, colon and heart. The fact that tubular cells of the aldosterone-sensitive distal nephron were involved in this response and that this response was translated to the protein level was confirmed by the observation that the same treatment induced a strong upregulation of ATF3 at the protein level in CNT/CCD tubule segments selected using a complex object parametric

analyzer and sorter (COPAS). Finally, metabolic characterization of the ATF3 KO mouse revealed no gross phenotype and showed no impairment of kidney function compared to wildtype mice. Specifically, ATF3 KO and wild type mice displayed comparable food and water consumption as well as feces and urine excretion, even when stressed by water deprivation. Taken together, we conclude that ATF3 expression is exquisitely sensitive to stress, in particular in the kidney, as shown both *in vivo* in mouse kidney tubules and *in vitro* in $mCCD_{Cl6}$ cells. It is suggested that *in vitro* this activation is mediated via phosphorylation of JNK/SAPK1, ERK1/2 and p38.

2 Zusammenfassung

Das mineralocorticoid Hormon Aldosteron spielt eine Schlüsselrolle in der über die Niere gesteuerten Blutdruckregulation, wo es in den aldosteron-sensitiven Tubuli eine Anzahl von Genen induziert. Das Ziel der vorliegenden Arbeit war es, die spezifische Rolle des potentiell durch Aldosteron induzierten activating transcription factor 3 (ATF3) in der Niere, genauer im Verbindungstubulus und im kortikalen Sammelrohr zu untersuchen. Da die Hauptzelle derjenige Zelltyp ist, der in diesen zwei Nierentubulussegmenten aldosteron-sensitiv ist, haben wir die kortikale Sammelrohr-Mauszelllinie mpkCCD$_{Cl14}$ mit zwei lentiviralen Konstrukten transduziert, welche die Doxycyclin-induzierbare Überexpression von ATF3 erlauben. Epithelien, die von diesen Zellen und zusätzlich von einer anderen Zelllinie, mCCD$_{Cl6}$ gebildet wurden, wurden in einem Ussingkammer-Messsystem auf ihre transepithelialen Ionentransport-Eigenschaften untersucht. Diese Messungen führten jedoch nicht zu eindeutigen Resultaten bezüglich der Rolle von ATF3. Weiterführende Untersuchungen zeigten, dass die zuvor beobachtete Induktion von ATF3 eher durch Stress als durch Aldosteron ausgelöst wurde. Dies war der Fall sowohl *in vivo* in Mausnieren, als auch *in vitro* in den kultivierten epithelialen Nierenzelllinien. Die Untersuchung von Signaltransduktionswegen, die potentiell zu dieser Aufregulation aufgrund des Mediumwechsels führen könnten, hat eine erhöhte Phosphorylierung der drei mitogen activated protein kinase (MAPK) JNK/SAPK1, ERK1/2 und p38 innerhalb von sieben Minuten gezeigt. Interessanterweise schien dieser Effekt von einem tiefen CO_2-Partialdruck im Ersatzmedium abhängig zu sein. *in vivo* konnten wir zeigen, dass die Injektion einer physiologischen Salzlösung in Mäuse zu einer Erhöhung der ATF3 mRNA in der Niere führt, während dies nicht der Fall ist im Hirn, der Mucosa des Dickdarms oder im Herzen. Eine starke Aufregulierung von ATF3 aufgrund der selben Behandlung konnte auf Ebene der Proteinexpression im Verbindungstubulus und kortikalen Sammelrohr beobachtet werden, welche mit einem complex object parametric sorter and analyzer (COPAS) selektioniert wurden. Die metabolische Charakterisierung der ATF3 KO Maus zeigte keine gestörte Nierenfunktion verglichen mit

Wildtypmäusen. Auch die Futter- und Wasseraufnahme sowie die Stuhl- und Urinproduktion waren vergleichbar. Wir ziehen die Schlussfolgerung, dass ATF3 spezifisch in der Niere *in vivo* ein stress-reguliertes Gen ist und dies auch auch in $mCCD_{Cl6}$ Zellen *in vitro* beobachtet werden kann. Diese Aufregulierung kommt *in vitro* durch die Phosphorylierung der MAPK JNK/SAPK1, ERK1/2 und p38 zustande.

3 Introduction

General introduction

The rationale of my thesis initially came from experiments made before I joined the laboratory. The original aim was to identify genes displaying an early response to aldosterone, and then to determine their effect in aldosterone target cells in the so-called aldosterone sensitive distal nephron (ASDN). A first Microarray study made on RNA prepared from isolated tubules of mice injected with aldosterone 1 hour before yielded a list of early aldosterone regulated genes, two of which were the activating transcription factor 3 (ATF3, 3.5-fold upregulated) and Gremlin2 (Grem2, 7.2-fold upregulated). We sought to determine the role of these two proteins in aldosterone linked processes. After investing a large part of the time of this thesis following this aim, we realized these two candidates were not regulated by the hormone aldosterone itself but rather this effect was a stress-response of the mice. In the initial experiments, the negative controls (untreated animals) were literally untreated, meaning they did not receive any vehicle injection and instead were killed directly[1]. Furthermore, *in vitro* experiments with cultured cells showed that a medium change also induced ATF3 in these cells. An additional experiment injecting vehicle into mice confirmed our hypothesis that ATF3 was upregulated by stress. In consequence the project was reoriented towards the mechanism leading to ATF3 induction. Interestingly, this stress response turned namely out to be quite organ specific; being strong in the kidney, and not significant in other organs tested. This suggests that the response is specific and that there could be a rationale for it to be seen exclusively in the kidney. Because much of the work performed during this thesis was done based on the rationale that ATF3 is

[1] Practically tubules from three treatment conditions had been originally isolated and tested: from mice injected with aldosterone, canrenoate (MR antagonist) or not injected. Because of the observation that the canrenoate treatment per se induced some gene products, it had been decided to focus on the genes that were differentially expressed between aldosterone-injected versus not injected conditions.

regulated by aldosterone, I will now introduce the kidney, aldosterone and also lentiviral inducible expression systems, since we produced clonal kidney cell lines overexpressing ATF3, and that this same approach was then used by others to characterize their protein of interest.) In the later parts of the introduction, I will focus on the basic leucine zipper transcription factors, to which the ATF3 protein belongs and signalling cascades that induce ATF3 under stress conditions.

3.1 Anatomy and function of the kidney

In humans, the kidneys are paired bean-shaped organs of about 10 cm in length, which primarily serve the function of urine production and are of central importance for maintenance of body homeostasis (e.g. electrolyte balance, blood pressure control, acid-base regulation and excretion of metabolic waste products). In adults, each kidney weighs about 115-170 g. Blood enters the kidney via the renal artery and leaves it over the renal vein. The organ consists of two basic layers, namely the cortex (granular outer region) and medulla (darker inner region). A lot of so called glomeruli are found in the cortex, they are the reason for its granularity. Glomeruli are bundles of capillaries that form the primary urine by filtering the blood. The medulla being free from glomeruli is made up in humans by 8-18 conical pyramids constituted by a parallel arrangement of small blood vessels and tubules. The tip of each pyramid is perforated, which allows the urine to enter the renal sinus.

The kidneys receive 20% of the total cardiac output and produce around 170 liters of primary urine (ultrafiltrate) per day. The urine is transported from each kidney to the bladder via the ureters.

The functional unit of the kidney is the nephron. Each human kidney is made up of 800'000 to 1'2000'000 nephrons. The nephrons all function individually up to the point where the collecting ducts merge with the collecting duct of one or even several other nephrons.

A nephron is constituted of a glomerulus and a tubule. The glomerulus is a bundle of blood vessels that forms the ultrafiltrate from the urine. This ultrafiltrate is passed on into the so-called tubule; an epithelial structure showing many ultrastructural subdivisions with specific functions to convert the blood filtrate into urine. Thus, the nephron has a vascular component as well as an epithelial one. They both converge in the so-called Bowman's capsule which surrounds the glomerulus and is contiguous with the lumen of the proximal end of the tubule, where the ultrafiltrate is taken up from the blood. There are two types of nephrons: superficial nephrons that have short loops extending only onto the border between outer and inner medulla and medullary nephrons which are important for the concentration of the urine and have long loops reaching the tip of the medulla [1].

The tubule of the nephron is subdivided into specialized segments which carry out very specific roles in the concentration of the primary urine due to specialized transporters that are characteristic for this segment. The tubule starts with the proximal tubule (see Fig.1). First, the proximal tubule is convoluted (proximal convoluted tubule: PCT, alternatively categorized as S1 and S2), and then straightens along the way to the more distal parts of the tubule (proximal straight tubule: PST, alternatively S3). In the proximal tubule the apical membranes of the epithelial cells that line the tubule show many infoldings, this is called the brush border membrane. Due to its variety of inserted transporters it allows high reabsorption of amino acids, glucose, certain ions (e.g. Na^+ Cl^-, HCO_3^- Ca_2^+) and water but is also responsible for secretion of NH_4^+ and other solutes. Adjacent to the proximal tubule is the loop of Henle (subdivided into thin descending limb, thin and thick ascending limbs). This loop is mainly involved in the dilution or concentration of the urine by building up a hyperosmotic gradient in the medulla by juxtamedullary nephrons. Depending on the body's needs, the gradient can be used to concentrate the urine in the distal medullary collecting ducts if necessary.

The loop of Henle terminates at the so called macula densa, which is part of the

juxtaglomerular apparatus (JGA). The JGA is important for the regulation of filtration rate, blood flow, sodium balance and maintenance of systemic blood pressure. The macula densa is the region where the thick ascending limb touches its glomerulus. It is made up by specialized epithelial cells lining the wall of the tubule, having large nuclei and being closely packed. This is the reason why this region of the tubule appears to be more "dense" when analyzed with a light microscope.

Granular cells are specialized smooth muscle cells lining the walls of the afferent arteriole in the JGA. They produce and store the renal hormone renin. Upon registration of a drop in blood pressure in the JGA, renin is released from the granular cells to regulate blood pressure via the mechanisms of the renin-angiotensin-aldosterone-system RAAS (see 3.1.1) [1].

The fine control of water and salt excretion takes place in the distal tubule and collecting duct system. The distal convoluted tubule (DCT) begins at the macula densa and merges into the connecting tubule (CNT) which ends in the cortical collecting duct (CCD). The CNT and collecting ducts show two distinct cell types, the principal cells and the intercalated cells, which are further subdivided into α- and β- intercalated cells. Principal cells constitute about two thirds of the initial and cortical collecting tubules; they have a characteristic central cilium on the apical membrane and are responsible for Na^+ and Cl^- absorption as well as K^+ secretion. α -intercalated cells secrete H^+ while β- intercalated cells secrete HCO_3^-. The collecting duct branches of several nephrons join to form the cortical collecting tubule (CCT) further divided into the outer medullary collecting duct OMCD and inner medullary collecting duct IMCD (see Fig. 1) [1].

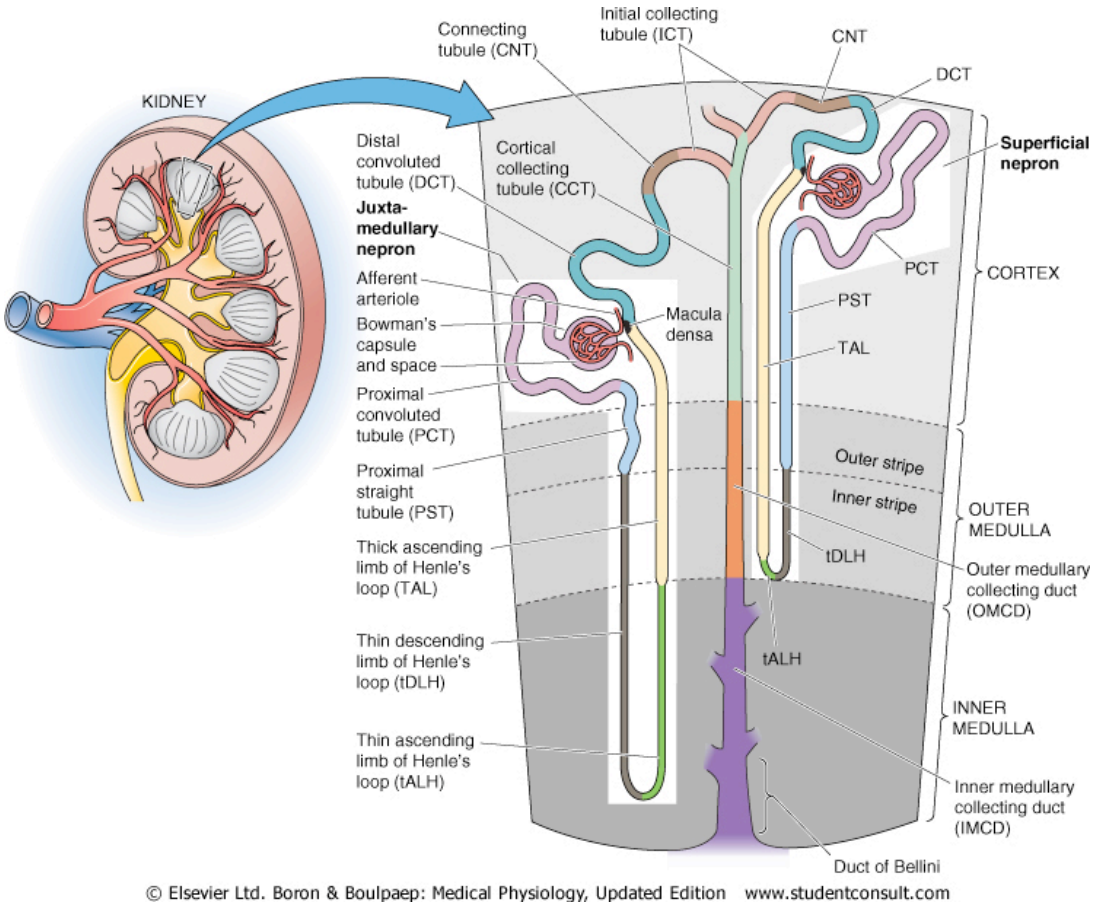

Figure 1: Structure of the nephron. Figure taken from the Textbook Boron & Boulpaep Updated Edition 2005 [1]

3.1.1 The Renin-Angiotensin-Aldosterone System RAAS

The Renin-Angiotensin-Aldosterone System RAAS is a hormone system regulating salt and water homeostasis of the human body by influencing the cardiovascular system (blood pressure) in parallel with kidney function (salt retention/water excretion/blood volume control).

Angiotensin

Angiotensinogen ("renin substrate") is synthesized in the liver and constitutively released into the blood circulation. Renin, a protease produced and stored in the granular cells of the JGA of the kidney, cleaves the deca-peptide from Angiotensinogen to Angiotensin I (Ang I). Renin is released from the granular cells of the macula densa (specialized smooth muscle cells in the wall of the afferent arteriole proximal to the glomeruli) when there are decreases in effective circulatory volume and subsequently also in blood pressure. This drop can be sensed by several systems:

- Decreased systemic blood pressure: Baroreceptors located in the central arterial circulation sense the decrease, signal the medulla to increase the sympathetic outflow to the JGA
- Decreased renal perfusion pressure: Stretch receptors in granular cells of the afferent arterioles sense a decreased distention
- Decreased luminal NaCl concentration at macula densa (independent of renal nerve activity)

All of the above mentioned control mechanisms lead to an increase in Renin release, enhancing the Ang I levels in the circulation. Ang I is still an inactive molecule, it needs to be cleaved into active Angiotensin II (Ang II) by the dipeptidyl carboxypeptidase angiotensin-converting enzyme (ACE), which is found on the luminal surface of vascular endothelia throughout the whole body, but mostly prominently resides in the lungs [2]. Ang II is the most potent effector of the RAAS; it has vasoconstrictive, pro-inflammatory and pro-fibrotic properties. There are two receptors for Ang II. Most actions of Ang II are mediated upon binding to the angiotensin receptor1 (AT1) (see Fig.2). This includes aldosterone secretion form the adrenal gland, vascular smooth muscle constriction, adrenergic

stimulation and sodium retention. Ang II is able to counterbalance its own actions by binding to the AT2 receptor, which triggers NO release, leading to vasodilatation [1]

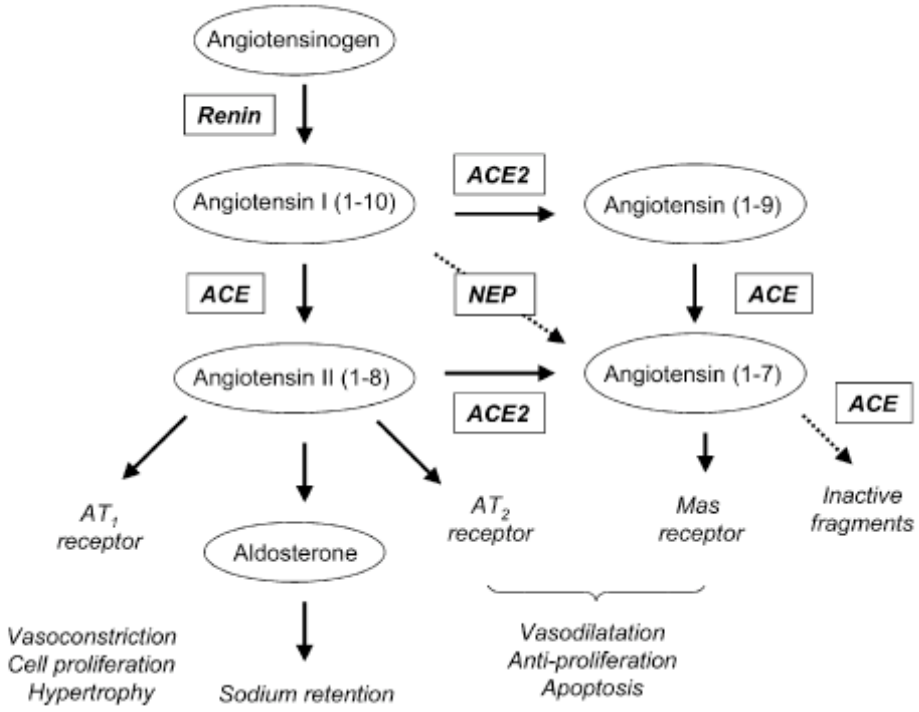

Figure 2: Scheme of the renin-angiotensin-aldosterone system RAAS. Scheme by Hamming et al. 2007. [3]

The main function of Ang II is to balance effective circulatory volume by controlling Na^+ reabsorption through the following mechanisms:

- Stimulation of aldosterone release from the glomerulosa cells of the adrenal cortex leading to Na^+ reabsorption via the epithelial sodium channel (ENaC) in the so called aldosterone sensitive distal nephron (ASDN, see 3.1.2.)

- Reduced blood flow through the vasa recta prevents NaCl and urea from being washed out of the medulla

- Stimulation of Na/H exchangers (proximal tubule and thick ascending limb of loop of Henle) promotes Na^+ reabsorption
- Stronger constricting the efferent arteriole compared to the afferent one maintains filtration rate and then supports Na^+ reabsorption in the proximal tubule
- Stimulation of thirst sensation in hypothalamus and release of the peptide hormone arginine vasopressin (AVP, also called anti-diuretic hormone ADH) from the posterior pituitary leading to an increase in total-body free water
- Enhanced tubuloglomerular feedback (see Fig 3) [1].

An increase in total-body free water and Na^+ retention result in a raise of blood pressure.

Aldosterone

Aldosterone regulates salt and water homeostasis. As mentioned earlier, aldosterone is released from the so-called granulosa cells of the cortex of the adrenal gland upon renin secretion and subsequent Ang II production as a response to a drop in blood pressure (see Fig. 3). It is a mineralocorticoid hormone belonging to the class of steroid hormones, since it is synthesized from cholesterol. Aldosterone production is unique to granulosa cells because they are the only cells in the body producing the aldosterone synthase, an enzyme needed for the last step of aldosterone creation. The synthesis and release of the mineralocorticoid hormone is tightly regulated by several factors. Apart from Ang II, elevated plasma K^+ levels also stimulate the production and release of aldosterone. K^+ depolarizes the membrane of granulosa cells, triggering an intracellular signalling cascade that finally leads to aldosterone secretion [2]. In turn, aldosterone increases the

renal secretion of K^+ in a negative short feedback loop.

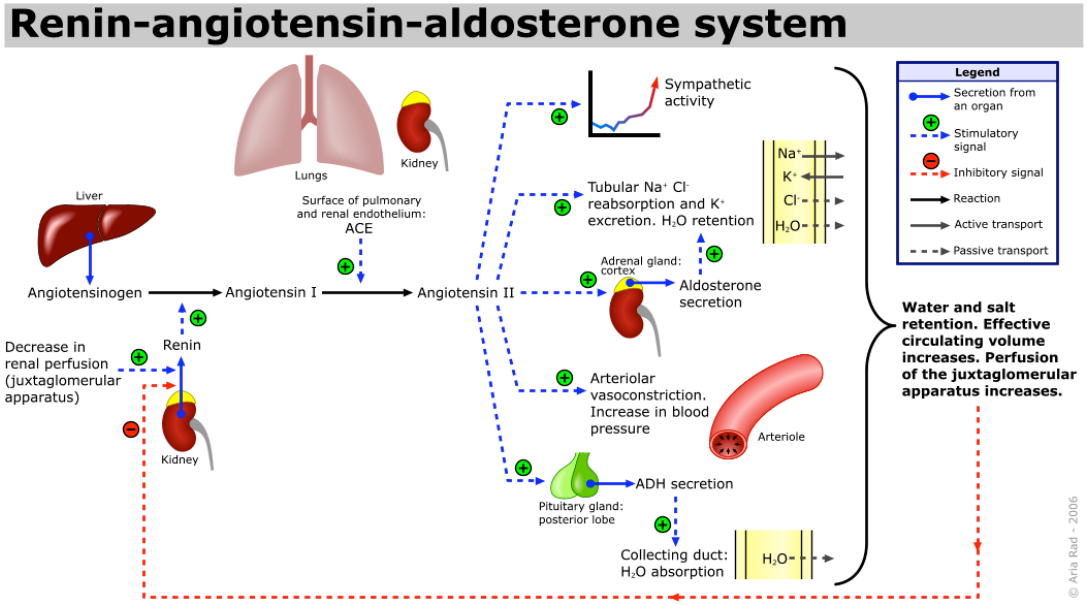

Figure 3: Schematic representation of coupling of vascular and renal system through the renin-angiotensin-aldosterone axis. Figure by Rad et al. 2006. [4]

Aldosterone also regulates Na^+ retention in the kidney in the principal cells of the collecting ducts. In the current definition, the aldosterone sensitive distal nephron (ASDN) includes the late distal convoluted tubule (DCT2), the connecting tubule and the cortical collecting duct (see Fig. 4) [5]. The ASDN is the most important site of fine-tuning for salt and water reabsorption. In this part of the nephron, ENaC, 11-β-hydroxysteroid dehydrogenase type 2 and the aldosterone receptor mineralocorticoid receptor (MR) are co-expressed. The target cells for aldosterone are the principal cells of the collecting duct, even though also intercalated cells have been shown to be to some extent responding to aldosterone action [6].

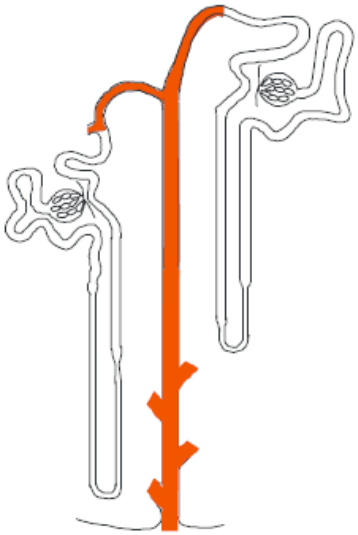

Figure 4: The aldosterone sensitive distal nephron ASDN. Scheme by Gabriele Adam (PhD), 2007 (unpublished).

Since aldosterone is a steroid hormone it can freely diffuse through the plasma membrane of the principal cell. In the cytoplasm the hormone binds to its receptor, the mineralocorticoid receptor (MR). This complex then translocates to the nucleus and initiates or inhibits transcription of target genes. It is known that the proteins induced by aldosterone are involved in regulation of Na^+ retention (see Fig. 5). For example they act on ENaC, enhancing the number of channel molecules in the plasmamembrane, stabilizing them and preventing them from being ubiquitinated and internalized into the membrane [7]. The increase in Na^+ absorption form the kidney tubules causes enhanced retention of water which elevates the extracellular fluid volume, which rises arterial pressure.

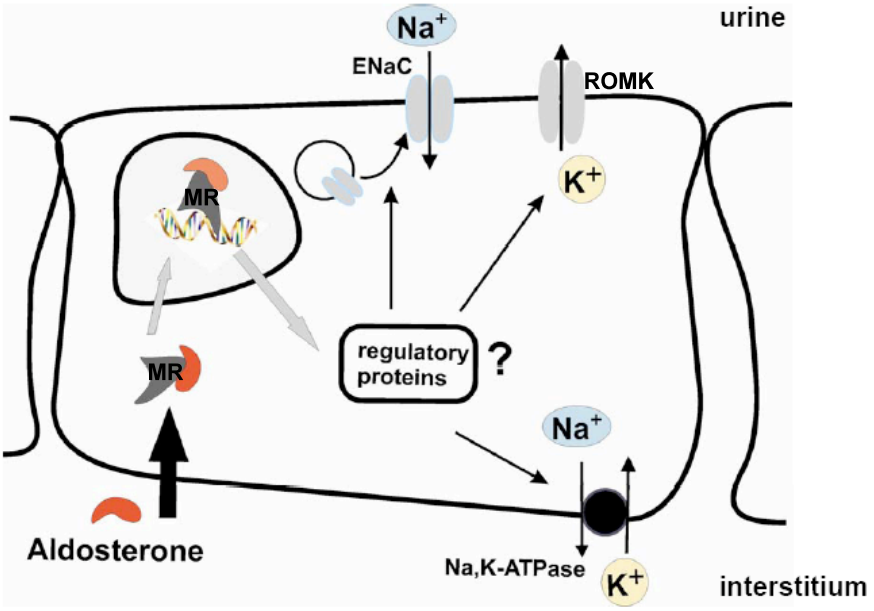

Figure 5: Action of aldosterone: Aldosterone freely diffuses through the membrane (steroid hormone) and binds to the cytoplasmic mineralocorticoid receptor (MR). This complex translocates to the nucleus and binds to specific regions in promoters of target genes. The transcription of the target gene is enhanced or suppressed, the protein products of these genes are involved in sodium retention via the epithelial sodium channel ENaC. Scheme by Gabriele Adam (PhD), 2008 (unpublished).

Thus aldosterone as well as Ang II is very important for control of blood pressure. The RAAS is often involved in cases of hypertension. For example when patches of the kidney are not properly supplied with blood, they start to constantly secrete high amounts of renin, Ang II is formed, aldosterone is released and the kidney starts to reabsorb big amounts of Na^+ and water, leading to a permanent rise in blood pressure and eventually tissue damage. In obese patients, Ang II and aldosterone are significantly higher than in slim people. The reason for this might be an elevated sympathetic nerve stimulation that leads to secretion of Renin, triggering the RAAS cascade. Today hypertension is treatable with different drugs. Vasodilative drugs either inhibit sympathetic nerve signals that would

cause Renin release or they directly relax the smooth muscle of the vasculature in the kidney. Another effective way of regulating blood pressure is by blocking the Ang II receptor or using ACE inhibitors.

3.2 Basic leucine zipper (bZIP) transcription factors

In our initial experiment with mice injected with aldosterone, we found the basic leucine zipper (bZIP) transcription factor ATF3 to be upregulated [7] and it was only later that we came to the conclusion that this induction was stress-related. I will describe the bZIP transcription factor family with a special emphasis on ATF3, and will also give a short insight into ATF3 in stress-responses.

The mammalian ATF/CREB (activating transcription factor/cAMP responsive element- binding) family of transcription factors constitutes a large group of basic region-leucine zipper (bZIP) proteins. The basic region of the bZIP domain is the DNA binding domain of this kind of transcription factor, which was classified in the late 1980s. The leucine zipper contains a coiled coil structure with heptad repeats of leucines. When the hydrophobic leucine occurs at every seventh position of an α-helix, the aliphatic side-chains are all oriented on the same side of the helix so that they can interact with each other, leading to a coiled coil structure (see Fig. 6) [8]. The leucine zipper of the bZIP domain is responsible for transcription factor dimerization.

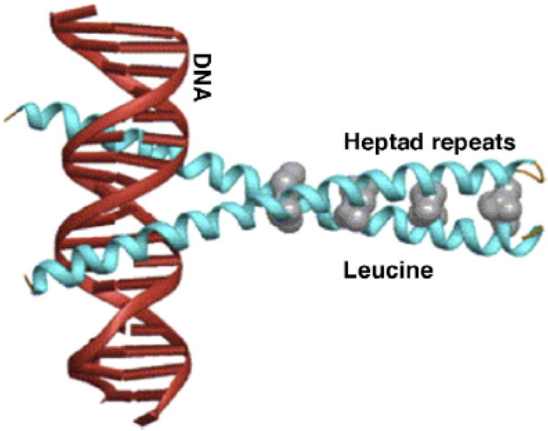

Figure 6: Schematic representation of the bZIP domain bound to double stranded DNA: DNA is represented in red, bZIP helices are in blue, heptad repeats of leucines are depicted in grey. Figure by Manna et al. 2009. [20]

The bZIP transcription factors represent one of the most important classes of enhancer-type transcription factors; they play a role in many physiological processes such as development, differentiation, tumor progression, metabolism and stress [9] [10]. There are three subfamilies of bZIP transcription factors: (1) cAMP responsive element-binding/ cAMP responsive element modulator/ ATF1 (CREB/CREM/ATF1), (2) Fos/Jun and (3) Caat-enhancer-binding protein (C/EBP), they all form (homo- and/or hetero)dimers, but bind to different DNA sequences unique to each subfamily. The bZIP domain allows selective formation of homo- and/or heterodimers among family members. Electrostatic interactions between amino acids along the dimerization sequence favor either the homo- or heterodimerization [11] [12]. The dimers then recognize related palindromic sequences in the DNA. Up to date as much as 53 human genes have been found to contain bZIP motifs which lead to a potential of 2700 different dimers to be formed [13] [14]. The heterodimeric complexes formed between jun, Fos and ATF family members are called AP-1 transcription factors. These AP-1 dimers are subdivided into 2 distinct classes, Jun/Fos and Jun/ATF. Depending on the combination of transcription factors involved, they can regulate cell proliferation,

differentiation and apoptosis either positively or negatively [15].

Expression and effects of the bZIP proteins are controlled by several signalling pathways, including cAMP-dependent protein kinase A (PKA), PKC, TGF-β signalling [16] and mitogen activated kinases MAPK such as the extracellular signal-regulated kinase (ERK), c-jun-N-terminal Kinase JNK and p38 kinase [17] [18] [19]. Depending on the cell type, its malignancy status and also the environment the cell faces, certain bZIP proteins are upregulated and interact with the transcriptional control of different targets genes.

In the following I would like to take a closer look at the ATF transcription factor family, with special emphasis on ATF3.

3.2.1 Activating transcription factor ATF

All proteins belonging to the ATF/CREB family have in common that they are responding to extracellular signals.

There are many cellular proteins having potential ATF binding sites in their promoters. ATFs in most cases bind to the so called cAMP response elements (CRE) in the promoter of the target gene. The CRE is required for gene inducibility via cAMP signalling [21]. The consensus binding sequence of all ATFs is 5'-TGACGTCA-3'. There are also promoters that are not responsive to cAMP that are bound by ATFs.

Truncated versions of ATFs leaving them only with their bZIP domain have been shown to bind DNA. In order to bind to DNA, it is required for the ATF proteins to dimerize. All of the 8 different ATF proteins can homodimerize, however, not all combinations of ATF proteins can heterodimerize [22]. Heterodimerization partners of ATF3 are C/EBP, CHOP/DDIT3, ATF2, Jun, JunB, p21SNFT/JDP1, and Nrf2/NFE2L2. Depending on the different dimerization patterns, ATF

proteins can be activators of gene expression, while in another combination they would rather be repressors. For example homodimers of ATF3 rather suppress gene transcription. Furthermore ATF/CREB family members can also heterodimerize with bZIP proteins belonging to other transcription factor families, e.g. AP-1 or C/EBP family members. This leads to a tremendous possibility of combinations of heterodimers, which are believed to have differing DNA binding specificities and therefore pleiotropic effects on gene expression regulation [23].

All ATFs show high sequence similarity in their leucine zipper and adjacent basic domain, however, outside of this region, they can be quite diverse in amino acid sequence [22]. Nowadays the ATF/CREB family of transcription factors is further subdivided into 6 subgroups, based on their amino acid similarity (see Table 1). Members of the same subgroup show significant sequence similarity inside as well as outside of the bZIP subdomain. Between the groups, the proteins do not share much similarity other than the bZIP motif. Hence, even though they have the same prefix (e.g. ATF or CREB), they should indeed be considered as distinct proteins [24]. However, some names of the proteins rather reflect their history of discovery rather than the belonging to one family. For example, ATF3 is much more homologous to the fos proteins (which belongs to the AP-1 family) rather than to other subgroups of the ATF/CREB proteins [11]. Also proteins belonging to one family can regulate transcription in the manner of the other family, e.g. C/EBP proteins can activate certain promoters by binding to a CRE site instead of the C/EBP site [25].

The mammalian ATF/CREB family of transcription factors[a]

Subgroup	Members	Alternative names
CREB	CREB	ATF-47
	CREM	
	ATF1	TREB36, TCRATF1, ATF-43
CRE-BP1	CRE-BP1	ATF2, HB16, TREB, TCR-ATF2, mXBP
	ATFa	
	CRE-BPa	
ATF3	ATF3	LRF-1, LRG-21, CRG-5, TI-241
	JDP-2	
ATF4	ATF4	CREB2, TAXREB67, mATF4, C/ATF, mTR67
	ATFx	hATF5
ATF6	ATF6	ATF6α
	CREB-RP	G13, ATF6β
B-ATF	B-ATF	
	JDP-1	

[a] This table is not meant to be comprehensive; for details and the original references, see a previous review (Hai et al., 1999).

Table 1: The mammalian ATF/CREB family of transcription factors with its 6 subgroups: Due to historical reasons, the nomenclature of the ATFs shows many different synonyms for each protein. This table is not comprehensive. Table by Hai et al, 2001. [24]

3.2.2 ATF3

ATF3 was originally isolated from HeLa cells that were treated with tetradecanoylphorbol acetate (TPA) which is a potent tumor promoter often employed in biomedical research to activate the signal transduction via protein kinase C [22]. ATF3 is a 181 amino acid protein that is ubiquitously expressed but its level is maintained low in the absence of cellular stresses [26], residing in the nucleus. Upstream factors of ATF3 include for example p53 [27], ATF2 [15], ATF4, protein kinase A (PKA), HIF-1a, the mitogen-activated kinases (MAPK) and C/EBP. Therefore ATF3 is regulated on the RNA level (e.g. by ATF4) as well as posttranslationally modified (e.g. by phosphorylation by MAPK) [28].

The ATF3 homodimer is a transcriptional repressor while heterodimeric complexes of ATF3 with c-Jun have been demonstrated to act as activators of transcription. Other bZIP protein dimerization partners for ATF3 are ATF2 [22], c-Jun [29], JunB [30], JunD [31] and gadd153/CHOP10. Transient transfection experiments have shown that ATF3/c-Jun and ATF3/JunD activate promoters containing ATF/CRE or related sites, while ATF3/JunB can either activate or repress a promoter, depending on the promoter context [30].

There are two different splice variants of ATF3 in humans: The longer isoform represses rather than activates transcription from promoters with ATF binding elements. The two shorter isoforms (ΔZip and ΔZip2 see Fig.7.) lacks the bZIP motif and therefore does not bind to DNA [32]. It is believed to sequester co-repressors from the promoters of the target genes, therefore activating their promoters. The full length form of ATF3 is also capable of activating promoters that do not contain ATF3 binding sites, probably also due to keeping away negative factors from the promoters of target genes [33]. In mice, so far only one isoform of ATF3 was identified (corresponding to the longer one in humans). ATF3 is early (within 2 h) and transiently induced during cellular responses to stress [28].

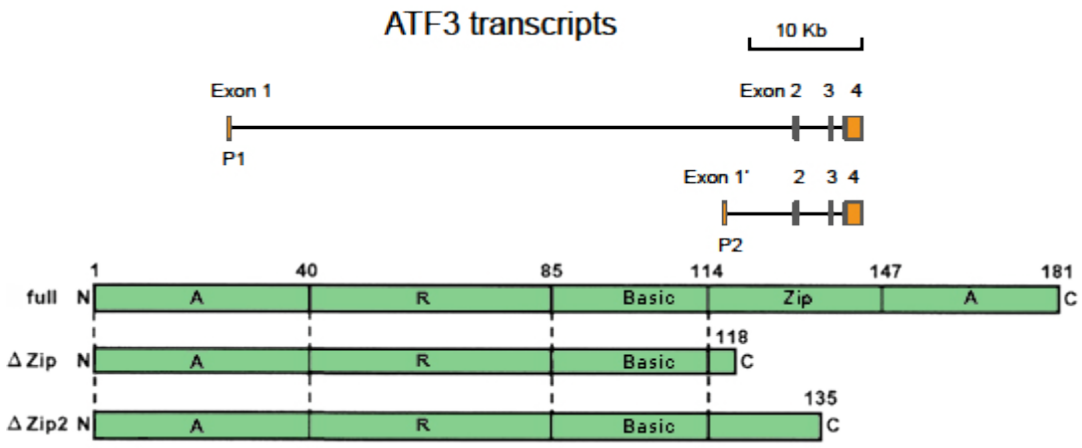

Figure 7: Isoforms of the ATF3 transcript in humans: The ATF3 gene has two promoters P1 and P2 that are differentially activated by external stimuli such as growth factors. The P1 and P2 transcripts differ in the first exon but share common exons 2, 3, and 4 encoding the same protein sequence. Both promoters give rise to the same transcripts, however, these proteins can be spliced differentially. The full length protein is made up of 181 amino acids, containing the basic region which binds the DNA and the bZIP region, which is the leucine zipper that allows dimerization of ATF3 either with itself (homodimerization, leading to a negative regulator of transcription) or other bZIP proteins, including the ones from other families e.g. c-Fos [34]. The ΔZip and ΔZip2 splice variants of the protein are shorter, due to a lack of the bZIP domain. Therefore these isoforms cannot dimerize, which leads to an inability to bind DNA. Thus, these two isoforms of ATF3 have a rather activating function on target genes, due to potential sequestering of transcriptional co-repressors. Figure by Kitajima et al, 2009 [34].

ATF3 in stress responses

There is overwhelming evidence from many laboratories that ATF3 is an early stress-inducible gene, its mRNA expression increases dramatically when cells are exposed to stresses such as amino acid deprivation [35] [36] [37], UV irradiation [38], x-rays [39], hypoxia [40] [41], ischemia-reperfusion injury in kidney [42], toxins like LPS via interferons [43] [44], cytokine release such as TNFα [19] or interleukin 4 (IL-4) [45] and many other stressors. All stressors seem to have in common that they injure the cell. Stresses that do not injure the cell seem

to fail to induce ATF3 transcription [46]. ATF3 is induced very immediately when the cell faces the stress and its induction remains only transient. In most of the systems that have been examined so far, a transient induction of ATF3 mRNA is seen within 2 h. This early and transient induction suggests that there is a mechanism to turn off ATF3 expression after its induction. Indeed it has been shown that ATF3 being a transcriptional repressor can shut down its own transcription by binding to its promoter [47]. Many of the target genes of ATF3 might themselves be other transcription factors, to orchestrate an early stress response of the cell.

Up to date there are around 40 target genes of ATF3 known, including interleukins, the inhibitor of differentiation 1 (Id1) [48], the transcription factor Nrf2, the nuclear protein gadd153/CHOP10 [49] [50], cyclin D1 which controls cell cycle arrest and phosphoenolpyruvate carboxykinase [51] which is important in gluconeogenesis. ATF3 also has a target site in its own promoter, repressing its own transcription via a negative feedback loop [47]. This explains partially the transient nature of ATF3 induction. Also other bZIP proteins like c-Fos [52] or ICER [53] show this autorepression.

Signalling pathways acting on ATF3 expression include TGF-β signalling, p53-dependent signalling, protein Kinase A (PKA), nuclear factor kappa B (NF-κB) and the mitogen activated kinases (MAPK). MAPK are activated by upstream kinases in response to extracellular stimuli like growth factors, hormones, stress and cytokines. There are 4 major signalling pathways via the MAPK ERK1/2, the p38, the c-Jun-N terminal kinase (JNK) and ERK5, which then in turn act on transcription factors by phosphorylating them regulating their transcriptional activity (see. Fig.8). The MAPK can be differentially involved in the regulation of ATF3 expression: JNK and p38 kinase seem to upregulate ATF3 mRNA expression, while it is suppressed by the extracellular-signal related kinase (ERK) [19].

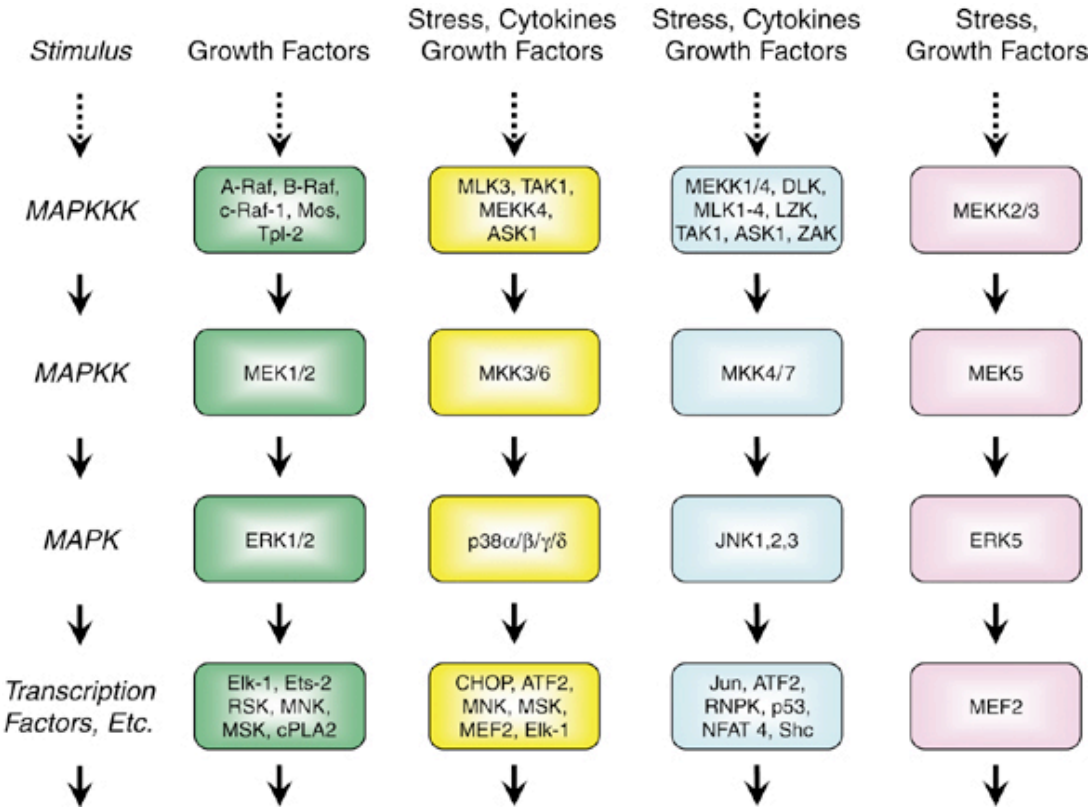

Figure 8: The four major MAPK signalling pathways. Scheme by Roberts et al. 2007 [54].

The physiological role of ATF3 is still controversially discussed. Targeted disruption of ATF3 in mice causes no obvious phenotype; the animals are viable and grow normally [55]. ATF3 was first believed to have detrimental outcomes for the cell when it is expressed. This was shown in several overexpression systems *in vitro* but also *in vivo* in flies and mice. However this ectopic expression is entirely out of context and ATF3 effects depend strongly on other proteins that might be induced and interact with ATF3. Nevertheless, ATF3 seems to be involved in tumor progression, promoting metastasis [56] by supporting cell cycle progression [30] [57]. A big variety of cancers including solid tumors in the breast, lungs, prostate and colon overexpress ATF3, supporting the notion that ATF3 is a

tumor progressor and positive regulator of cell cycle progression and cell survival. Under other conditions using other cell lines, ATF3 seems to have the opposing function, supporting cell death and preventing tumorigenesis. ATF3 is a marker for injured neurons that are regenerating [58] and is activated by JNK when cerebellar granule neurons undergo apoptosis due to potassium deprivation [59]. Another example of ATF3 dependent apoptosis is observed in beta cells of the pancreas, where ATF3 suppresses the expression of the insulin receptor substrate 2 (IRS2), resulting in cell death [60]. So the effects of ATF3 seem to clearly depend on the cell type and also its malignancy status. The group of Tsonwin Hai, which created the ATF3 knockout mouse was the first to state a dichotomous role for ATF3 in cancer development. They performed loss- and gain of function studies using a breast cancer cell line (MCF10A) that comes in different sub-states of malignancy but all of them have the same genetic background. MCF10A is spontaneously immortalized but shows normal characteristics of breast epithelium whole MCF10CA1a is a highly malignant form of this breast epithelial cell line. In the non-malignant MCF10A cell line, ATF3 enhanced apoptosis, while in the aggressive MCFCA1a it protected from apoptosis, enhanced the cell motility and upregulated the transcription of genes involved in metastasis formation e.g. caveolin-1, Slug and the Basic helix-loop-helix (bHLH) transcription factor TWIST1 [61].

ATF3 regulation in the kidney

In an initial experiment that was at the origin of the present thesis work, it was sought to determine aldosterone regulated genes in the aldosterone sensitive distal nephron using the Affymetrix Microarray approach. The strategy was to inject mice with aldosterone for 1 h, to micro-disect the tubules of the ASDN and to extract total RNA from the tissue. This RNA was then subjected to Microarray analysis, yielding a list of potentially aldosterone regulated genes. In this list we found ATF3 mRNA to be upregulated 3.5-fold. Only later we realized

that this upregulation was not due to the specific effect of the mineralocorticoid hormone but rather to the injection per se, manifested in the stress reaction of the mouse to being restrained and injected. This seemed to be reasonable since the literature comprises many papers dealing with the role of stress induction of ATF3 as mentioned earlier. Interestingly the induction of ATF3 by stress seemed to be very specific for the kidney and might even be specific for this kidney segment (the ASDN). An induction of ATF3 under the same treatment conditions was not seen in heart or colon.

According to the literature, only little is known about the specific function of ATF3 in the kidney. Nevertheless it has been found to be involved in stress-reactions of the kidney. It is upregulated 12-fold in human proximal tubule (HK2) cells treated with hydrogen peroxide H_2O_2 (oxidative stress) and 6-fold in a mouse model of renal ischemia-reperfusion injury, which is an insult that usually leads to subsequent apoptosis of tissue. Overexpression of ATF3 could reduce the injury, which was associated with a decrease in p53 [42]. ATF3 was found in urinary exosomes of rats with cis-platin injury or ischemia-reperfusion injury. Exosomes are secreted vesicles from all nephron segments that contain intracellular kidney injury biomarkers. Also human patients with acute kidney injury excrete ATF3 containing exosomes in the urine, in contrast to patients with chronic kidney failure, where there is no ATF3 detected in the urinary exosomes, suggesting that ATF3 might be a new marker for renal acute injury [62]. This is also supported by another study in acute renal failure (ARF) models in rat kidney, where ATF3 was transiently upregulated not only on the mRNA but also on the protein level after 8 h and 24 h in whole kidney samples [63]. The before mentioned studies only show the upregulation of ATF3 in kidney injuries due to hypoxic stress, toxic stress and as a result of this eventually apoptosis, but they never propose a mode of action of the transcription factor in these pathophysiological conditions. Therefore the group of Guanghui Hu sought to unify all the Microarray data available and tried to reveal possible signal transduction cascades involved in human kidney pathologies. They found ATF3

mRNA to be induced by the TGF-β signalling pathway, which is involved in many diseases (e.g. glomerular- and tubulointerstitial pathologies) and also controls many processes in the kidney [64]. It regulates the basal expression of collagen IV which is the main constituent of the basement membrane of the glomerulus. ATF3 has been reported to repress expression of type IV collagenase (matrix metalloproteinase-2 MMP-2) by inhibiting trans-activation of the MMP-2 gene by p53 [65]. Therefore it is reasonable to suspect ATF3 to possibly contribute to TGF-β mediated kidney diseases by interfering with the healthy balance of collagen production and breakdown.

TGF-β is linked to renal dysfunction during diabetes-induced processes (e.g. diabetic nephropathy via hypertrophy matrix accumulation), in which an excessive production and secretion of glucagons takes place (the hormone which is the counter-regulator of insulin). ATF3 has been shown to act positively on the expression of glucagons in several cell types [66], therefore possibly being a player taking part in the events that lead to kidney end stage disease. In addition, ATF3 gene expression was reported to be up-regulated by TGF-β- treatment in epithelial cells [48].

Not only will TGF-β-induced ATF3 decrease MMP-2 mRNA transcription and enhance glucagon secretion, in addition it also acts on Cyclin D1 which is an important control protein in cell cycle progression. Cyclin D1 allows the cell to go from the resting G1 phase into the S-phase. In mouse chondrocytes ATF3 represses the expression of Cycline D1 [67], leading to a cell cycle exit, prevention of cell division and subsequent terminal differentiation, which can result in hypertrophy of the kidney tissue.

There could be two different pathways via which ATF3 is upregulated by TGF-β. One pathway involves the MAPK p38 which was mentioned earlier. p38 phosphorylates the heterodimer of c-Jun and ATF2 which in turn translocates to the nucleus and induces the transcription of the ATF3 gene by binding to the ATF/CRE site in its promoter region [32]. The other pathway would be

the more classical pathway over the so-called Smads. Smads are transcription factors involved in TGF-β signalling. Smad3 is phosphorylated upon binding of TGF-β to its receptor, then it binds the co-Smad4, translocates to the nucleus and initiates ATF3 transcription (see Fig. 9).

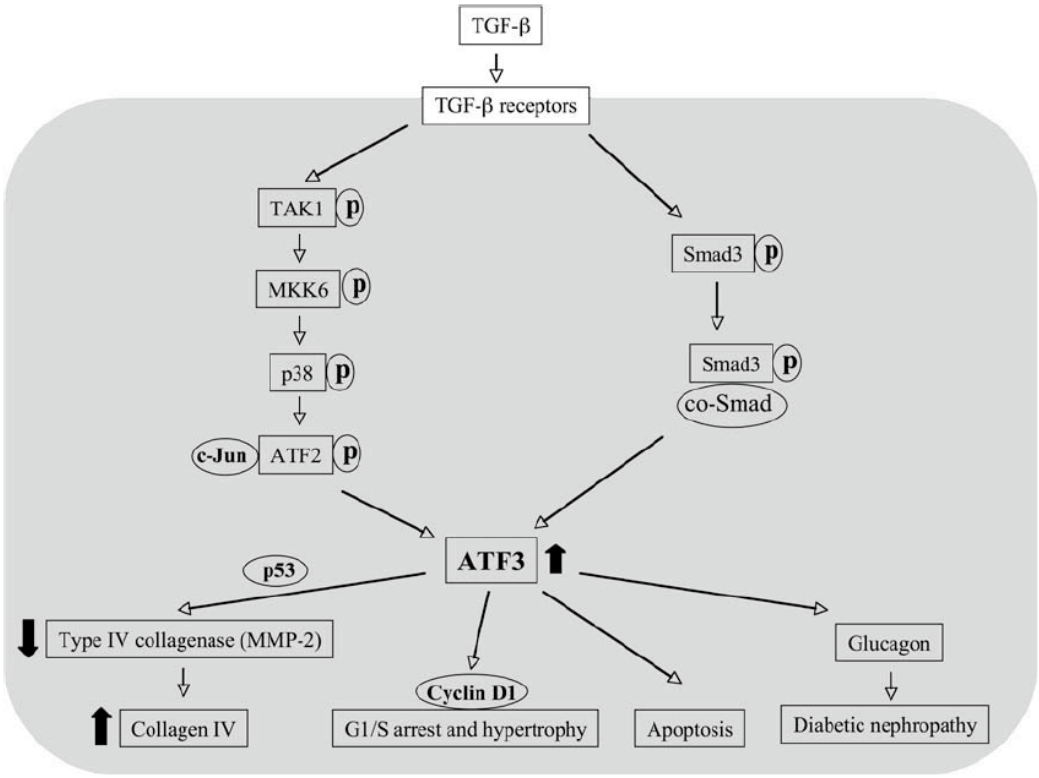

Figure 9: Proposed regulation of ATF3 by TGF-β signalling in the kidney: There is a possible regulation of ATF3 gene transcription via a Smad dependent and Smad independent pathway. Both regulation pathways are mainly controlled by phosphorylation rather than gene expression. On the contrary, once the ATF3 is activated, it stimulates or suppresses a number of down-stream genes involved in many biological processes and kidney diseases such as fibrosis, hypertrophy, and diabetic nephropathy. Scheme by James et al. 2006 [64].

So far only the negative role of ATF3 with detrimental outcomes for the kidney was discussed. However, there is also evidence that ATF3 can exert a protective role for the kidney cells. A very recent study showed that ATF3 deficient mice have a higher ischemia-reperfusion induced mortality, as well as kidney dysfunction,

inflammation and apoptosis. When they specifically rescued ATF3 expression in the kidney, the ischemia-reperfusion injuries were reduced. Here ATF3 seems to be regulating interleukin 6 and 12 expression in an epigenetic way: ATF3 directly binds to the histone deacetylase 1 (HDAC1) and recruits the enzyme to the ATF/NF-κB sites of the promoters of the two interleukins. The DNA in this region then condensates which makes it harder for transcriptional co-factors and the RNA polymerase to reach promoter. This leads to an epigenetic repression of IL6 and 12 in acute kidney injuries, mediated by ATF3 [68]. As mentioned earlier, the human kidney cell line HK2 increases ATF3 expression upon H_2O_2 treatment. When ATF3 was introduced into this cell line using adenoviruses, the cells were protected from apoptosis in a p53-dependent manner. When overexpressing ATF3 in mice using the same viruses, the animals were protected from ischemia-reperfusion injury [42].

Thus, just like for its involvement in cancer, one cannot make a clear statement for ATF3 mediated effects in the kidney, they might be very controversial depending on the insult. Many papers describe ATF3 as a promising novel target for treating kidney injuries. However, it is not always the "bad guy", which makes it harder to use as a therapeutic target.

3.3 Retroviruses

Since we used lentiviral vector systems for this study, in the following an overview of lentiviruses is provided.

General introduction

Over the last few years, virus-based vectors have become very important tools for research using overexpression systems. They have also been implicated in first attempts of gene transfer to diseased cells, trying to genetically cure illnesses. Also due to the very high transduction rate, they have been used to create transgenic animals [69]. Nowadays, various types of virus-derived gene transfer systems are available based either on DNA or RNA viruses. The vectors either integrate stably into the host cell genome or express their genetic information episomally (replicating autonomously in the cytoplasm or as part of a chromosome).

Retroviruses have been used since the early 1990s to transfer DNA into host cells. As already described in 1970, retroviruses are single-stranded RNA (ss) viruses replicating through a double-stranded (ds) DNA intermediate [70]. They display a broad host range, including humans and many other mammals as well as birds. Some of the earliest ever studied retroviruses were the murine leukaemia virus (MLV), mouse mammary tumor virus (MMTV) and avian leucosis virus (ALV). All of them were found to associate with tumor development in their host organisms, which made them very interesting for studying cancer development. They helped to discover the oncogenes. While some viruses seemed to deliver oncogenes to the cell, others were interacting directly or more indirectly with the oncogenes encoded by the host cell, therefore contributing to malignant tissue formation [71].

Based on their pathogenicity the retroviruses were divided into three groups: (1)

the onco-retroviruses (e.g. MLV), (2) the lentiviruses (e.g. human immunodeficiency virus HIV) and (3) the spumaviruses (foamy viruses, with prominent spikes on their surface e.g. human foamy virus) [72]. In the following lentiviruses shall be discussed closer.

3.3.1 Lentiviruses

Lentiviruses (latin: slow) have long incubation periods and characteristically cause diseases with a prolonged latent period. Lentiviruses (e.g. Human immunodeficiency virus HIV) have the ability to infect a broad range of dividing and non-dividing host cells and stably integrate DNA segments into the cell genome. The lentivirus docks to the target cell surface and releases RNA into the target cell, which is transcribed into the DNA by the reverse transcriptase that is also encoded by the virus. This DNA then forms a preintegration complex with the accessory protein Vpr, the integrase and the protein matrix. These proteins all contain localization sequences, allowing the preintegration complex to cross the nuclear membrane. This is a specific feature of lentiviruses and the reason why they can also infect non-dividing cells. Vectors based on other viruses cannot enter the nucleus through its membrane, they have to wait until the cell starts dividing and therefore the nuclear membrane is broken down in order to get through to the host cell DNA [73]. When the vector DNA has reached the host cell DNA, it is stably integrated via the enzyme integrase (see Fig.10). Another feature of lentiviruses constituting an advantage over working with other retroviral classes is the fact that they preferentially insert in introns of chromosomal regions rich in expressed genes. Therefore chances are less that they insert in an exon of a gene, disrupting its expression [13] [14].

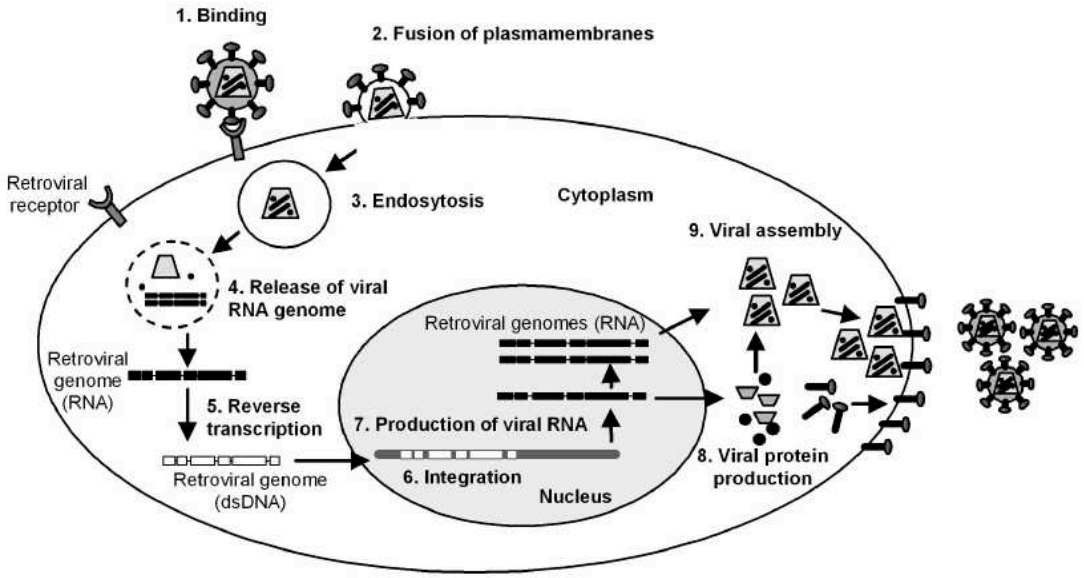

Figure 10: Lentiviral life cycle: Lentivirus based vectors (e.g. HIV) have the ability to infect dividing as well as non-dividing cells. 1. The virus specifically binds via retroviral receptors located on the surface on the host cell to its plasma membrane. 2. The viral lipid-layer surrounding the viral nucleocapsid fuses with the host cell membrane and allows entry of the virus via endocytosis (3.) 4. The viral genome is released into the cytoplasm along with the two viral enzymes reverse transcriptase (RT) and the integrase. The vector RNA is transcribed into DNA by the RT, which forms a preintegration complex with the accessory protein Vpr, the enzyme integrase, and the protein matrix. These proteins contain localization sequences, allowing the preintegration complex to cross the nuclear membrane [73. After entering the nucleus the viral cDNA is stably integrated into the host genome by integrase as a pro-virus. 7. The viral DNA is transcribed by the host cell machinery into new retroviral genomes (RNA). 8. While some RNA molecules reside in the cytoplasm as they are, others are translated and viral proteins are produced from them. These proteins help to assemble new viruses and package the viral RNA molecules into nucleocapsids. 9. The virus buds from the cell, leaves it via exocytosis taking along a lipid-bilayer envelope of plasmamebrane with viral proteins on its surface. These proteins will again bind to new retroviral receptors on the next host cell. Since the integration of the pro-virus into the host cell genome is stable, it is passed on to the daughter cells also after cell division. Scheme by Hemminki et. al 2005 [73] [74].

Structure of lentiviruses

Lentiviruses are around 80-100 nM in diameter. They enclose an RNA genome in a lipid-bilayer enveloped nucleocapsid (see Fig. 11 and 12).

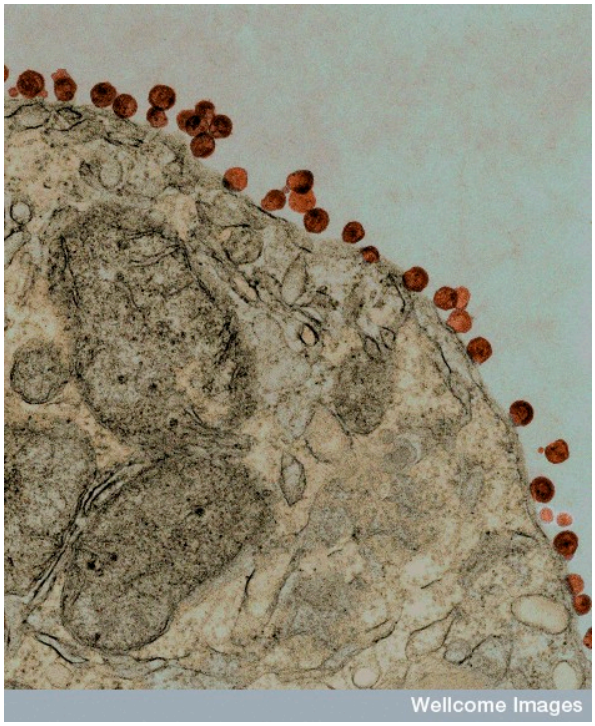

Figure 11: Electron microscopy picture of HIV budding from an infected host cell. Picture from Wellcome images photolibrary, number B0005754.

The lentiviral genome comprises two linear positive-sense single stranded 8-12 kb stranded RNA molecules. Its basic structure is the same as the one of all retroviruses: The genome is flanked on both sides by long terminal repeats (LTR). These are short DNA sequences repeated up to thousands of times. The LTRs mediate the integration of the retroviral DNA via an LTR specific integrase into the host chromosome. The lentiviral genome contains three essential genes: *gag* encodes a precursor protein of the viral structural proteins that is cleaved by a

viral protease into the matrix (MA), capsid (CA) and nucleocapsid protein. *pol* encodes three enzymes; a protease important in virion maturation, the reverse transcriptase needed to convert the RNA molecules of the lentiviral genome into insertable cDNA molecules and the integrase to insert the cDNA molecule into the host genome as a pro-virus. Finally *env* encodes the envelope glycoprotein that allows attaching of the virus to the host cell membrane and entry into the cell.

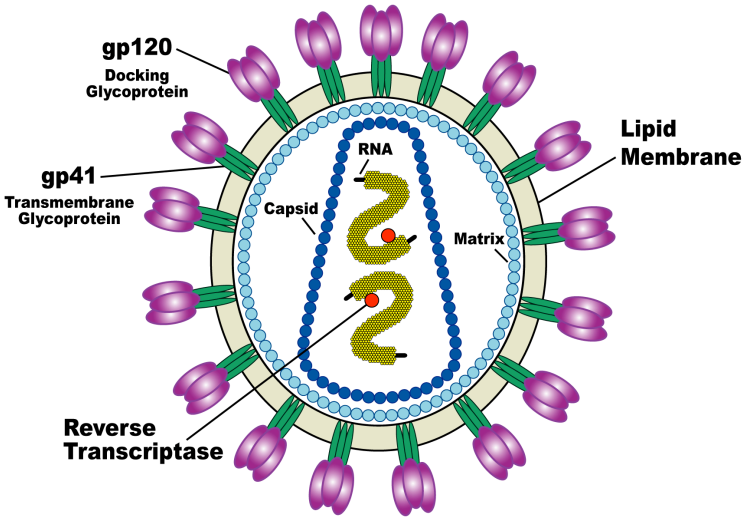

Figure 12: Schematic representation of HIV virus morphology. Scheme by Shen group Shang Hai Jiao Tong University.

Lentiviral genomes are more complex than the ones of more simple retroviruses (e.g. onco-retroviruses, see Fig. 13).

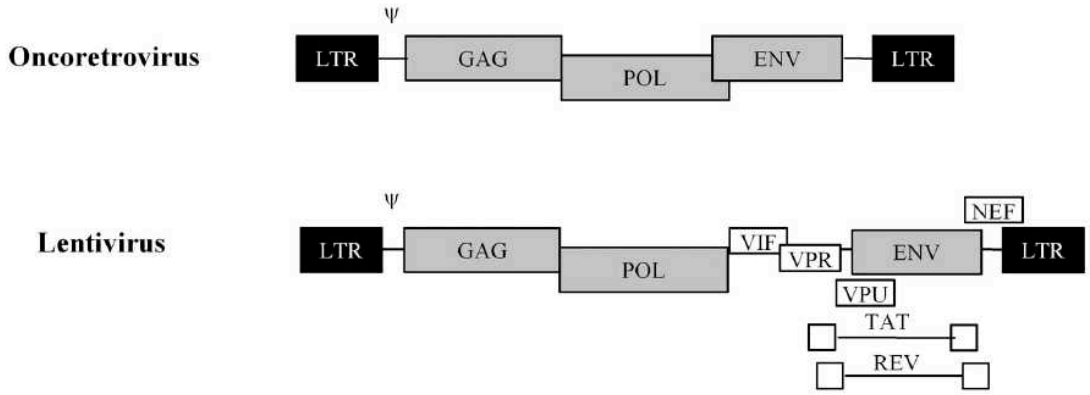

Figure 13: The retroviral genome structure: The onco-retroviral genome consists of three genes, gag, pol and env encoding the structural proteins, the reverse transcriptase and integrase, and envelope proteins respectively. The lentiviral genome contains additional genes encoding for regulatory proteins (tat, rev) or accessory proteins (*vif, vpr, vpu, nef*) that help the virus enter the host cell and ensure a prolonged infection of the host cell. The psi (Ψ) element found in both types of retroviruses is a packaging element and is involved in regulating the encapsidation of the retroviral RNA [76]. Scheme by Hemminki et al. 2005 [74].

Lentiviruses have evolved better mechanisms to optimize all steps of infection. Unlike onco-retroviruses, lentiviruses have additional accessory genes, e.g. in the HIV-1 genome there are the *vif, vpr, vpu, tat, rev* and *nef* genes, encoding proteins required for more efficient viral replication and maintenance of infection in the target cell [75]. Herein, Tat is a positive regulator of transcription, while Rev is responsible for export of spliced or partially spliced viral transcripts from the nucleus (see Fig. 14).

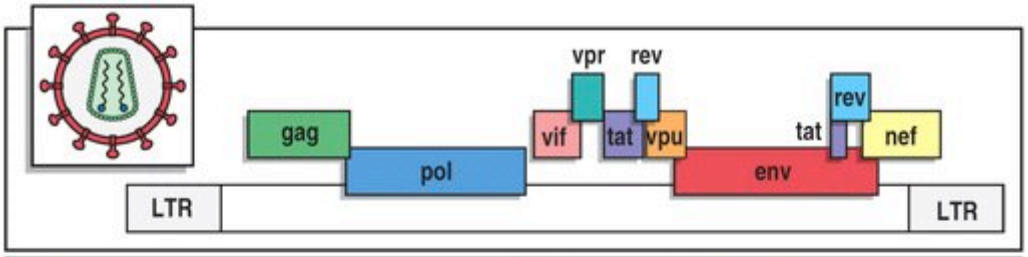

Gene		Gene product/function
gag	Group-specific antigen	Core proteins and matrix proteins
pol	Polymerase	Reverse transcriptase, protease, and integrase enzymes
env	Envelope	Transmembrane glycoproteins. gp120 binds CD4 and CCR5; gp41 is required for virus fusion and internalization
tat	Transactivator	Positive regulator of transcription
rev	Regulator of viral expression	Allows export of unspliced and partially spliced transcripts from nucleus
vif	Viral infectivity	Affects particle infectivity
vpr	Viral protein R	Transport of DNA to nucleus. Augments virion production. Cell cycle arrest
vpu	Viral protein U	Promotes intracellular degradation of CD4 and enhances release of virus from cell membrane
nef	Negative-regulation factor	Augments viral replication *in vivo* and *in vitro*. Downregulates CD4 and MHC class II

Figure 14: Summary of lentiviral genes and the function of their corresponding proteins. Scheme from "The Immune system", Garland Science 2005).

3.3.2 Lentiviral vector expression systems

Seven years after the discovery of HIV in 1983, a first HIV-based vector DNA delivery system was described [76] [77]. These are replication-defective HIV-1 vector due to deleted envelope (env) protein sequences. They are co-transfected with expression vectors that encode heterologous Env proteins from other viruses, e.g. human T cell leukemia virus type I- HTLV-I Env protein yielding so-called

HIV-1 pseudotypes (chimeric lentiviral vectors). These first gene delivery systems have constantly been improved and also become safer. Since there would be a potential of the viral RNA to recombine and a cross-species transmission could take place, the vector systems of the first generation were further developed including a deletion of almost all the accessory and regulatory genes and splitting the vector genome into parts (several vector constructs). These measures reduce the risk of vector recombination and mobilization to a minimum. The most sophisticated vectors nowadays are third generation lentiviral vectors that are based on HIV-vectors (see Fig. 15). Deletion of the env gene apparently still allows formation of viral particles, however, they are non-infectious. The broad variety of available env genes allows to pseudotype viruses with other envelope glycoproteins, offering a wider range of target host cells to the virus [78].

3rd generation lentiviral vector systems:

The latest 3rd generation vector systems were developed based on the concept of separating the *cis*-acting elements (essential for RNA synthesis, packaging, reverse transcription and cDNA integration) from the *trans*-acting elements (viral enzymes, structural and accessory proteins). These systems consist of a packaging vector, a transfer vector and an envelope expression cassette (see Fig. 15. A-C).

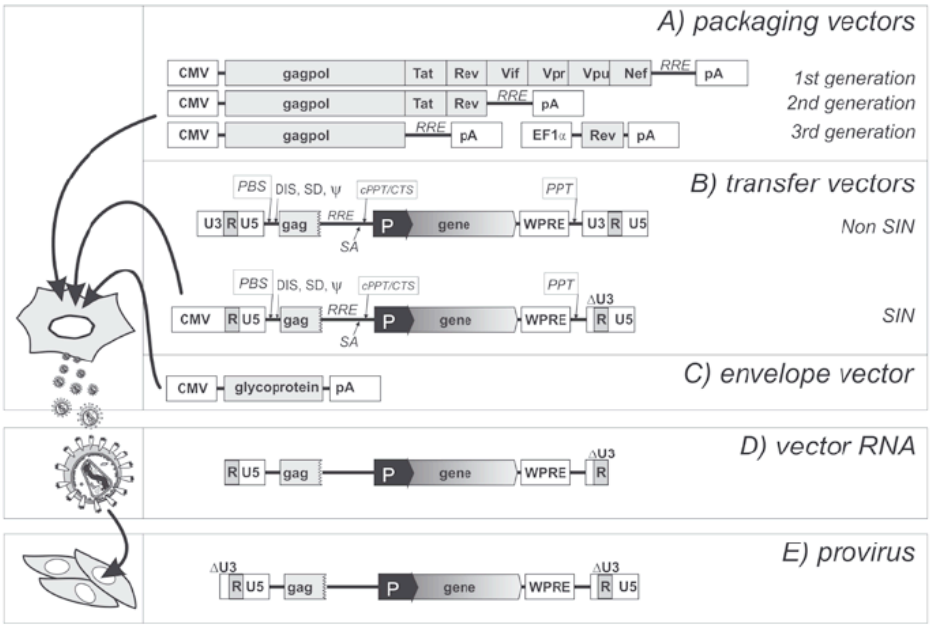

Figure 15: Vectors of lentivirus-based gene delivery systems: A–C: Packaging vectors, transfer vectors and the envelope vector are the plasmids utilized for transient transfection of a producer cell line (e.g. HEK 293T). **A**: Packaging vector plasmids: The original first-generation vectors contained all regulatory and accessory viral genes expressed from CMV promoter, while second-generation vectors encode only Tat and Rev proteins. The latest third-generation packaging systems are split onto of two plasmids: one encoding Gag and Gag-pol polyproteins, the second encoding the Rev protein. **B**: Transfer vector plasmids: In non-SIN (self-inactivating) vectors, viral RNA is expressed from intact 5' LTR. SIN vector have a deletion in U3 region (ΔU3), leading to an inactivation of the entire viral RNA after pro-virus integration. **C**: Envelope vector. Depending on the glycoprotein encoded by the vector, the virus is pseudotyped with different envelope proteins, enhancing the tropism of the virus. **D**: Vector genomic RNA: Co-transfection of either second-generation packaging vector or third-generation vectors in co-transfection with the SIN transfer vector and envelope vector leads to formation of viral particles that contain dimeric RNA bearing ΔU3 mutation. E: After stable provirus integration into host cell DNA, the transcription from the mutated 5' LTR (duplicated 3' ΔU3) is stopped. Abbreviations: CMV, cytomegalovirus immediate-early promoter; EF1α, human elongation factor 1-α promoter; gag, 5' portion of *gag* gene containing dimerization/packaging signals; PBS, primer binding site; DIS, dimerization signal; SD, splice donor site; SA, splice acceptor site; ψ, packaging signal; cPPT, central polypurine tract; CTS, central termination sequence; RRE, Rev response element; PPT, polypurine tract; pA, polyadenylation signal; ΔU3, SIN deletion in U3 region of 3' LTR; P, internal promoter for transgene expression; WPRE, woodchuck hepatitis virus (WHV) post-transcriptional regulatory element. Figure by Pluta et al. 2009 [69].

Packaging vector

All genes necessary for viral enzyme and structural protein expression for infectious particle formation are found on this vector. The *env* gene is missing, as well as the ones encoding the accessory proteins Vpu, Vpr, Nef and also the regulatory proteins Rev and Tat which used to be included on the packaging plasmids of the first generation of lentiviral vectors. Moreover, also the LTRs and ψ packaging sequences were eliminated [79], preventing full-length mRNA encoding *trans* elements from being packed into vector particles. RNA synthesis was driven by other viral promoters, usually CMV (cytomegalovirus) or RSV (Rous sarcoma virus) (instead of the LTRs), the polyA signal was taken from SV40 (simian virus) or the insulin gene. While *tat* is completely deleted on the final 3rd generation packaging vector, *rev* was placed on another vector. The function of Tat was substituted by modified 5' LTR enhancer promoter elements, which usually contain strong constitutive active RSV or CMV-derived promoters [80]. Astonishingly, all these manipulations did not affect vector production or infectivity much.

Transfer vector

This vector expresses full-length mRNA containing all *cis*-acting elements needed for the packaging, reverse transcription, nuclear import and integration of the cDNA into the host genome. Inserted in this vector is the transgene that should be delivered to the host cell and be stably integrated for long-term overexpression. This gene of interest is driven by an internal promoter, which usually resides between the 3' Tat/Rev SA site and the 3' LTR (see Fig. 15 B). Earlier transfer vectors still contained the tat sequence, Tat-independent transcription of the vector cassette was achieved by replacing the enhancer/promoter sequences in the 5'LTR with a strong promoter derived from CMV (see Fig. 15 B) [81]. These transfer vectors are an essential part of the 3rd generation packaging systems that lack Tat. Deleting the enhancer/promoter sequence in the 3' LTR has led to the creation of so-called self-inactivating (SIN) vectors (see Fig. 15 B [82] [83] [84]. When infecting host cells with viruses made from these transfer constructs,

this deletion is reproduced in the 5' LTR during the reverse transcription which leads to the transcriptional inactivation of the pro-virus (see Fig. 15 D, E). This SIN design also reduces the expression of full length transcripts for packaging, therefore the possibility of vector mobilization is minimized [85].

Envelope vector

The envelope vector is the third part of the 3rd generation lentiviral vector systems. It encodes the envelope glycoproteins (see Fig. 15 C). Since the original lentiviral *env* gene is deleted from the system, this additional vector expressing a heterologous glycoprotein is used for the virus production. As mentioned before, this technique is called pseudotyping, it increases the safety because the sequence homology with wild-type virus is reduced. Furthermore this broadens the tropism of the virus, a wider range of host cells can possibly be infected. Finally pseudotyping enhances the stability of the virus particle, which allows concentration with ultra-centrifugation and further long-term storage at very low temperatures [76] [78]. The most commonly used glycoprotein nowadays is the vesicular stomatitis virus-glycoprotein (VSV-G). Virions with this glycoprotein show excellent stability and infect virtually all mammalian and insect cells. In addition, the VSV-G facilitates virus entry via endocytosis, which reduces the requirement for viral accessory proteins, still ensuring full virus infectivity [86] [87]. So far, it remains unclear, which are the binding targets of the VSV-G on the host cell membrane.

One disadvantage of the production of VSV-G pseudotyped viruses is, that it can be toxic to some mammalian cells, if it is constitutively expressed [88]. The solution to this problem was found in using producer cell lines like HEK293T cells, which are transiently transfected with the 3 vectors (packaging, transfer and envelope vectors). These viruses are then used to transduce the host cells, but they will not be able to produce the virus themselves.

3.3.3 Tetracycline inducible expression using lentiviral gene delivery systems

Since one use of lentiviral gene delivery systems is the approach of gene therapy of human diseases, it is important that the expression of the gene of interest can be controlled within the host cell. Depending on what the protein is, it might be toxic if expressed in high amounts. One solution to this problem is the creation of tetracycline controlled lentiviral vector systems. These systems are fully prokaryotic, they use components of the *E. coli* Tet-resistance operon and are therefore not showing pleiotropic effects in eukaryotic host cells [89]. Tetracycline (tet) and its synthetic derivative Doxycycline (Dox) induce or inhibit expression of the gene of interest by controlling its tet-responsive promoter. They can be administered in the growth medium of cell *in vitro* or oral *in vivo* and are able to penetrate all tissues, including passage of the blood brain barrier. The Dox concentrations used to control gene expression are below the level of those needed for bacteriostatic function. Additionally it has a relatively short half-life, therefore gene expression responses are fast and can be reverted within short time [90]. The Dox response is dose-dependent.

The first tet-controlled expression system was a so-called Tet-off system, in which a Tet-controlled transactivator (tTA) binds the Tet-responsive element (TRE) and induces gene expression in the absence of Tet or Dox [91]. The TRE is made up of seven tandem copies of Tet operator (*tetO*) sequences and resides upstream of the CMV minimal promoter (TRE/CMV). tTA is a chimeric protein consisting of the bacterial Tet-repressor (tetR) fused to the HSV (herpes simplex virus) VP16 transactivation domain.

The Tet-on system uses a mutated version of the tTA, the reverse Tet-controlled transactivator (rtTA). The rtTA binds the *tetO* sequences in the TRE and only when Dox is administered the rtTA is sequestered away from the DNA allowing the transcriptional enzymes to access the promoter and start gene transcription (see Fig. 16) [92].

Both, the inducible transgene and the transactivator need to be present in the same cell. This is made possible by lentiviral vector delivery. The first lentiviral vectors used were Tet-off systems [94] [95] [96]. Up to 500-fold induction of gene expression over background was observed, but the background levels in the un-repressed state were unacceptably high. Another drawback of this system is, that in a clinical setting, the patient must be under constant medication with Dox, to not express the transgene at all times. To overcome this disadvantage, the first lentiviral Tet-on systems were tested, continually optimized to finally lead to the development of the Tet-on system using a fusion protein of rtTAKRAB to suppress gene expression in the absence of Dox. The Krüppel-associated box (KRAB) protein domain of human KOX1, is a Krüppeltype zinc finger factor [97]. It is a transcriptional repression module, suppressing the polymerase II and polymerase III mediated transcription stretching over a distance of 2-3kb from its DNA binding site (see Fig. 17). This might be mediated via formation of heterochromatin [98]. Therefore the repression of transcription mediated by the fusion protein of KRAB with rtTA is not only drug dependent but also exerts its effects on an additional epigenetic level.

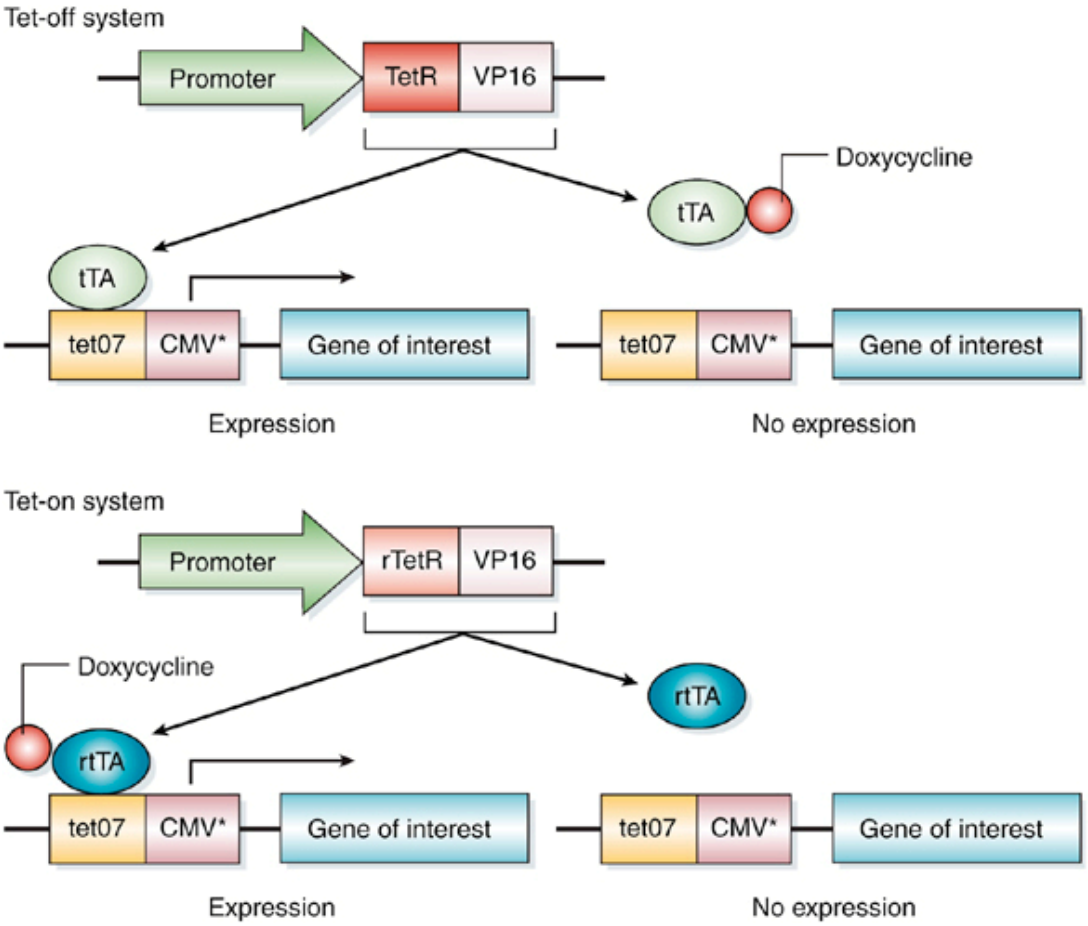

Figure 16: Doxycycline-regulated gene expression. Shown is a tet-off system, where the chimeric tetracycline transactivator protein (tTA) consists of the TetR domain that recognizes the tetO fused to the VP16 transactivating domain of herpes simplex virus. tTA binds to seven *tetO* domains (*tetO7*) connected to a minimally active CMV promoter (CMV*), allowing transcriptional induction of the gene of interest. Doxycycline binds the tTA and prevents gene activation. In the tet-on system, TetR is mutated to rTetR (rtTA). Here the gene of interest can only be transcribed if Dox is present in the system, so that it can bind to the *tetO7* and activate gene expression. Scheme by Kafri et al. 2000 [93].

Figure 17: Lentiviral vector construct expressing the Dox-responsive fusion protein tTR-KRAB and dsRed II as a fluorescence marker. Scheme by Wiznerowicz et. al 2003. [99]

In the lentiviral vector system developed by Trono et al. (Lausanne, Switzerland), the rtTA (or herein tTR: tet-Trans-Repressor) fused to the KRAB protein is expressed on one vector, while the gene of interest is on another transfer vector, also containing the TRE (pLV-T, unpublished vector).

The KRABtTR fusion protein is expressed from the ubiquitously active EF1-α promoter as part of a bicistronic transcript (that also produces the dsRed II marker) and modulates transcription from an integrated promoter that is next to the *tet* operator (*tetO*) sequences. Both the gene of interest and the *tetO* are on a second vector called pLV-T (unpublished vector, also see methods section 4.2.). When both vectors are delivered to the host cell, the tTR-KRAB fusion protein inhibits expression of the marker gene in the absence of Dox by binding to the *tetO* sequences upstream of the maker gene. Cells that express the transrepressor should have a red fluorescence (ds RedII). Adding Dox to the cell medium allows binding of the drug to the tTR portion of the transcriptional repressor, sequestering it away from the DNA and allowing the transcription machinery to access the promoter [99] (See Fig. 18, depicted is the one vector system, where tTR-KRAB and the gene of interest are on the same vector).

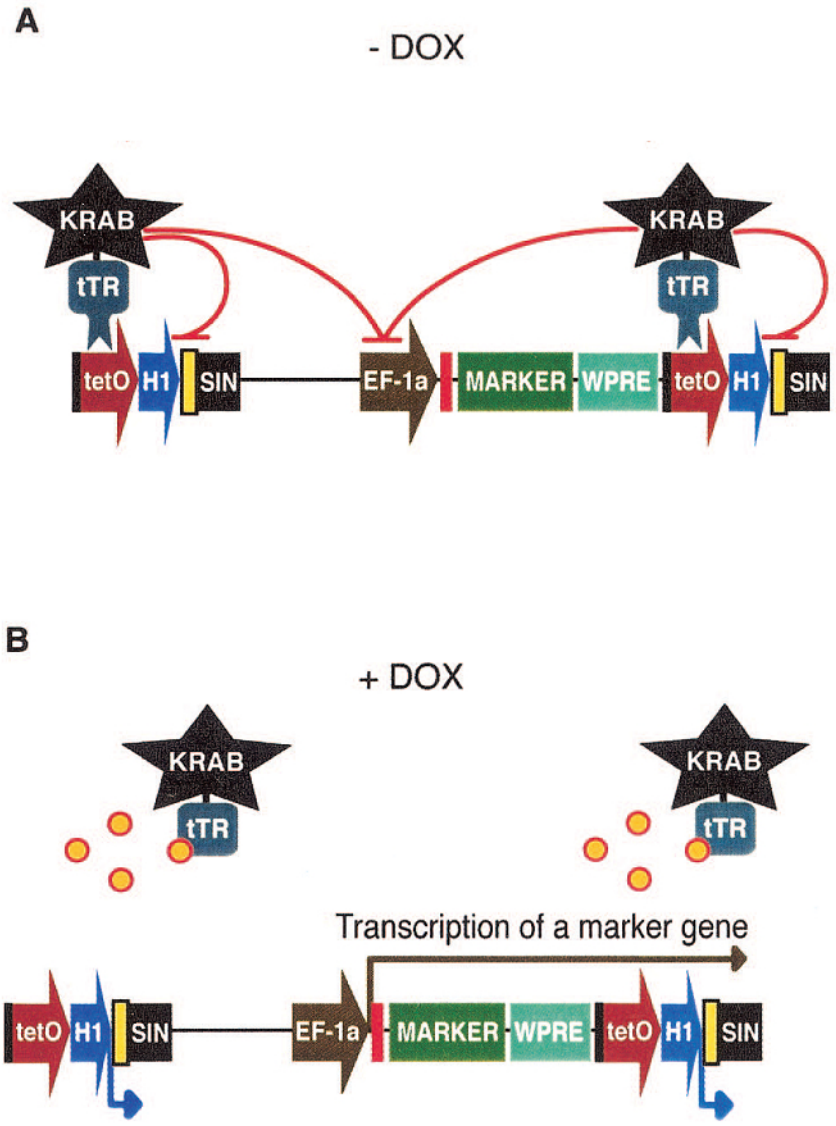

Figure 18: Mechanism of Doxycycline inducible expression of a target gene. Shown is the one vector system, where both tTR-KRAB and the marker gene lie on one vector only. (A) In the absence of DOX, tTR-KRAB binds to the *tetO* and suppresses transcription of a target gene (Marker) (B) In the presence of DOX, tTR-KRAB cannot bind to the *tetO*, allowing transcription and expression of the target gene [99]. H1: human H1 promoter (mtDNA), *tetO*: Tet: Operator, SIN: self-inactivation domain, EF-1α: ubiquitously active elongation factor 1-α promoter. WPRE: Woodchuck hepatitis virus posttranscriptional regulatory element: enhancer of transcription of the marker gene in the host cell. Scheme taken from Wiznerowicz et. al 2003 [99].

4 Materials and methods

4.1 Cell lines

mpkCCD$_{Cl14}$ is an immortalized mouse cortical collecting duct cell line that was originally described by Bens et al. in 1999 [100]. For maintenance of the culture and for lentiviral transductions, cells were seeded into plastic dishes (Corning Costar) in standard medium (DMEM:Ham's F12 without phenolred, 1:1 vol/vol Invitrogen; 60 nM Na^+-selenate, 5 mg/ml Apo-Transferrine, 2 mM glutamine, 50 nM dexamethasone, 1 nM triiodothyronine, 10 ng/ml epidermal growth factor, 5 mg/ml insulin, 20 mM D-Glucose, 2% fetal calf serum (FCS Amimed #2-01F10-I, Lot A127772P, Bioconcept, Allschwil, Switzerland) and 20 mM Hepes pH 7.4) and incubated at 37°C in 5% CO_2 / 95% air. For fluorescence stainings, western blot analysis and electrophysiological experiments in Ussing chamber, cells were cultured on 12 mm diameter snapwell permeable filter supports (polycarbonate membrane, Corning Costar #3107) for 5 days in standard medium, 5 days in filter medium (standard medium without FCS, Apo-Transferrine and EGF) and starved 1 day in DMEM: Ham's F12 1:1 vol/vol only.

mCCD$_{Cl1}$ cells were originally described by Gaeggeler et al. [101]. They are another immortalized mouse kidney cortical collecting duct cell line. Unlinke the mpkCCD$_{Cl14}$ cells, the mCCD$_{Cl1}$ cells do express the mineralocorticoid receptor. We obtained mCCD$_{Cl1}$ cells as well as a newer clone 6 from the lab of Prof. Dr. Olivier Staub in Lausanne. The mCCD$_{Cl6}$ has shown more stable properties in terms of transepithelial transport measurements over several passages compared to its predecessor clone 1. They were grown 5 days in complete medium DMEM/Ham's F12 (1:1 vol/vol) (Invitrogen, Switzerland), 5 mg/ml insulin, 5 mg/ml Apo-Transferrine, EGF 10 ng/ml, 60 nM Na^+-selenate, 1 nM triiodothyronine, 50 nM dexamethasone at 37°C/5% CO_2, then 5 days in filter medium (same as complete medium except 3 nM dexamethasone and no EGF, Apo-Transferrine and FCS). Cells were starved overnight in minimal medium

(DMEM F12 (1:1 vol/vol) only) and then used for the experiments.

Human embryonic kidney cells (HEK293T) were kindly provided by the lab of Prof. Dr. Daniel Schümperli, University of Berne and grown in plastic culture dishes (Corning Costar) in DMEM (Invitrogen Cat no. 41965-039), 10% FCS (heat inactivated), 1% NEAA and 4 mM L-glutamine at 37°C / 5% CO_2.

4.2 Cloning of ATF3 into lentiviral constructs and lentiviral transduction of mpkCCD$_{Cl14}$ cell lines

Mouse total kidney RNA was isolated with the Qiagen RNeasy Mini Kit, according to the manufacturer's protocol (Qiagen, Hombrechtikon, Switzerland). Reverse transcription was performed with oligo dT primers using the TaqMan Reverse Transcription Kit (Applied Biosystems, Foster City, USA). cDNA of ATF3 was amplified by PCR using 2.5 U of a proof reading polymerase (Pfu) (Promega, Madison, USA), 1x Pfu-reaction buffer (Promega), 2 mM dNTPs, 0.5 µM 5'-forward-primer, 0.5 µM 3'-reverse-primer for 35 cycles (5 min 95°C, then cycles: 30 sec 95°C, 30 sec 64°C, 2 min 68°C, then finishing with 10 min 68°C, o/n 4°C). Primers for cloning ATF3 were designed to contain restriction enzyme sites for subsequent digestion of PCR product and vector for ligation.

Primers:

ATF3 fwd with BamHI restriction site: 5 - AAA AGG ATC CTG GAG CCA ATC GGC TAA C - 3'

ATF3 rev with XmaI restriction site: 5' - AAA CCC GGG GAG TGG GAC AAT GCA GTA GG - 3'

The ATF3 PCR-product was cloned into the pLV-T vector, containing a Tet operator (*tetO*) (unpublished vector). All vectors needed to produce lentiviruses

of this Tet-on system were obtained from the Tronolab EPFL Lausanne [99]. Briefly, this inducible overexpression system relies on a tetracycline-controlled hybrid protein called tTR-KRAB. tTR is the tetracycline repressor with a DNA binding domain from *Escherichia coli Tn10* which is fused to the human KRAB domain which is an epigenetic transcriptional repressor (see Fig. 19).

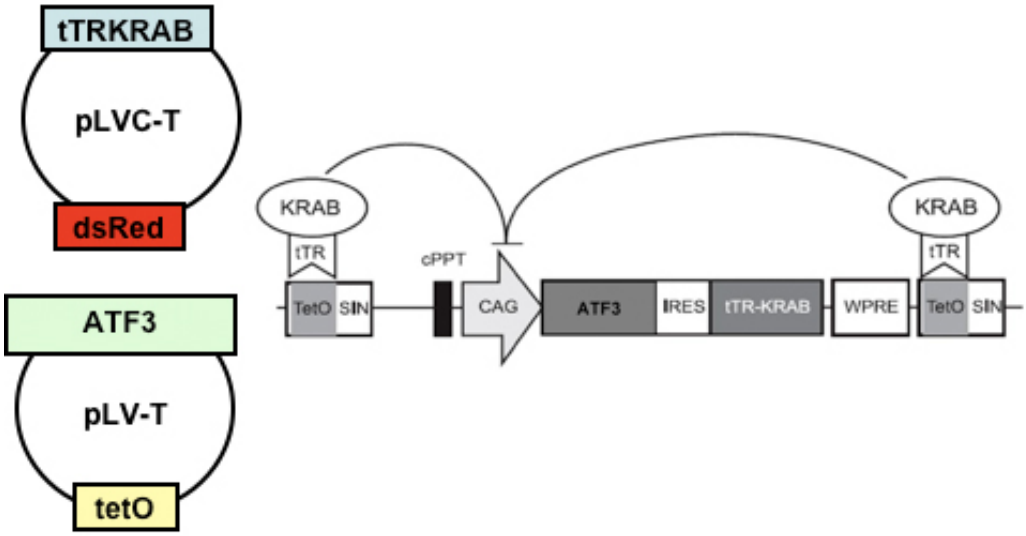

Figure 19: The lentiviral Tet-On vector system from the Tronolab, EPFL Lausanne: The KRABtTR fusion protein is expressed from the ubiquitously active EF1-α promoter as part of a bicistronic transcript (that also produces the dsRed marker) and modulates transcription from an integrated promoter that is next to the tet operator (*tetO*) sequences. ATF3 was cloned downstream of the *tetO*. Two lentiviruses based on the human immunodeficiency virus type 1 were used as delivery vehicles for the two vectors (pLVCT-tTRKRAB-dsRed and pLV-T-ATF3). When cells were grown with no Dox in the medium, ATF3 expression was suppressed. Upon addition of 1 mg/ml Dox to the cell culture medium, the tTR binds the Dox and is sequestered away from the promoter, ATF3 or a GFP control are expressed within 3 days (see Fig. 18). Figure modified from Wiznerowicz et. al 2003 [99].

Protocol of virus production:

All vectors needed for the following lentivirus production protocol were constructed in the Tronolab (Prof. Dr. Daniel Trono, EPFL Lausanne) and obtained either via Addgene (www.addgene.org) or in the case of pLV-T from the Lab of

Prof. Dr. Schümperli, University of Berne. The vectors were amplified using HB101 *E.coli* cells for subsequent Maxipreps of the constructs (with Qiagen Maxi Kit, Endonuclease free Cat.no. 12362l). Human embryonic kidney cells (HEK293T) were grown in DMEM with 10% fetal calf serum, 1% NEAA and 4 mM L-glutamine seeded at 6 x 106 cells per 10 cm dish. On the following day, they were co-transfected with the packaging plasmid pMDG.2 (5 µg), the envelope plasmid pCMVΔR8.91 (10 µg) and the vector with the gene of interest either, pLV-T ATF3, pLV-T-EGFP or pLVCT-tTRKRAB-dsRed (15 µg) using the calcium phosphate DNA precipitation method. Corresponding amounts of plasmids were mixed and volume was added up to 450 µl with 0.1 TE pH 8.8, add 50 µl of $CaCl_2$ and 500 µl of 2x HBS, mixed well and let complex for 20 min at room temperature. The precipitates were added dropwise to the cells and cells incubated with the virus overnight at 37°C / 5% CO_2. The medium was changed the next day and left on the cells for 3 days. On the second day the target cells, in this case $mpkCCD_{Cl14}$ were seeded at 1x105 cells into 6-well plates. On the third day the virus supernatant of the HEK293T cells was centrifuged at 1000 rpm for 5 min at 4°C, then filtered through a 0.22 µm filter and polybrene was added to a final concentration of 4 µg/well. 1 ml of virus was applied to the $mpkCCD_{Cl14}$ cells and 1 ml of mpkCCD complete medium was added. Cells were incubated overnight at 37°C / 5% CO_2. The next day the medium was completely replaced with mpkCCD complete medium.

$mpkCCD_{Cl14}$ cells were first transduced with the pLVCT-tTRKRAB vector and checked for red fluorescence. Subsequently a second virus transduction with the pLV-TATF3 or as a control pLV-T-EGFP construct was performed. These cells were then subjected to limiting dilution in 96-well plates, where cells were seeded at very low density of 0.5 cells, 1 cell or 2 cells per well. These clones were observed for 2 weeks; wells with only 1 cell population growing were selected and transferred to bigger growth areas. Finally, the clones were functionally tested for their inducible and long-term stable expression of ATF3 or GFP.

4.3 Western blot of ATF3 overexpressing mpkCCD$_{Cl14}$ cells

mpkCCD$_{Cl14}$ ATF3/KRAB transduced cells were grown in 6-well plastic plates and harvested after 3 days of 1 mg/ml Doxycycline induction. 100 µl RIPA buffer (150 mM NaCl, 1% Igepal (NP40), 0.5% DOC, 0.1% SDS, 50 mM Tris pH 7.5, protease inhibitor cocktail PIC, Sigma) by scraping them off the plastic and sonicating the samples for 30 seconds. Cell debris was pelleted with centrifugation at 100 x g for 10 min. Protein concentration of the samples was determined using the Bradford protein assay (Biorad 500-0113, 500-0114, 500-0115) to ensure equal protein amount loading. Samples were diluted in 4x loading buffer (4x SDS 8%, Tris-HCl 200 mM pH 6.8, 40% Glycerol, 0.4% Bromphenolblue) with 10% β-Mercaptoethanol. 20-40 µg were loaded on a 12% polyacrylamide gel, separated by SDS-PAGE and electrophoretically transferred to a PVDF-membrane (Immobilon-P, Millipore, USA). After blocking with 5% low-fat milk powder in Tris buffered saline / 0.1%-Triton (TBS-T) for 1 h at room temperature, the blots were incubated with primary antibodies rabbit-anti-mouse ATF3 (ATF3 C-19, sc-188 rabbit polyclonal IgG, Santa Cruz) diluted 1:500 in 2.5% milk-TBS-T over night (o/n) at 4°C. After washing the blot with TBS-T, it was incubated with secondary antibody diluted 1:1000 (donkey-anti rabbit conjugated with horseradish peroxidase, BD transduction laboratories, Franklin Lakes, USA) in 2.5% milk-TBS-T for 1 h at room temperature. Antibody binding was detected with the Immobilon Western Chemiluminescent HRP Substrate (Millipore, USA) and visualized with a DIANA III camera (Raytest, Straubenhardt, Germany). Images were further processed using Photoshop 7 (Adobe, San Jose, USA).

4.4 Immunofluorescence staining of ATF3 overexpressing mpkCCD$_{Cl14}$ cells

mpkCCD$_{Cl14}$ ATF3/KRAB transduced cells were grown on glass coverslips and stained after 3 days of 1 µg/ml Dox induction. Cells were washed with PBS and fixed with 3% paraformaldehyde (PFA). After 15 min of blocking with 2% BSA / 0.2% Triton-X100, cells were incubated at 4°C o/n with primary antibody against ATF3 diluted 1:500 in 2% BSA / 0.2% Triton-X100. After washing, cells were incubated 1 h at room temperature with conjugated secondary antibody (Alexa Fluor 488 goat-anti-rabbit IgG, Invitrogen, USA) diluted 1:1000 in 2% BSA/0.2% Triton-X100. Images were acquired using the Nikon Eclipse TE3000 inverted fluorescence microscope (Nikon AG Küsnacht, Switzerland) equipped with a DS-5M Standard CCD camera (Nikon) and the NIS-Elements software (Nikon). Images were further processed using Photoshop 7 (Adobe, San Jose, USA).

4.5 Transepithelial electrophysiological measurements

The transepithelial electrical resistance across intact monolayers of mpkCCD$_{Cl14}$ WT or ATF3 transduced cells grown on permeable filter membranes was measured using an EVOHM device (World Precision Instruments, Sarasota, Florida, USA). A transepithelial resistance of >1 kΩ was considered as a perquisite for using the filter cultures for subsequent electrophysiological measurements in an Ussing chamber set-up [102] [103]. 200'000 cells per filter (1 cm^2 area) were grown for 11 day as mentioned earlier (see 4.1.). On the day of the experiment, filters were carefully mounted in a multichannel current clamp device of an Ussing chamber (Model VCC MCC Revision B, Physiological Instruments) and monolayers maintained under current clamp conditions at a DC clamp level of 0 µA. Bipolar pulses of 5 µA lasting 620 ms were given every 60 sec. Cells were allowed to equilibrate to the given circumstances in the chamber (37°C,

continuous bubbling with 5% CO_2 / 95% O_2 bubbling to maintain stable pH) for 1 hour. Aldosterone was then applied to the media in the chamber (300 mM - 1 µM) currents were further traced for 2 hours. After this, optionally 10 nM arginine-vasopressin (AVP) was added to the medium and currents were traced for another 30 min. To finish, Na^+ currents mediated via ENaC were specifically blocked using 10 µM amiloride.

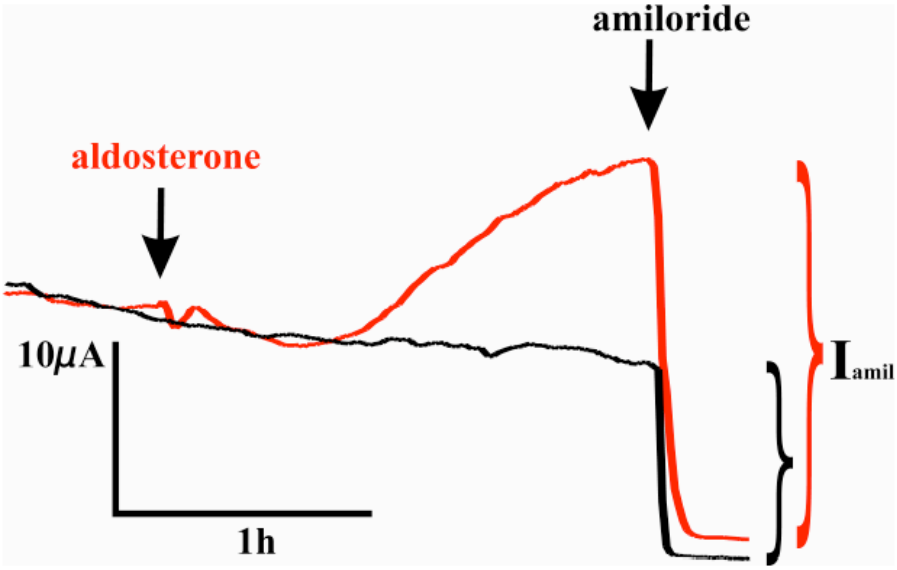

Figure 20: Original transepithelial current trace using an Ussing chamber system: mpkCCD$_{Cl14}$ cells were grown on permeable filter membranes and treated with aldosterone 300 µM (red) in the Ussing chamber set-up. After 150 min amiloride (10 nM) was added to the medium in the chambers to block ENaC mediated current. In parallel, another filter with cells was mounted and treated with the vehicle as control (black). Amiloride sensitive current (Iamil) is significantly higher in aldosterone treated cells. This trace is missing the optional AVP addition after aldosterone incubation. Figure taken from PhD Thesis of Dr. Gabriele Adam. [104].

4.6 Western blot of MAPK p38, JNK/SAPK1 and ERK1/2

$mCCD_{Cl6}$ cells were grown on filter supports as described in 4.1. To check for MAPK phosphorylation induced by a medium change the cells were serum and growth factor starved overnight. Then the cells underwent different medium changes: (1) A mock change, where the medium was aspirated and the same medium was added back to the cells immediately, (2) a medium change where the old medium was replaced by fresh minimal medium that was pre-warmed in a tube, (3) a medium change where the old medium was replaced by fresh medium that was CO_2-equilibrated and pre-warmed in the incubator, and (4) a conditioned medium change where the medium was taken from one well of cells and put onto another. All cells were lysed seven min after the medium change took place. The lysis buffer contained 10 mM Tris in HCl pH 7.4, 1% SDS, 1x protease Inhibitor Cocktail (Sigma), 1 mM Na Orthovanadate and 1x Phosstop (Roche) to stop dephosphorylation of the proteins. Samples were sonicated, 4x Laemmli buffer with 10% β-Mercaptoethanol added and cooked for 3 min at 95 °C. Approximately 5 µg were loaded on a 10% SDS-Polyacrylamidgel and transferred onto a PVDF membrane after running the gel. For the transfer a semi-dry blotter was used to ensure equal transfer also on the sides of the membrane. Transfer was 45 min at 25 V. The total- and phosphospecific mouse antibodies against JNK/SAPK1, p38 and ERK1/2 were from the MAPK sampler kit (BD Pharmingen 612544):

Antibody	Cat#	Isotype	MW	WB	IP	IF	IH	Human	Dog	Rat	Mouse	Chick	Control	Dilution
ERK1	610030	IgG1	44/42	+	den	+	+	+	+	+	+	+	Rat Cerebrum	1:4000
ERK1/2 (pT202/pY204)	612358	IgG1	44/42	+		+		+		+	+		A431+EGF	1:1000
pan-JNK/SAPK1	610627	IgG1	49	+	-	+	+	+	+	+	+	+	PC12	1:250
JNK (pT183/pY185)	612540	IgG1	43/56	+				+		+	+		HeLa+Anisomycin	1:250
p38a/SAPK2a	612168	IgG1	42	+		+		+	+	+	+		Jurkat	1:5000
p38 MAPK	612280	IgG1	42	+		+		+		+	+		HeLa+Anisomycin	1:2500

Table 2: Table taken from Technical Data Sheet MAPK sampler Kit 612544 BD Pharmingen.

Membranes where phosphospecific antibodies were used to detect the MAPK were blocked with 2% Topblock in TBS-0.1% Triton for 1h, while membranes for total

MAPK detection were blocked with 5% non-fat dry milk in TBS-0.1% Triton. Antibodies were diluted according to the table above either in 1% Topblock in TBS-0.1% Tween for the phosphospecific antibodies or in 2.5% non-fat dry milk in TBS-0.1% Tween. All primary antibodies were incubated overnight at 4°C. Secondary anti-mouse AP antibody was diluted 1:5000, incubated at RT for 1 h and developed with AP chemiluminescence substrate (Millipore Cat. No. WBKDS0100). For actin detection, membranes were washed thoroughly with TBS-Tween 0.1%, stripped with a low pH stripping buffer (1% SDS/Glycine, pH 2) for 10 min, washed again and incubated with anti-mouse-β-actin antibody 1:5000 (Sigma) in 2.5% non-fat dry milk in TBS-0.1% Tween at RT for 1h. Secondary anti-mouse-HRP antibody 1:5000 was diluted in 2.5% non-fat dry milk in TBS-0.1% Tween and applied for 1h RT. Membranes were developed using HRP chemiluminescence substrate (Millipore Cat. No. WBKLS0500).

4.7 ATF3 knockout mouse

The ATF3 knockout mouse (C57BL/6 background) was kindly provided by Prof. Dr. Tsonwin Hai, USA [105]. Wildtype C57BL/6 (Harlan Animal Laboratories, Holland), and ATF3 knockout mice were housed in standard conditions and fed a standard diet. Pups from ATF3 knockout breedings were weaned at 28 days as opposed to the common weaning of wildtype mice after 21 days (T. Hai, personnel communication). All procedures for mouse handling and housing were conducted according to the Swiss Animal Welfare laws and approved by the Kantonales Veterinäramt Zürich.

ATF3 knockout mouse genotyping

The genotyping protocol was obtained from the lab of Prof. Dr. Tsonwin Hai.

Primers:

186 AGA GCT TCA GCA ATG GTT TGC

187 TGA AGA AGG TAA ACA CAC CGT G

188 ATC AGC AGC CTC TGT TCC AC

Primers (100 µM) were mixed in a ratio of 10:5:5 of #186, #187, and #188 respectively. 2 µl template mouse tail DNA was mixed with 2 µl 10x Eurobio Taq buffer, 1 µl $MgCl_2$ (25 mM), 0.4 µl dNTPs 2 µl primer mix, 9.6 µl mili-Q H_2 and 1 µl Eurobio Taq for 1 PCR reaction. PCR program: 1. 94°C 4min, 2. 94°C 30 sec, 3. 57°C 30 sec, 4. 72°C 30 sec, 5. 72°C 10 min, 4°C o/n. The wildtype band: 329 bp, knockout band: 236 bp.

4.8 B1EGFP mouse

The B1EGFP mixed background mouse (C57BL/6 x CBA) specifically expresses EGFP under the promoter of the V-ATPase B1 subunit. Therefore EGFP is specifically expressed in tissues expressing V-ATPase, namely the kidney, the male reproductive tract, and the lung (nonciliated airway cells). In the kidney tubule EGFP is specifically expressed in intercalated cells of the collecting duct and connecting tubule [106]. This allows sorting of green fluorescent tubules with COPAS (complex object parametric analyzer and sorter, see 4.12.) and subsequent RNA and protein extraction from the tubule material (see Unionbio webpage for COPAS).

B1EGFP mouse genotyping

Primers:

Fw B1-EGFP 5‘ - CCC TCT TCC CTT CTC CCT CCA - 3‘
Rev B1-EGFP 5‘ - CGC TGA ACT TGT GGC CGT TT - 3‘

The PCR reaction of 25 µl final volume was composed as follows: 2.5 µl 10x PCR Buffer with $MgCl_2$ (Sigma), 1.0 µl 10 mM dNTP Mix, 0.75 µl 10 µM fwd primer, 0.75 µl 10 µM rev primer, 0.2 µl Taq Polymerase 5 U/µl (Sigma D1806), 17.8 µl H_2 and 2 µl of genomic DNA extracted from mouse tails. Expected amplicon size: 366 bp.

PCR Cycling Conditions:

1. 94°C 5 min; 2. 94°C 30 sec; 3. 65°C 30 sec; 4. 72°C 1 min ; back to step 2 for 10 cycles, 5. 95°C 30 sec; 6. 60°C 30 sec; 7. 72°C 1 min 45 sec; back to step 5 for 10 cycles; 8. 95°C 30 sec; 9. 55°C 30 sec; 10. 72°C 1 min 45 sec; back to step 8 for 30 cycles; 11. 72°C 5 min; 12. 4°C pause. The B1EGFP WT mouse was further bred with the ATF3 KO mouse to generate the ATF3 KO B1EGFP mouse. This mouse is a complete ATF3 knockout, the GFP expression allows to analyze the effect of ATF3 lack specifically on gene expression in the CNT/CCD (see section 4.12. COPAS).

4.9 Metabolic cages

11-week-old wildtype C57BL/6 mice and ATF3 knockout mice were adapted to metabolic cages (Tecniplast, Buguggiate, Italy) for two times two days with breaks

in normal cages in between (see Fig. 21). Animals had free access to standard mouse diet (18.5% crude protein, Kliba-Nafag, Kaiseraugst, Switzerland) and drinking water. Daily food/water intake, urine/feces output and body weights were measured.

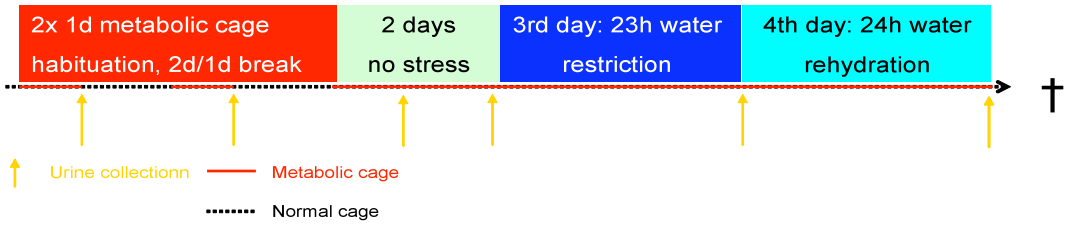

Figure 21: Protocol of metabolic cage experiment comparing ATF3 KO mice to wildtype mice.

4.10 Mouse perfusion

Mice were anesthetized either with isofluorane or via i.p. injection with ketamine (90 mg/kg body weight, Narketan 10, Vétoquinol, Lure, France) and xylazine (10 mg/kg body weight, Xylazin, Streuli, Uznach, Switzerland) and perfused through the left cardiac ventricle with phosphate buffered saline (PBS, pH 7.4) followed by a buffered paraformaldehyde solution (4%, pH7) as previously described [107]. The kidneys were then harvested, the capsule was removed and the organs were snapfrozen in liquid nitrogen for subsequent RNA or protein extraction.

4.11 Real-Time RT-PCR

100 ng of total RNA extracted with the RNeasy Kit (Qiagen) either from mouse kidney, brain, heart, colon mucosa cells (from mice perfused with PBS, see above section 4.9.), $mCCD_{Cl6}$ cell cultures or extracted with the RNAequous kit

(Ambion) for COPAS sorted kidney tubules were used for reverse transcription using the TaqMan® Reverse Transcription Kit (Applied Biosystems). Real-time PCR was performed using the SYBR®Green JumpStart™ Taq ReadyMix™ (SIGMA) with 1 ng (for COPAS study see Methods 4.11.) or 2 ng (for whole organ and cell culture specific expression studies) of cDNA per reaction.

Primers:

Mouse ATF3 fwd	5' - AGA CCC CTG GAG ATG TCA GTC A - 3'
Mouse ATF3 rev	5' - CGC CTC CTT TTC CTC TCA TCT T - 3'
Mouse SGK1 fwd	5' - GAG GGA GCG CTG CTT CCT - 3'
Mouse SGK1 rev	5' - GCA GAT AGC CCA GGG CAC T - 3'
Mouse ATF4 fwd	5' - CTC GGC CCA AAC CTT ATG - 3'
Mouse ATF4 rev	5' - CTT CTA TCA GGT CTT TCA GAT ACT - 3'
Mouse CHOP10 fwd	5' - AGC TGG AAG CCT GGT ATG AGG - 3'
Mouse CHOP10 rev	5' - AGC TGG AAG CCT GGT ATG AGG - 3'
Mouse αENac fwd	5' - GGT GCA CGG GGA TGA G - 3'
Mouse αENac fwd	5' - TAG TTG CCT CCG AGG CTT TC - 3'
Mouse NaPi2a fwd	5' - TGA TCA CCA GCA TTG CCG - 3'
Mouse NaPi2a rev	5' - GTG TTT GCA AGC TGC CCG - 3'
Mouse AQP2 fwd	5' - TGG TGC TGT GCA TCT TTTG CCT - 3'
Mouse AQP2 rev	5' - ACT TGC CAG TGA CAA CTG CTG - 3'
Mouse NCC fwd	5' - ACA TCT GCT GGA AGG TGG AC - 3'
Mouse NCC rev	5' - TGA CCT GCA TTC ATT CCT CA - 3'
Mouse HPRT fwd	5' - TTA TCA GAC TGA AGA GCT ACT GTA ATG ATC - 3'
Mouse HPRT rev	5' - TTA CCA GTG TCA ATT ATA TCT TCA ACA ATC - 3'
Mouse β-Actin fwd	5' - CCA CCG ATC CAC ACA GAG - 3'
Mouse β-Actin rev	5' - GAC AGG ATG CAG AAG GAG - 3'

PCR cycling protocol:

1. 95° C 2 min; 2. 95°C 3 sec, 60 °C 30 sec, repeat 40 times; 3. Dissociation curve step: 95°C 15 sec, 60°C 1 min, 95°C 15 sec, 60 °C 15 sec

The expression of the mRNA of genes of interest was calculated relative to Hypoxanthine Guanine Phosphoribosyltransferase (HPRT) or β-Actin as reference genes. Relative expression ratios were estimated as $R = (2^{(Ct(reference) - Ct(test))}$. Ct: cycle number at the threshold, test : tested mRNAs (e.g. ATF3).

4.12 COPAS

As described in 4.8. we used WT B1EGFP mice to sort green fluorescent CNT/CCD tubules to analyze gene expression in these kidney segments (referred to as the ASDN). 2 groups of mice were analyzed: 4 non-injected WT B1EGFP C57BL/6 mice (1 female, 3 males) versus 4 WT B1EGFP mice (2 females, 2 males) that were injected for 1 h with 0.9%Na-Cl / 0.3% EtOH-injected. Additionally we also sorted green fluorescent tubules of 4 non-injected ATF3 KO B1EGFP C57BL/6 mice (2 females, 2 males), to see if a lack of ATF3 might make a difference on upstream and downstream factors when compared to the WT mice.

Mice were perfused through the left cardiac ventricle first with 10 ml PBS (room temperature) and afterwards with 10 ml of a mix containing 1 mg / 10 ml DNAse I (Sigma DN25), 10 mg /10 ml Collagenase Type-1 (Worthington 4196) and 10 mg / 10 ml Hyaluronidase (Sigma H3884) in cold KREBS buffer. The kidneys were removed from the mice and the cortex was dissected with razor blades for further processing. The cortex was minced with the razorblade and digested for 10 min, 5 min and finally 2 min in 10 ml of the digestion enzyme mix at 37°C with vortexing in between the incubation times. Afterwards the digestion mix was sieved through a 212 µm and a 250 µm sieve (coated with 5% BSA-KREBS), then filtered through a 100 µm nylon filter (Cell restrainer, BD Falcon 352340) and a 40 µm filter (Cell restrainer, BD Falcon 252360). The remains left on the 40 µm nylon filters were flushed off with cold KREBS buffer and diluted to yield 50 ml of sorting material. From this tubule suspension, a

green fluorescent fraction of tubules, a GFP-negative selected fraction (whole kidney cortex without CNT/CCD) and a fraction containing the whole kidney cortex were sorted using a COPAS (complex object parametric analyzer and sorter, Unionbio). 800 tubules per tube were sorted, for each mouse between 2400 and 4000 tubules of the different kidney fractions were sorted. To sort one sample cup of tubule suspension it took between 5-8 min. During this time the sample was not cooled. The tubule suspension and the samples that were already sorted were kept on ice. Sorting the tubules of 2 kidneys from each mouse took about 8 h. The samples were kept on ice during the sort and centrifuged at 800 rcf for 5 min at 4°C to pellet the tubules. 800 tubules per sample were lysed either in 50 µl of RNA lysis buffer from the RNAequous micro kit (Ambion, Cat. No. AM1931) or 20 µl of protein lysis buffer (10 mM Tris in HCl pH 7.4, 1% SDS, 1x protease Inhibitor Cocktail (Sigma), 1 mM Na Orthovanadate with 1x Laemmli buffer, and 10% β-Mercaptoethanol. 400 tubules per lane were used for Western Blot. ATF3 was detected using the polyclonal antibody mentioned in 4.4. AQP2 was detected using a polyclonal rabbit antibody (kindly provided by Prof. Johannes Loffing) 1:5000 in 2.5% milk-TBS-Triton. Total RNA of the tubules lysed in RNA lysis buffer was extracted using the Ambion RNAequous micro RNA kit, yielding 20 µl of RNA per sample. Total RNA was reverse transcribed and qPCR was performed following the procedure described in section 4.11. To ensure that the green fluorescent tubules sorted were truly CNT/CCD, qPCR was performed for NaPi2a (proximal tubule), NCC (TAL), AQP2 (CCD), ?ENaC (CCD) and SGK1 (mostly ASDN). Gene expression in GFP-positive sorted fractions was compared to GFP-negative sorted fractions (whole kidney cortex without the green fluorescent tubules) and whole kidney cortex fraction of all mice. Also the relative mRNA expression of ATF4 (upstream of ATF3), ATF3 and CHOP (downstream of ATF3) was analyzed in all 3 fractions sorted for the 3 groups of mice (WT B1EGFP non-injected, WT B1EGFP injected 1 h 0.9% NaCl / 0.3% EtOH and ATF3 KO B1EGFP non-injected).

KREBS buffer

Powder		**for 1 l**	**for 2 l**	**for 5 l**
NaCl (58.5 g/mol)	145 mM	8.45 g	13 g	42.5 g
HEPES (238.3 g/mol)	10 mM	2.38 g	4.8 g	11.9 g
KCl (74.5 g/mol)	5 mM	0.37 g	0.75 g	1.86 g
NaH_2PO_4*1 H_2O(138 g/mol)	1 mM	0.14 g	0.28 g	0.69 g
$CaCl_2$ (147 g/mol)	2.5 mM)	0.37 g)	0.74 g)	1.84 g
$MgSO_4$ (246.5 g/mol)	1.8 mM	0.44 g	0.89 g	2.22 g
Glucose (180.1 g/mol)	5 mM	0.9 g	1.8 g	4.5 g

All chemicals used for KREBS buffer obtained from Sigma Aldrich.

4.13 Statistics

Data were expressed as means ± standard error of the mean (SEM). Calculations were carried out with Microsoft Excel, while the graphs were created using GraphPad Prism™ Version 5.0 (GraphPad Inc.). Significance was tested with GraphPad Prism™ using students T-Test unpaired) or one-way ANOVA, as indicated. Statistical significance was accepted at $P < 0.05$.

5 Results

5.1 Regulation and impact of ATF3 expression in kidney CCD cell lines

5.1.1 Aldosterone stimulates ATF3 expression in mpkCCD$_{Cl14}$ cells

As mentioned in the introduction, this project was originally a continuation of another study (by Fakitsas et al.) that showed that an aldosterone injection strongly upregulates ATF3 on mRNA level within 1 hour in WT mice. Therefore an *in vitro* model was created to study the role of ATF3 in the action of aldosterone, on principal cells of the cortical collecting duct of the kidney. For this model the mouse kidney cortical collecting duct cell line mpkCCD$_{Cl14}$ was used. Even though this principal cell line does not express the mineralocorticoid receptor (MR, aldosterone receptor), aldosterone can exert its effects through the glucocorticoid receptor (GR), although significantly higher doses are required to do so [101]. To investigate whether the ATF3 mRNA induction seen *in vivo* in aldosterone-injected mice can be reproduced *in vitro* in mpkCCD$_{Cl14}$, a former collaborator (Dr. Gabriele Adam) had analyzed ATF3 mRNA levels in mpkCCD$_{Cl14}$ cells upon treatment with 1 µM aldosterone over a timecourse of 3 h. Similar to the response in mice, also cortical collecting duct kidney cells upregulated ATF3 mRNA expression *in vitro* upon aldosterone treatment with a peak after 1 h. After this point of time, ATF3 mRNA levels decreased back to almost baseline levels after 3 h (see Fig. 22). Thus, ATF3 appeared to be an early aldosterone-induced gene in mpkCCD$_{Cl14}$ cells *in vitro*.

ATF3 expression in mpkCCD$_{Cl14}$ cells treated with 1 μM aldosterone

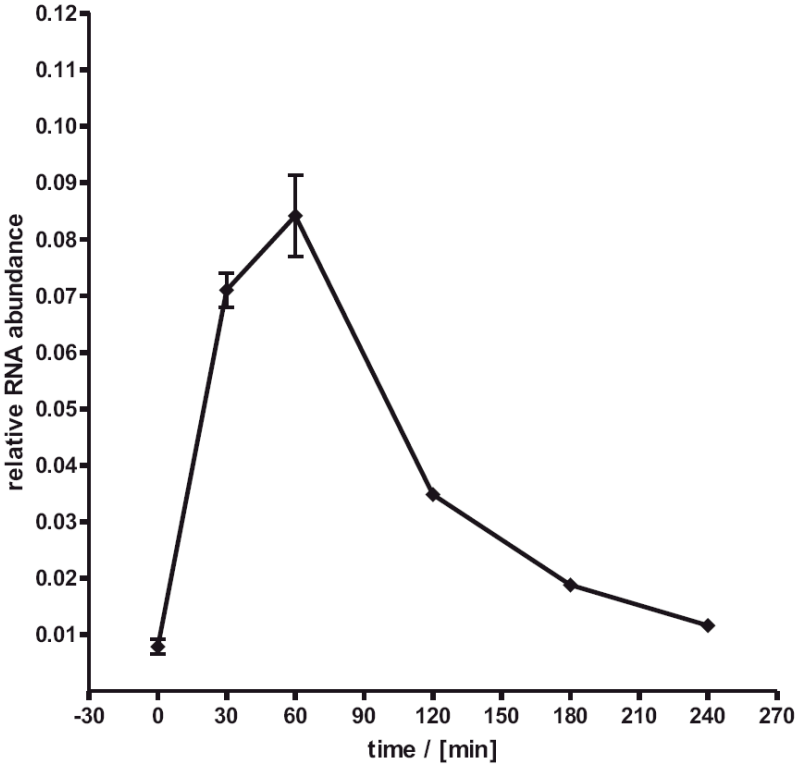

Figure 22: Aldosterone upregulates ATF3 mRNA levels in mpkCCD$_{Cl14}$ cells: Cells were cultured with 1 μM aldosterone over a timecourse up to 3 hours. Subsequent qPCR analysis showed an approximately 8-fold upregulation of ATF3 mRNA levels after 1 h of hormone treatment. After 3 h ATF3 mRNA levels were almost back to baseline. Errorbars: SEM. Graph by Dr. Gabriele Adam, unpublished data.

Since the same effect was observed *in vitro* as was the case *in vivo*, namely that ATF3 expression was stimulated by aldosterone also in the mpkCCD$_{Cl14}$ cells, it was decided to use this cell line as a system to create a cell line which shows inducible overexpression of ATF3 using lentiviral vector systems.

5.1.2 Overexpression of ATF3 in a mixed population of mpkCCD$_{Cl14}$ cells using a lentiviral Tet-On system

The ATF3 coding sequence was cloned into the pLV-T vector of a lentiviral two-vector system (see methods section 4.2.). Both the pLV-T vector with ATF3 under the control of a tet operator (*tetO*) and the vector expressing the tet-responsive transrepressor (tTR) fused to a KRAB protein were transduced sequentially into the mouse cortical collecting duct cell line mpkCCD$_{Cl14}$. Overexpression of ATF3 was induced with 1 µg/ml Dox for 3 days. Western blot analysis of the ATF3/KRAB mpkCCD$_{Cl14}$ mixed cell population showed a clear induction of ATF3 expression at the expected band size level (approximately 23 kD) as opposed to WT mpkCCD$_{Cl14}$ cells or GFP/KRAB mpkCCD$_{Cl14}$. However, also the two control cell lines as well as un-induced ATF3/KRAB mpkCCD$_{Cl14}$ showed a weak band at the same level that probably corresponds to endogenous baseline levels of ATF3 expression, as well as unspecific bands in the lower kD range (see Fig. 23).

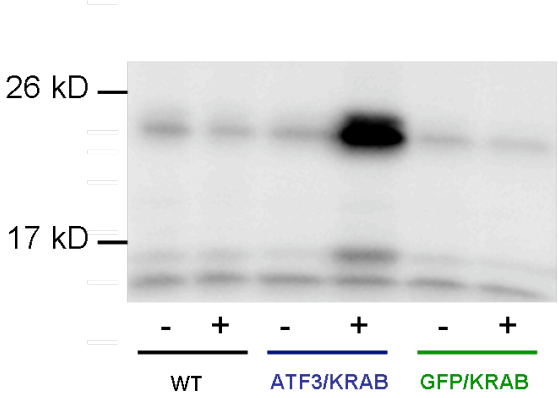

Figure 23: Dox-induced overexpression of ATF3 in a mixed population of mpkCCD$_{Cl14}$ cells: WT mpkCCD$_{Cl14}$ cells were transduced with the tTRKRAB fusionprotein lentiviral vector pLVCT-tTRKRAB and the pLV-T vector expressing ATF3 under the control of the *tetO*. Cells were grown for 3 days in medium containing 1 µg/ml Dox (+) or without the antibiotic (-). As controls WT mpkCCD$_{Cl14}$ cells and cells expressing inducible GFP were used. A clear overexpression of ATF3 (ca. 23 kD) was seen after 3 days of induction with Dox in this Western Blot. All cell lines used express low endogenous levels of ATF3.

The Dox-inducible ATF3 overexpression could also be confirmed with immunofluorescence of mixed populations of mpkCCD$_{Cl14}$ cells expressing KRAB and ATF3 (green). In WT mpkCCD$_{Cl14}$ cells, the endogenous ATF3 expression was below the detection limit of the antibody in immunofluorescence (as opposed to the Western blot, see Fig. 23). This was also not altered by the treatment with Dox. ATF3/KRAB transduced cells showed a low level of ATF3 expression when no Dox was added, indicating the repression by KRAB being leaky to a low extent. Addition of 1 µg/ml Dox to ATF3/KRAB transduced mpkCCD$_{Cl14}$ cells grown on coverslips during 3 days showed an induction of ATF3 expression which was mostly located in the nucleus (see Fig. 24).

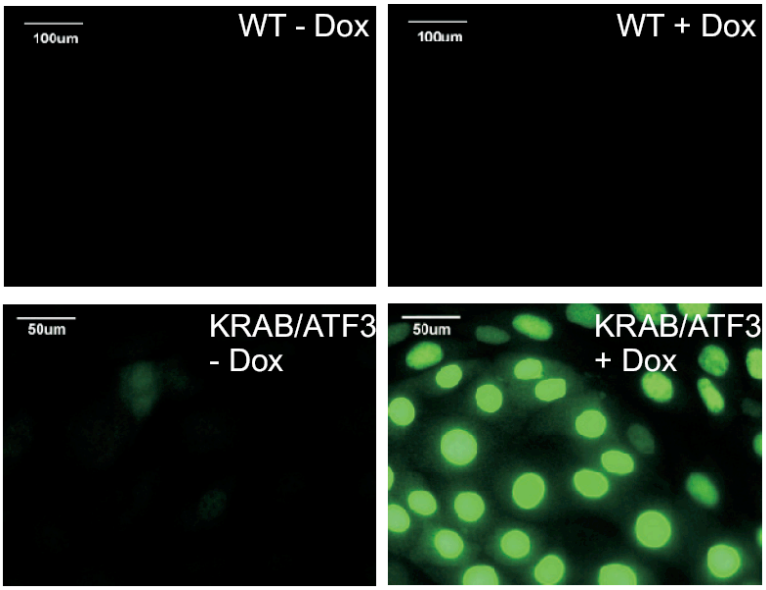

Figure 24: Overexpression of ATF3 in mpkCCD$_{Cl14}$ cells after 3 days of 1 mg/ml Dox: Immunofluorescence staining using a polyclonal anti-ATF3 antibody (1:500). KRAB/ATF3 mpkCCD$_{Cl14}$ cells grown without Dox showed only very low levels of ATF3 expression as compared to Dox-induced cells. WT mpkCCD$_{Cl14}$ cells served as a control where endogenous ATF3 expression was below the detection limit of the antibody.

Selection of mpkCCD$_{Cl14}$ clonal cell lines co-expressing ATF3 and KRAB

Limiting dilution led to isolation of clonal cell lines expressing both KRAB and ATF3. These clones showed a Dox-inducible overexpression of the transcription factor upon treatment with 1 µg/ml Dox for 3 days (see Fig. 25). Shown are the examples for clones 1 and 11. In total 9 clonal mpkCCD$_{Cl14}$ ATF3/KRAB expressing cell lines displayed Dox-inducibility of the transcription factor. An endogenous level of ATF3 expression was seen in the WT mpkCCD$_{Cl14}$ cells, however, it was not increased by Dox.

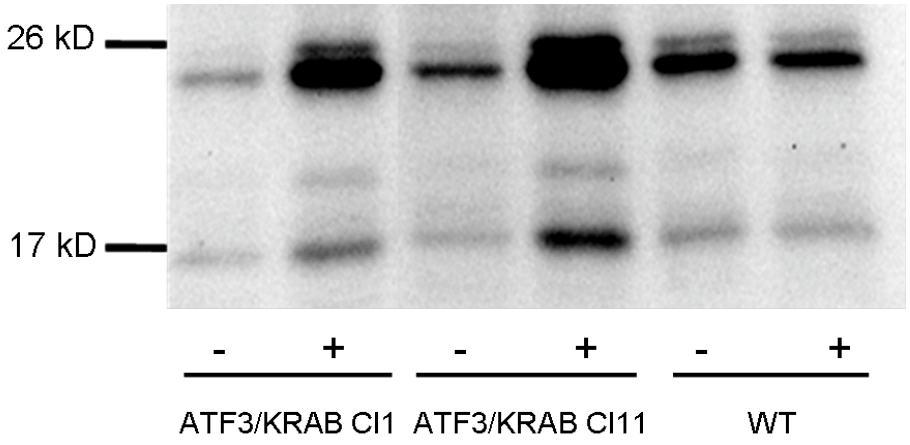

Figure 25: Dox-inducible ATF3 clonal mpkCCD$_{Cl14}$ cell lines: ATF3/KRAB mpkCCD$_{Cl14}$ Clones 1 and 11 were isolated by limiting dilution. They were grown ± 1 µg/ml Dox for 3 days to analyze induction of ATF3 overexpression (approximately 23 kD). WT mpkCCD$_{Cl14}$ cells were grown in parallel as a control. A clear induction of ATF3 expression was seen by Western Blot after 3 days in ATF3KRAB mpkCCD$_{Cl14}$ clones treated with Dox when compared to non-treated ATF3/KRAB mpkCCD$_{Cl14}$ transduced or WT mpkCCD$_{Cl14}$ cells.

ATF3 overexpression is induced upon treatment with low Dox concentrations in ATF3/KRAB transduced mpkCCD$_{Cl14}$ cells

To characterize the Dox-inducible overexpression of ATF3 in the mpkCCD$_{Cl14}$ cell lines, it was first tested whether the amount of overexpressed protein can be regulated by varying the concentration of Dox in the medium. Fig. 26 shows the dose response to different Dox concentrations of clone 9 ATF3/KRAB mpkCCD$_{Cl14}$ cells obtained by limiting dilution. Already the low dose of 0.1 µg/ml Dox showed a clear induction of ATF3 overexpression in ATF3/KRAB mpkCCD$_{Cl14}$ cells compared to non-induced cells (0 µg/ml Dox) or non-transduced WT mpkCCD$_{Cl14}$ cells. This effect increased with higher Dox doses up to 1 µg/ml.

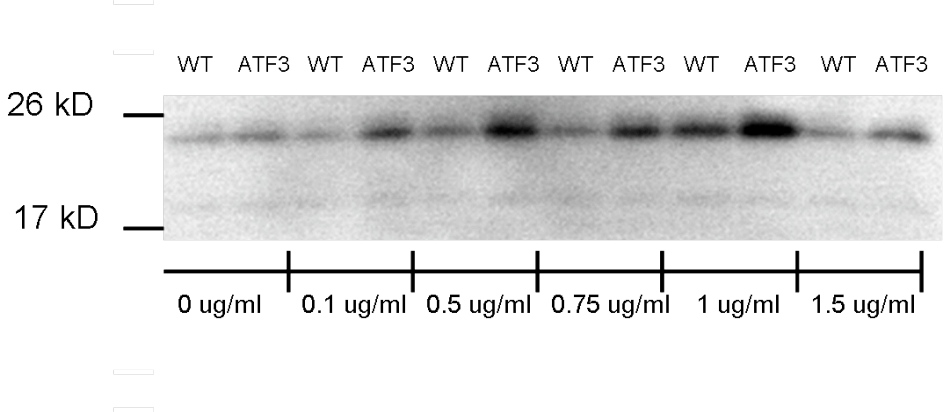

Figure 26: Dose response of Dox-induced ATF3 expression. mpkCCD$_{Cl14}$ cells transduced with ATF3 and KRAB were exposed to 0.1 µg/ml; 0.5 µg/ml; 0.75 µg/ml; 1 µg/ml and 1.5 µg/ml of Dox in the medium over a period of 3 days. Induction of ATF3 expression (approximately 23 kD) compared to WT mpkCCD$_{Cl14}$ cells or no Dox treatment of ATF3/KRAB mpkCCD$_{Cl14}$ clone 9 cells is observed even with the lowest dose of Dox (0.1 µg/ml). The protein overexpression increases, the more Dox is added to the medium (up to 1 µg/ml).

Dox-inducible overexpression of ATF3 in ATF3/KRAB transduced mpkCCD$_{Cl14}$ cells is maintained over long periods of time

Next it was tested whether the cells do not lose the ability to induce ATF3 expression upon Dox-treatment over a longer culturing period including passaging of the cells. The ATF3/KRAB transduced mpkCCD$_{Cl14}$ clone 1 cells (ATF3/KRABCl1) were grown in two different concentrations of Dox (1.5 and 3 µg/ml) over a period of 15 days, with being passaged once. Furthermore the Dox concentration at which ATF3 would be maximally induced was to be determined. It was observed that ATF3/KRABCl1 mpkCCD$_{Cl14}$ cells were able to maintain the expression of the transcription factor over the tested time period of 15 days. At this timepoint, the induction was still as strong as it was after 3 days of Dox treatment. Moreover, in the case of this particular clone, the strongest possible induction seemed to be already reached with 1.5 µg/ml Dox, using twice this dose of the antibiotic did not increase the overexpression of ATF3 any further (see Fig. 27).

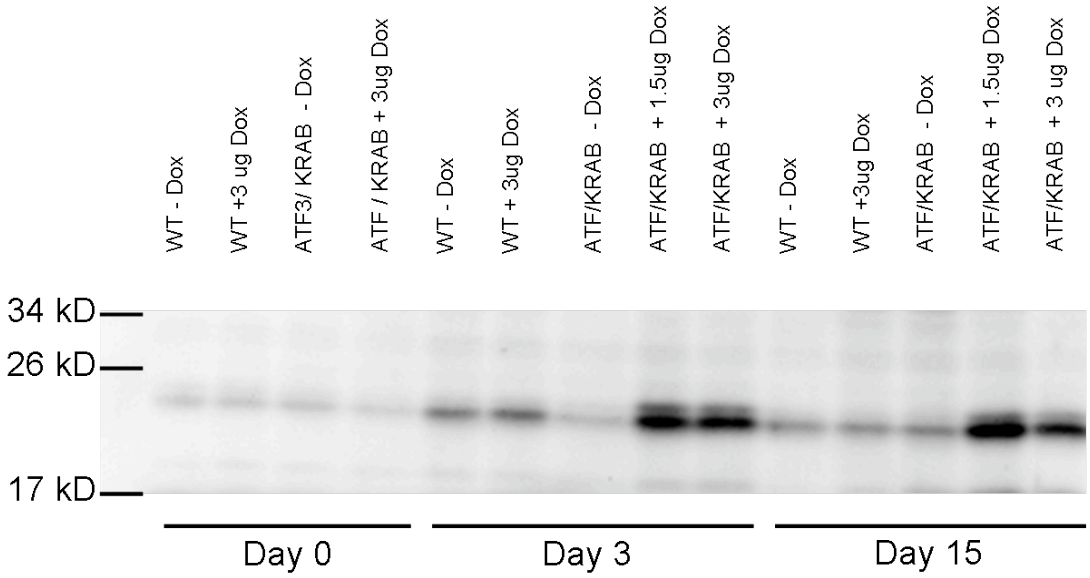

Figure 27: Timecourse of Dox-induced ATF3 expression: WT mpkCCD$_{Cl14}$ cells transduced with ATF3 and KRAB (clone 1, selected by limiting dilution) were exposed to 1.5 or 3 µg/ml of Dox in the medium over a period of 15 days, including passaging of the cells once. Induction of ATF3 expression compared to WT mpkCCD$_{Cl14}$ cells or not Dox-treated ATF3KRABCl1 mpkCCD$_{Cl14}$ cells was maintained over 15 days. The induction was similar, regardless whether cells were grown in 1.5 µg/ml or 3 µg/ml Dox. Furthermore, the induction did not lose its effectiveness even after 15 days.

Since we were able to demonstrate that clonal mpkCCD$_{Cl14}$ cell lines transduced with ATF3 and KRAB showed Dox-inducible and dose dependent overexpression of the transcription factor, which was maintained even after passaging, we considered these cell lines to be suitable for functional studies of these cells. Since ATF3 had been identified as aldosterone-induced gene product, we were interested to test whether the ENaC-mediated Na^+ current and its regulation by aldosterone were altered in ATF3 overexpressing mpkCCD$_{Cl14}$ cells compared to WT mpkCCD$_{Cl14}$ cells.

5.1.3 Functional tests of ATF3/KRAB mpkCCD$_{Cl14}$ cell lines in Ussing chamber

Before the mpkCCD$_{Cl14}$ ATF3 overexpressing cells were subjected to transepithelial voltage clamp in an Ussing chamber set up, the transepithelial resistance (TER) of the monolayer was confirmed to be sufficient (TER $\geq$ 1 kΩ), meaning the cells formed a tight epithelium on the filter supports.

First the mpkCCD$_{Cl14}$ ATF3/KRAB mixed cell population and the clonal cell line ATF3/KRABCl11 that were grown $\pm$ 1 µg/ml Dox for 3 days were compared in terms of their transepithelial transport characteristics. The cells were voltage clamped (see methods section 4.5) and transepithelial short circuit current was measured. The cells were allowed to stabilize in the new environment of the chamber (minimal medium warmed to 37°C and pH equilibrated with constant gas supply of 95% O_2 and 5% CO_2) until the short circuit currents measured reached a stable plateau, in the case of this first experiment after approximately 2 h. 1 µM aldosterone was then added to the medium in the chamber surrounding the cells (residing on filters) to stimulate Na^+ transport by the epithelial Na^+ channel ENaC via the glucocorticoid receptor (GR), since mpkCCD$_{Cl14}$ cells do not have endogenous expression of the aldosterone receptor mineralocorticoid receptor (MR). After about 3 h, arginine-vasopressin (AVP) was added to the medium to stimulate ENaC mediated Na^+ transport via another signalling route, namely the cyclic AMP (cAMP) signalling pathway for approximately 2 h. At the end of the transepithelial current measurements, the diuretic amiloride was added to specifically block ENaC and abrogate Na^+ transport (see Fig. 28 A+B).

All cells showed a steep increase in transepithelial currents during the first two hours of the experiment. The levels of the currents observed once they stabilized were very different from one filter to the other ranging from approximately 13 up to 61 µA, once a stable condition was reached. After addition of aldosterone to the medium in the chamber, only cells treated with Dox showed an increase in

currents of approximately 10 µA for the mixed population and approximately 20 µA for the clonal cell line. However, both these filters showed lower currents after the stabilization period than were observed in their non-induced counterparts. Addition of AVP lead to an increase in currents measured in all samples, which was most pronounced in the clonal cell line overexpressing ATF3. Addition of amiloride blocked the currents to a comparable level of around 3.5 µA in all the samples (Fig. 28 A), suggesting that the currents measured were Na^+ currents mediated by ENaC. Also transepithelial resistances increased during the phase of stabilization until they reached approximately 3 kΩ which is considerably high. The transepithelial resistances decreased in the mixed population of ATF3/KRAB mpkCCD$_{Cl14}$ cells or the ATF3/KRABCl11 mpkCCD$_{Cl14}$ cell line treated with Dox as was expected to go along with the increases in transepithelial currents. Amiloride blocked ENaC and ablated Na^+ currents, which led to an increase of transepithelial resistance in all chambers up to 6 kΩ (see Fig. 28 B).

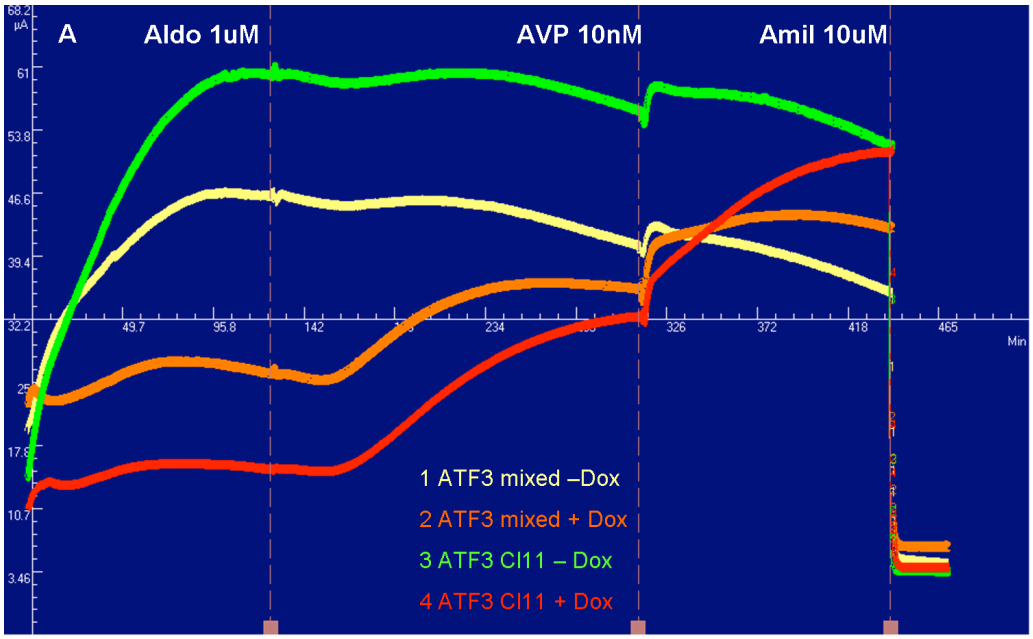

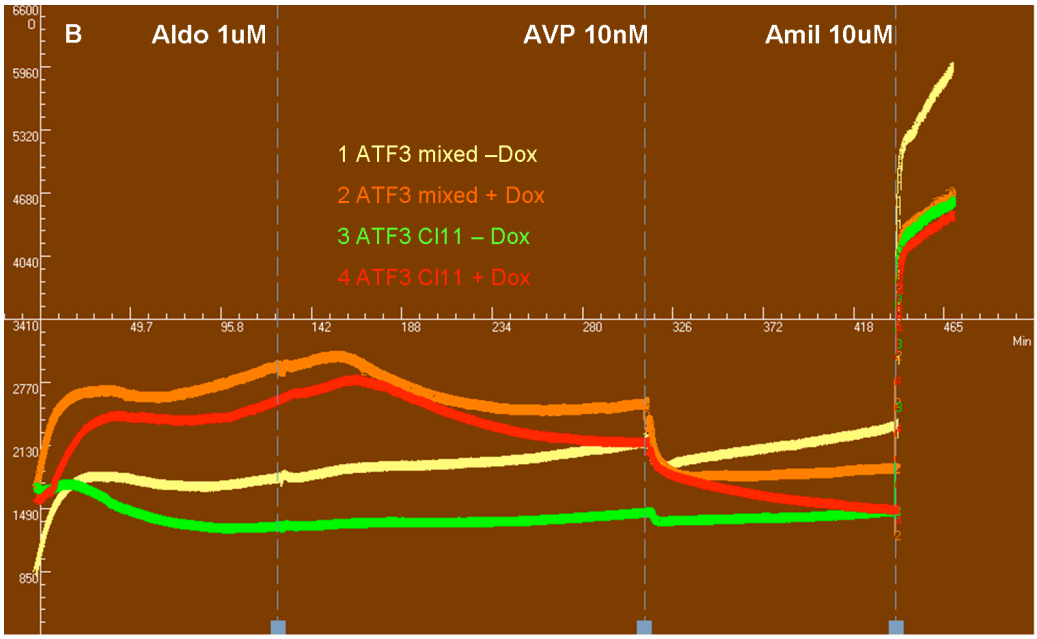

Figure 28: A: Original trace of Ussing chamber short circuit currents of ATF3/KRAB mpkCCD$_{Cl14}$ mixed population and ATF3/KRAB$_{Cl11}$ mpkCCD$_{Cl14}$ under voltage clamp: Addition of 1 µM aldosterone only stimulated transepithelial currents in cells treated 3 days with 1 µg/ml Dox in both clonal and mixed populations of ATF3 overexpressing cells, while addition of 10 nM AVP increased currents in all cell populations. Addition of 10 µM amiloride blocked the currents in all samples to 3.5 µA, suggesting that the observed transepithelial currents are ENaC-mediated Na^+ currents.
B: Transepithelial resistances of ATF3/KRAB mpkCCD$_{Cl14}$ mixed population and ATF3/KRABCl11 mpkCCD$_{Cl14}$ under voltage clamp: Transepithelial resistances of all cells measured confirmed that the cells grew in tight monolayers. Up to 3 kΩ of transepithelial resistance was reached as in the case of ATF/KRAB mpkCCD$_{Cl14}$ mixed population grown with 1 µg/ml Doxycycline for 3 days. The resistances decreased upon addition of 1 µM aldosterone or 10 nM AVP because these agents increased the transepithelial short circuit currents by opening a Na^+ conductance. Addition of 10 µM amiloride to the medium chambers immediately led to a rise of resistance in all samples measured up to 6 kΩ, confirming that the observed current and decrease in resistance was due to ENaC-mediated Na^+ transport.

In the next step the goal was to verify the data obtained from Fig. 28 using additional clones. Furthermore, it was to be confirmed that the transduction of ATF3 and KRAB per se, without inducing the Overexpression of ATF3 would not alter transepithelial currents compared to WT cells. Thus, we subjected

ATF3/KRABCl1 and Cl13 mpkCCD$_{Cl14}$ cells to transepithelial current measurements in Ussing chamber. ATF3/KRABCl13 mpkCCD$_{Cl14}$ cells showed approximately the same short circuit currents independent of whether they were induced to overexpress ATF3 or not (see Fig. 29 B respectively A). In clone 1 there was a clear difference in the cells grown for 3 days with Dox compared to non-induced cells. The baseline currents in the ATF3 overexpressing cells were around 30 µA higher (approximately 85 µA) than in the same clone grown without Dox (approximately 55 µA. However, the transepithelial resistance stayed about the same for both induced and non-induced ATF3/KRABCl1 cells, namely about 1 kΩ. Surprisingly stimulation by addition of 1 µM aldosterone to the chambers did not alter transepithelial currents in any of the tested cells (WT, ATF3/KRABCl1 or Cl13), independent of Dox-induction. ATF3/KRABCl1 mpkCCD$_{Cl14}$ cells always showed higher short circuit currents, than the WT mpkCCD$_{Cl14}$ cells (approximately 7-fold higher), no matter if they were induced to overexpress ATF3 or not. Unexpectedly, the currents of the WT mpkCCD$_{Cl14}$ were higher when grown with Dox than when grown without the Dox. In the whole experiment, neither aldosterone nor addition of 10 nM AVP had an effect on the currents measured in any cell type. Addition of 10 µM amiloride completely blocked the currents measured in all the cell populations, which was accompanied by a rise in resistance. Therefore the currents observed must have been ENaC-mediated Na^+ currents.

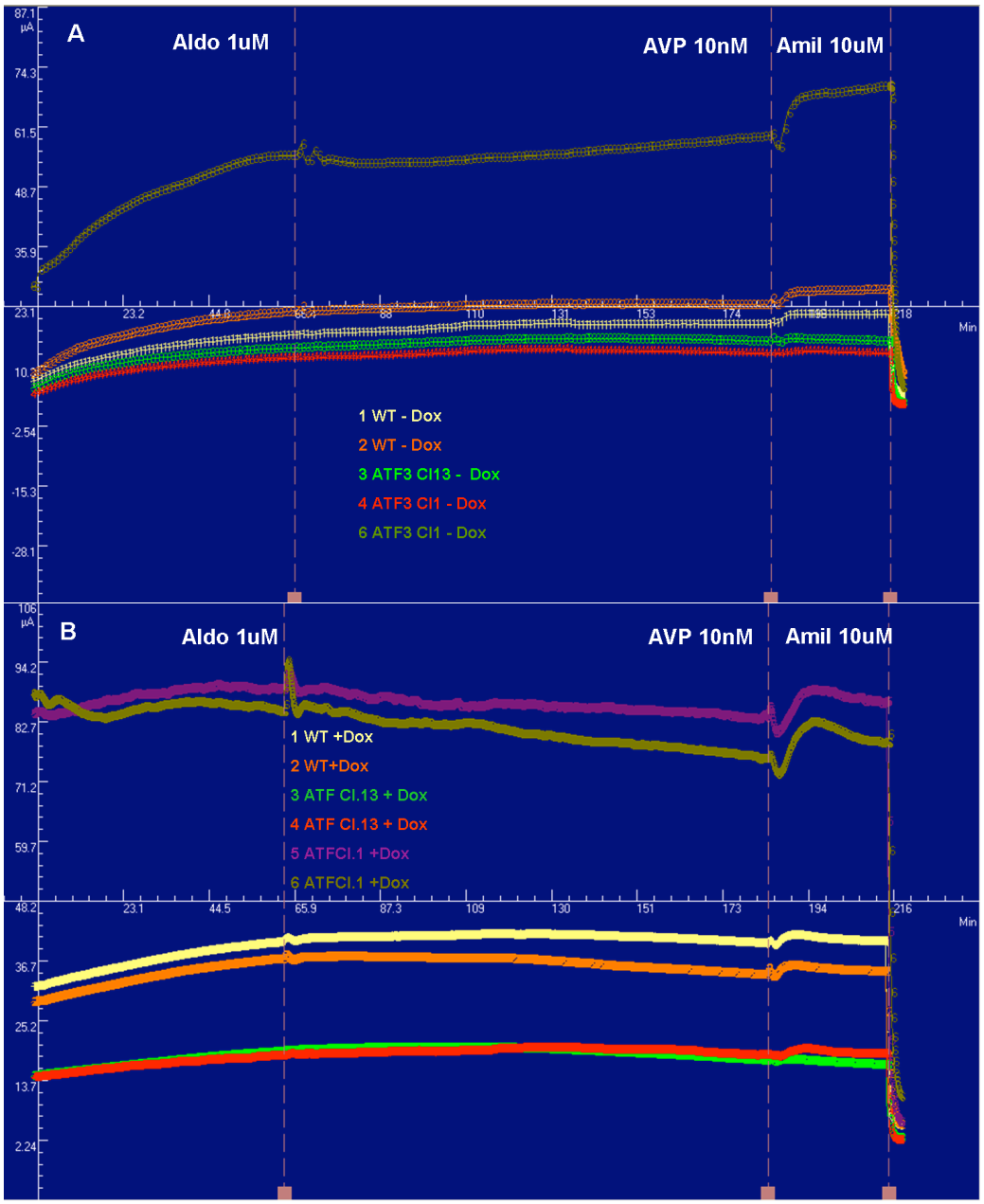
A
Aldo 1uM
AVP 10nM
Amil 10uM
87.1 µA
74.3
61.5
48.7
35.9
23.1
23.2
44.8
88
110
131
153
174
218
Min
10.2
-2.54
-15.3
-28.1
1 WT - Dox
2 WT - Dox
3 ATF3 Cl13 - Dox
4 ATF3 Cl1 - Dox
6 ATF3 Cl1 - Dox
B
Aldo 1uM
AVP 10nM
Amil 10uM
106 µA
94.2
82.7
71.2
59.7
1 WT +Dox
2 WT+Dox
3 ATF Cl.13 + Dox
4 ATF Cl.13 + Dox
5 ATFCl.1 +Dox
6 ATFCl.1 +Dox
48.2
23.1
44.5
65.9
87.3
109
130
151
173
194
216
Min
36.7
25.2
13.7
2.24

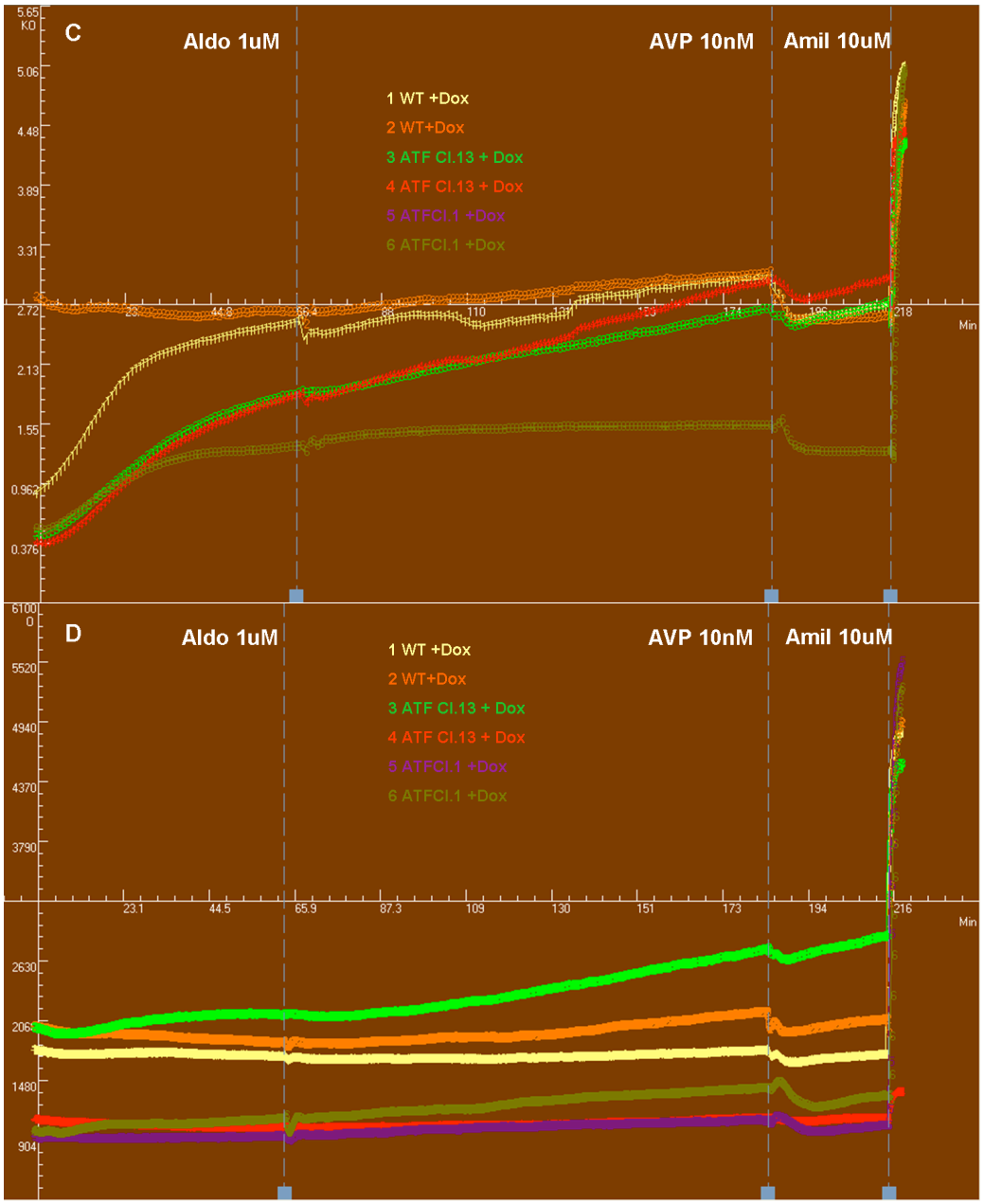
C
Aldo 1uM
AVP 10nM
Amil 10uM
1 WT +Dox
2 WT+Dox
3 ATF Cl.13 + Dox
4 ATF Cl.13 + Dox
5 ATFCl.1 +Dox
6 ATFCl.1 +Dox
5.65
KO
5.06
4.48
3.89
3.31
2.72
2.13
1.55
0.962
0.376
23.1
44.9
66.4
88
110
130
174
195
218
Min
D
Aldo 1uM
AVP 10nM
Amil 10uM
1 WT +Dox
2 WT+Dox
3 ATF Cl.13 + Dox
4 ATF Cl.13 + Dox
5 ATFCl.1 +Dox
6 ATFCl.1 +Dox
6100
0
5520
4940
4370
3790
2630
2060
1480
904
23.1
44.5
65.9
87.3
109
130
151
173
194
216
Min

Figure 29: A+B: Original trace of Ussing chamber short circuit currents of mpkCCD$_{Cl14}$ WT, ATF3/KRABCI1 mpkCCD$_{Cl14}$ and ATF3/KRABCI13 mpkCCD$_{Cl14}$ grown without Doxycycline (A) or with 1 μg/ml Doxycycline for 3 days (B): WT mpkCCD$_{Cl14}$ cells aswell as ATF3/KRABCI13 cells all showed about 10-20 μA throughout the whole experiment. Regardless of the baseline level of current of unstimulated cells, none of the cell populations showed any reaction in terms of transepithelial currents in response to stimulation with 1 μM aldosterone or 10 nM AVP, independent of ATF3 overexpression.
C+D: Transepithelial resistances of mpkCCD$_{Cl14}$ WT, ATF3/KRABCI11 mpkCCD$_{Cl14}$ and ATF3/KRABCI13 mpkCCD$_{Cl14}$ grown without Doxycycline (C) or with 1 μg/ml Doxycycline for 3 days (D): As can be observed in the transepithelial resistances, the cells formed tight monolayers. This was not altered upon hormone addition to the medium. 10 μM amiloride increased the transepithelial resistance in all the cell samples by blocking ENaC.

The experiment shown above was the first one not to give reproducible results from Ussing chamber measurements anymore. Additionally it was disturbing that Dox per se increased transepithelial currents in WT mpkCCD$_{Cl14}$ cells. We were also no longer able to reproduce the experiments that were formerly performed in the laboratory (by Dr. Gabriele Adam), even though we were controlling pH and temperature of the medium during the experiment. Surprisingly, even the mpkCCD$_{Cl14}$ WT cells did not seem to respond to aldosterone anymore by increased transepithelial currents. This problem was also observed in another mouse cortical collecting duct cell line, the mCCD$_{Cl1}$ cells, in two other laboratories (Prof. Olivier Staub in Lausanne, Switzerland and Prof. Johannes Loffing in Zurich, Switzerland). Trying to optimize growth and differentiation media, number of cells seeded on the filters, coating conditions of filters and testing of different lots of FCS did not improve the situation (data not shown).

The initial rational why mpkCCD$_{Cl14}$ cells were chosen over mCCD$_{Cl1}$ cells to be used as a cell culture model was that mpkCCD$_{Cl14}$ cells seemed much more stable in terms of transepithelial transport characteristics over the different passages during the culturing period. However, the disadvantage of working with mpkCCD$_{Cl14}$ cells is, that they do not express the mineralocorticoid receptor (MR) endogenously, which is the specific aldosterone receptor. This is the reason

why compared to the physiological level, which is in the nanomolar range, an unreasonably high dose of aldosterone has to be added to the medium (1 μM) to stimulate Na^+ transport in these cells more unspecifically over the glucocorticoid receptor (GR) signalling pathway (see Ussing chamber results Fig. 28) [108] [109]. The laboratories of Prof. Bernard Rossier and Prof. Olivier Staub isolated a new mCCD clonal cell line, the clone 6, which happened to be much more stable over the passages and gave considerable aldosterone responsiveness at lower levels of aldosterone in Ussing chamber experiments of these research groups. The cells were tested in our Ussing chamber and increased transepithelial short circuit currents with 300 nM aldosterone treatment after 1 h were observed. 10 nm AVP was able to further increase these currents. Final treatment of $mCCD_{Cl6}$ cells with 10 μM amiloride ablated the currents observed before to a minimum, therefore pointing to the fact that the currents observed are ENaC-mediated Na^+ currents (see Fig. 30).

Therefore from this time point on, we decided to continue our work with $mCCD_{Cl6}$ cells and to not further use the $mpkCCD_{Cl14}$ cells, neither the WT nor the ATF3KRAB transduced ones.

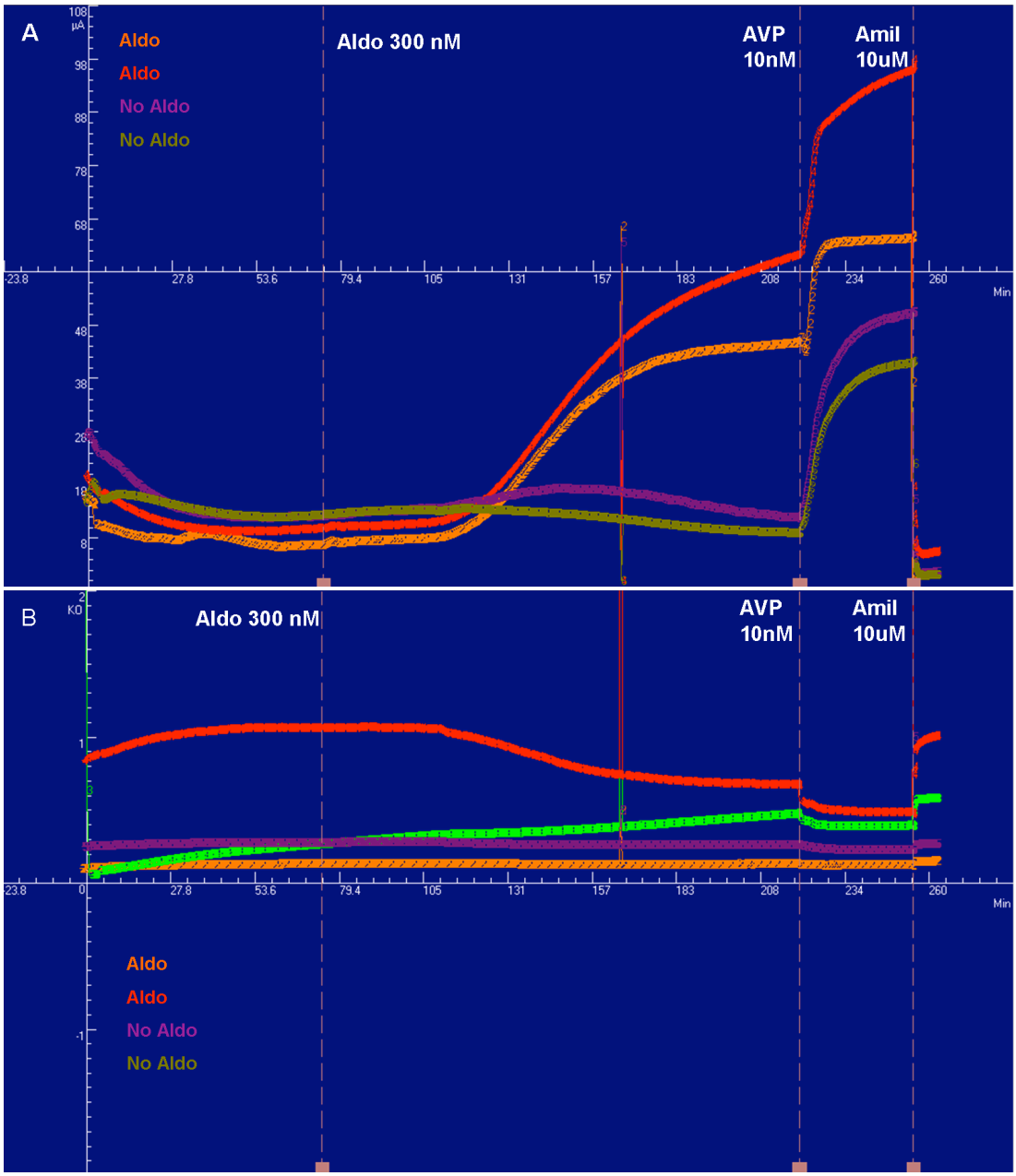
A
Aldo
Aldo
No Aldo
No Aldo
Aldo 300 nM
AVP
10nM
Amil
10uM
Min
B
Aldo 300 nM
AVP
10nM
Amil
10uM
Min
Aldo
Aldo
No Aldo
No Aldo

Figure 30: Original trace of Ussing chamber short circuit currents (A) and resistances (B) of mCCD$_{Cl6}$ WT cells: WT mCCD$_{Cl6}$ were tested for their capability to respond to aldosterone stimulation. After the initial stabilization period of approximately 1 h, 2 filters were treated with 300 nM aldosterone while 2 filters were left untreated. All filters had stabilized their short circuit currents around approximately 9-18 µA. After approximately 1 h, cells treated with aldosterone increased short circuit currents up to approximately 60 µA, while short circuit currents of non-treated cells remained stable. Addition of 10 nM AVP to all cells increased the short circuit currents in all samples, with a more pronounced increase in cells that had so far been unstimulated (approximately 30 µA). Treatment with 10 µM amiloride abrogated most of the transepithelial current seen, confirming that the increased short circuit currents in response to aldosterone or AVP treatment are Na^+ currents due to enhanced ENaC activity. The jump in currents and resistance after approximately 170 min is due to unstable electrodes.

5.1.4 ATF3 relative mRNA expression is upregulated upon medium change in mCCD$_{Cl6}$ cells *in vitro*

When we first aimed at characterizing the new mCCD$_{Cl6}$ cells, we were interested whether we could see an early aldosterone induced upregulation of ATF3 on the mRNA level, as we did in mpkCCD$_{Cl14}$ cells (see Fig. 22).

When treating mCCD$_{Cl6}$ cells with aldosterone in a time-course experiment, a student co-worker replaced the old medium that had been on the cells for 2 days with fresh medium containing aldosterone, instead of diluting the hormone directly into the medium that already had been on the cells. As a negative control cells were not treated with aldosterone, but also in this condition the medium was also replaced with fresh medium. This treatment of the negative control and the 24h-aldosterone treatment were performed at the same time. This had the effect of inducing ATF3 mRNA levels relative to this control. There was a most prominent ATF3 mRNA expression peak after 1 h during a 24 h-timecourse, showing an approximately 6-fold induction compared to control. SGK1 served as a positive control, since it is an aldosterone-induced gene. Relative SGK1 mRNA levels only showed a tendency to increase after 24 h (see Fig. 31). It was decided that the upregulation of ATF3 observed from this experimental set-up cannot

completely be attributed to be aldosterone-mediated, since the medium change per se might possibly have an effect on the expression of specific genes. It could have been the medium change per se and not the aldosterone added with the medium that was responsible for the upregulation of ATF3 mRNA levels after 1h. We suspected that it is possibly a kind of stress caused by the medium change that induces the expression of the transcription factor after 1 h rather than the hormone.

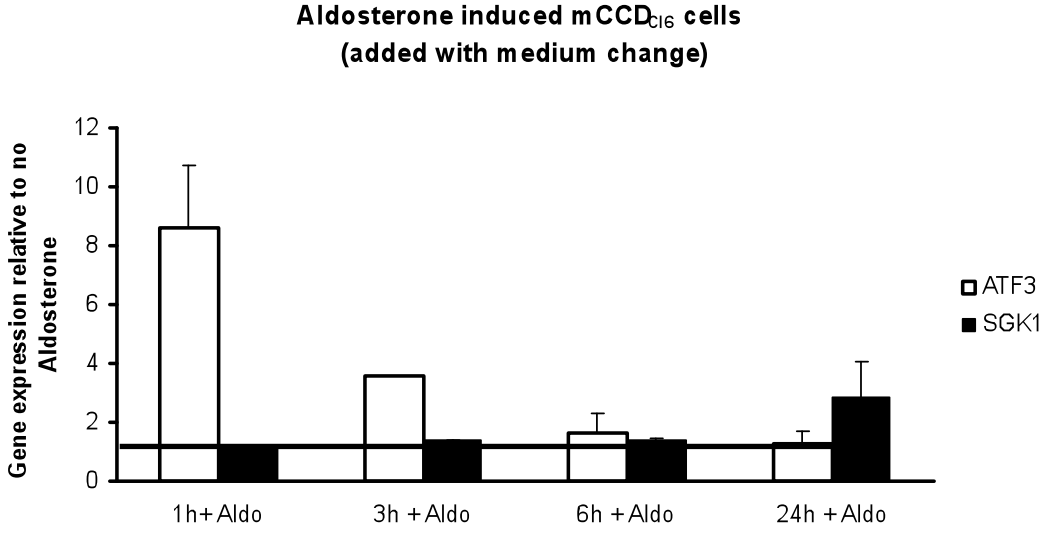

Figure 31: Aldosterone increases relative ATF3 mRNA expression when added with a medium change in mCCD$_{Cl6}$ cells. Relative mRNA expression of ATF3 and SGK1 in mCCD$_{Cl6}$ cells in response to 1 µM aldosterone treatment for 1 h, 3 h, 6 h and 24 h was analyzed. In this experimental set-up, 1 µM aldosterone was added to the cells by replacing the old medium on the cells with fresh medium in which the aldosterone was diluted. This led to an approximately 6-fold induction of relative ATF3 mRNA expression while SGK1 mRNA levels showed a tendency of increasing after 24 h. Values are expressed relative to a control (no aldosterone = 1, represented by the black line) in which the medium had been replaced with fresh medium (without aldosterone) at the same timepoint as the 24h-aldosterone treatment started. N=3, house keeping gene: HPRT, error bars= SEM. Unpublished Data (Cand. med. Christoph Rüst)

To further confirm the hypothesis, that the medium change and not the aldosterone had an effect on ATF3 expression, the co-worker performed an experiment

where he added the aldosterone directly to the medium that had already been on the $mCCD_{Cl6}$ cells for 24 h and lysed these cells after 1 h, 3 h, 6 h and 24 h to analyze mRNA expression patterns. A clear induction of SGK1 mRNA expression with a peak after 3 h could be observed, while relative mRNA levels of ATF3 seemed unaltered even though aldosterone was present in the medium (see Fig. 32).

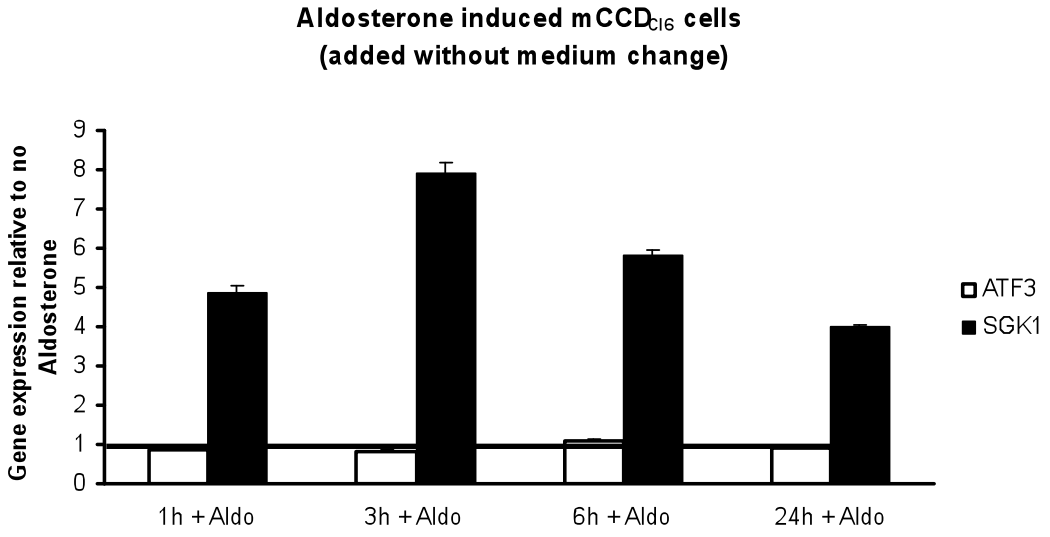

Figure 32: Aldosterone does not induce ATF3 expression in $mCCD_{Cl6}$ cells when added without a medium change: When 1 µM aldosterone was added to the WT $mCCD_{Cl6}$ cells without changing the medium, and incubated for 1 h, 3 h, 6 h or 24 h, there was only a relative upregulation of SGK1 mRNA, which was strongest after 3 h when expressed relative to non-treated cells. However, the ATF3 mRNA levels of cells treated with aldosterone that was added directly to the medium stayed unaltered over time. Values are expressed relative to a control (no aldosterone = 1, represented by the black line). N=3, house keeping gene: HPRT, error bars= SEM. Unpublished Data (Cand. med. Christoph Rüst).

An additional experiment in which $mCCD_{Cl6}$ cells underwent only a medium change with minimal medium (no aldosterone added), ATF3 mRNA levels were clearly increased after 1 h, namely 25-fold higher than after 24 h. SGK1 expression levels were slightly lower due to the medium change (see Fig. 33)

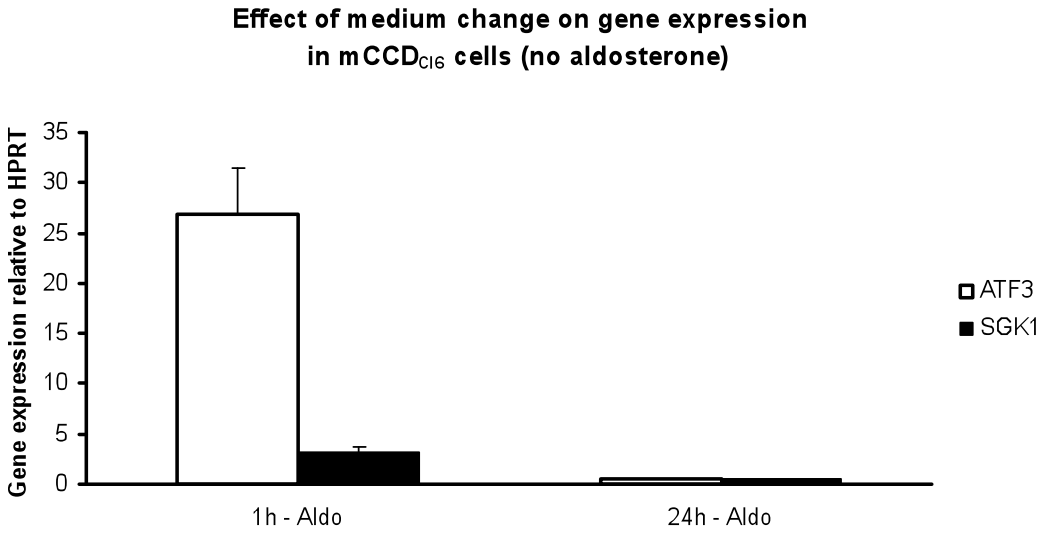

Figure 33: Changing the medium mCCD$_{Cl6}$ of cells induces relative expression of ATF3 mRNA: The minimal medium of mCCD$_{Cl6}$ cells was changed 1 h or 24 h prior to lysis. There is a strong increase in relative expression levels of ATF3 mRNA observed when cells were lysed after 1 h compared to cells lysed after 24 h. This effect was not as pronounced for relative SGK1 expression levels. N=3, all values relative to HPRT mRNA expression, error bars= SEM. Unpublished Data (Cand. med. Christoph Rüst).

The results from these cell culture experiments were unexpected and showed that a simple medium change is enough to stimulate ATF3 mRNA expression in mCCD$_{Cl6}$ cells and that it is not aldosterone that is responsible for this upregulation in this cell line*in vitro*. Moreover, this is not the case for SGK1, here a medium change only has a small effect, while it is up to 7-fold induced by the hormone.

Retrospectively, also the upregulation of ATF3 in mpkCCD$_{Cl14}$ WT cells upon aldosterone stimulation (see Fig. 22) could have been due to the medium change, since also this co-worker replaced the medium with fresh aldosterone-containing medium instead of diluting the hormone directly in the conditioned medium that had been on the cells before. It needed to be tested which aspect of the

medium change was responsible for the induction of ATF3 mRNA by the medium change. On one hand it could be due to the fact that when the old medium is replaced by fresh one, certain substances that were released into the supernatant were removed while fresh factors were supplied. On the other hand it might be simply the mechanical stimulation of the cells that lets them produce more of the transcription factor mRNA.

Hence, an experiment comparing $mCCD_{Cl6}$ cells not treated at all to cells that underwent two different kinds of medium change was carried out: First, a mock medium change, which meant to aspirate the conditioned minimal medium (without growth factors or FCS) from the cells that had been there for 24 h and immediately redistributing it back onto the cells and second, a real medium change where the old medium was discarded and fresh in a tube pre-warmed (37°C) minimal medium was put on the cells. Performing qPCR of cells treated with these different medium changes for 1 h revealed that a mock change showed a tendency to upregulate relative ATF3mRNA compared to non-treated controls. A real change of medium, replacing the old medium on the cells led to a approximately 5-fold upregulation of relative ATF3 mRNA expression (normalized to HPRT mRNA expression levels) compared to untreated cells (see Fig. 34). None of the medium changes had an effect on SGK1 expression. With this experiment the conclusion from the previous experiment could be confirmed, namely that ATF3 is an early stress-induced response gene, rather than an early-aldosterone induced gene.

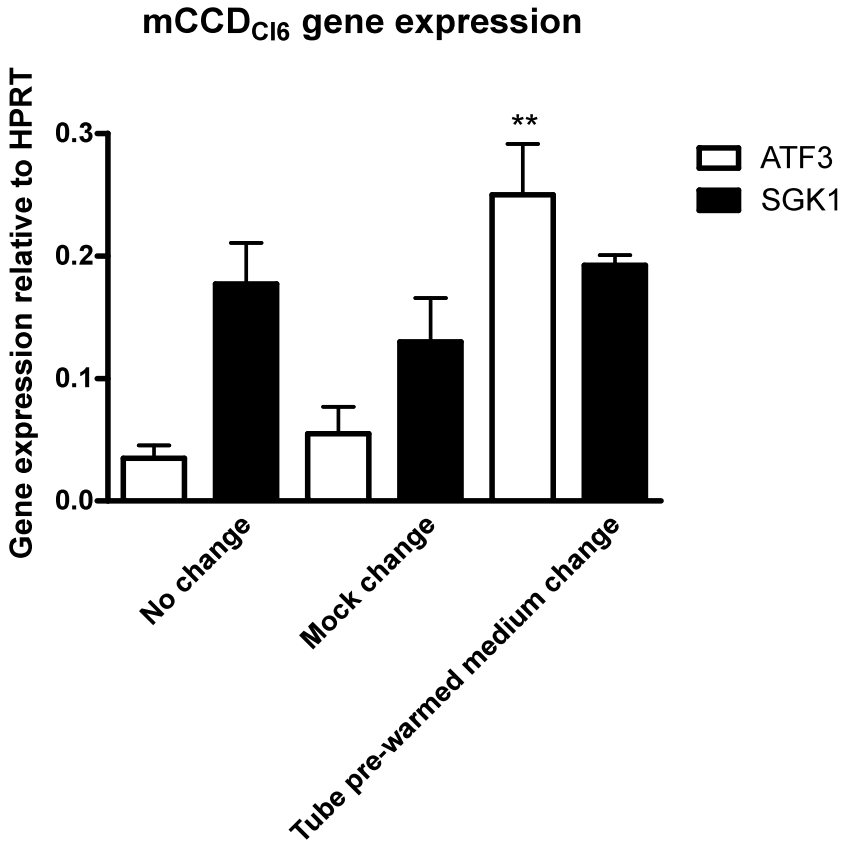

Figure 34: Relative ATF3 mRNA expression is induced after 1 h due to medium change in mCCD$_{Cl6}$ cells: mCCD$_{Cl6}$ cells were serum and growth factor starved for 24 h. Then cells either underwent no medium change, a mock change where the medium on the cells was withdrawn and put back on the cells immediately or a change of medium replacing the old medium with fresh minimal medium pre-warmed in a tube (37°C). After 1 h, only exchanging the old medium with fresh medium pre-warmed in a tube led to an approximately 5-fold increase of ATF3 mRNA expression (normalized to HPRT mRNA expression).This was not observed for SGK1 expression. N=4; ** = $p < 0.01$ t-test and 1-way ANOVA, error bars: SEM. The result relative to Actin is represented in supplementary figure 2.

When analyzing the expression of ATF3 on the protein level it was found to be endogenously expressed at very low levels in untreated mCCD$_{Cl6}$ cells. After treating the cells with either no medium change, a mock or a real medium change,

there was a slight increase in ATF3 protein levels seen 1 h after the treatment (see Fig. 35).

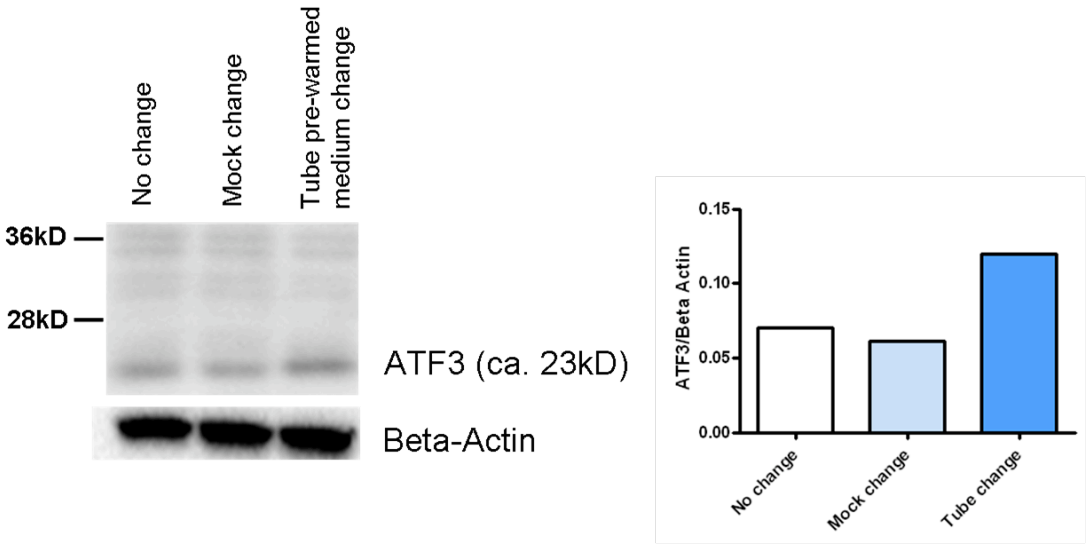

Figure 35: ATF3 expression is induced on the protein level after 1 h medium change in mCCD$_{Cl6}$ cells: mCCD$_{Cl6}$ cells were serum and growth factor starved for 24 h. Then cells either underwent no medium change, a mock change where the medium on the cells was withdrawn and put back on the cells immediately or a change of medium replacing the old medium with fresh minimal medium pre-warmed in a tube (37°C). Using a polyclonal antibody against mouse ATF3 (approximately 23 kD), a slight induction of ATF3 protein after 1 h after exchanging the old medium with fresh medium with pre-warmed in a tube is seen in Western blot (40 µg cell lysate loaded per lane).

5.1.5 JNK/SAPK1, ERK1/2 and p38 phosphorylation are increased mCCD$_{Cl6}$ cells upon the stress of medium change

This chapter describes the work that has been done to investigate which signal transduction pathways might be responsible for the observed increase in ATF3 mRNA and protein levels in mCCD$_{Cl6}$ after a medium change of 1 h (see Fig. 34 and 35).

The literature reports ATF3 to be induced by several pathways of MAPK signalling (see introduction 3.2.2.). We therefore tested whether the medium change induces an increase in phosphorylation of the MAPK p38, JNK or ERK, which could be responsible for the subsequent increase in ATF3 protein by phosphorylating transcription factors that control ATF3 gene expression. However, MAPK phosphorylation is a process of minutes, which might then lead in the end to a delayed ATF3 upregulation after 1 h. Therefore the cells were lysed shortly after the medium change, seven min instead of 1 h to be sure not to miss the phosphorylation events of the MAPK. Also the different properties of the medium change were redefined. The control cell lysates (no medium change) were compared to (1) mock medium changed lysates (aspirating and immediately putting back the same medium on the cells), (2) a medium change where fresh medium was used that was pre-warmed in a tube to 37°C, (3) a medium change where the fresh medium was allowed to CO_2-equilibrate and pre-warm in the incubator at 37°C, or (4) a conditioned medium change where the medium from one well of cells was transferred to another. This allowed investigating whether the cells might produce an inhibitor that would prevent MAPK phosphorylation.

A clear induction of phosphorylation of JNK/SAPK1 could be observed only in $mCCD_{Cl6}$ cells treated with a medium change with medium pre-warmed in a tube (see Fig. 36). For all other conditions phosphorylation levels of the MAPK remained low. Analyzing total JNK/SAPK1 content in the cells revealed that the tube pre-warmed medium change condition showed a band migrating slightly higher than in the other conditions. Admitting that this slightly higher band corresponds to the phosphorylated form of JNK, this would indicate that a substantial proportion of JNK was phosphorylated in this condition. This is coherent with the increased phosphorylation seen in this treatment when using the phospho-specific JNK/SAPK1-antibody.

Western blots using phospho-specific antibodies against the MAPK ERK1/2 also showed the similar patterns observed for JNK/SAPK1 phosphorylation: Only when the medium was replaced with fresh medium that had been pre-warmed

in a tube at 37°C, a higher phosphorylation of ERK1/2 was seen in $mCCD_{Cl6}$ cells compared to all other conditions (see Fig. 37), while total levels of ERK1/2 protein stayed approximately the same in all samples.

Finally, also p38, the third MAPK investigated showed similar behavior when treated with the different medium changes. Also in this case it is the change with medium pre-warmed in a closed tube that led to the strongest induction of p38 phosphorylation while the total protein content stayed mostly constant (see Fig. 38).

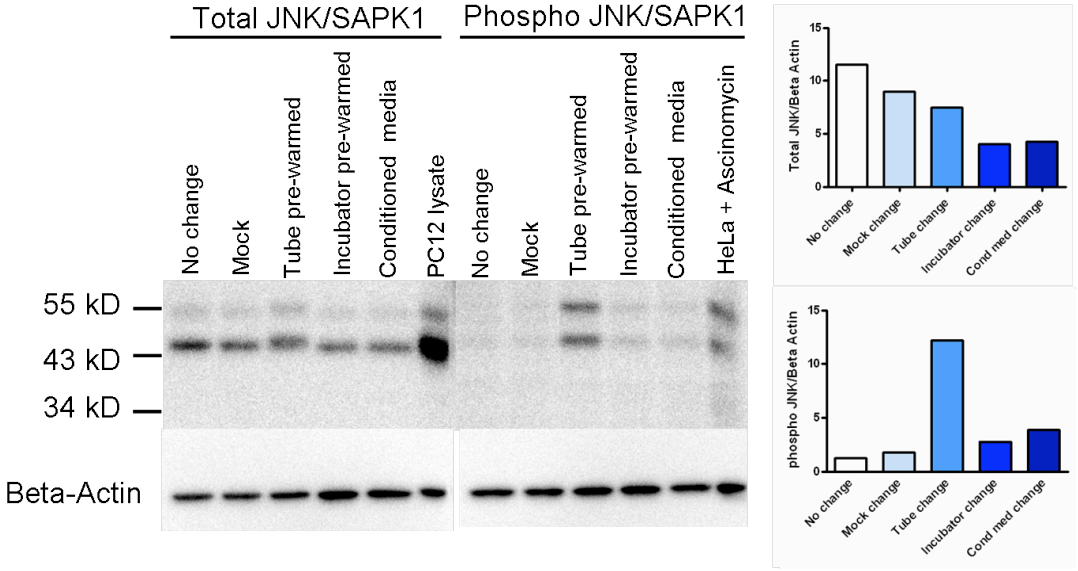

Figure 36: JNK phosphorylation is increased in $mCCD_{Cl6}$ cells upon the stress of medium change: $mCCD_{Cl6}$ cells were growth factor and serum starved overnight. Then they were subjected to different medium changes: (1) A mock change, meaning the medium is aspirated and the same medium is added back to the cells immediately, (2) a medium change where the old medium is replaced by fresh minimal medium that was pre-warmed in a tube, (3) a medium change where the old medium is replaced by fresh medium that was CO_2-equilibrated and pre-warmed in the incubator, (4) a conditioned medium change where the medium is taken from one well of cells and put onto another. All cells were lysed seven min after the medium change took place. As a control, cells were lysed immediately, without a medium change. A clear induction of JNK/SAPK1 (approximately 43 and 56 kD; positive control HeLa + Ascinomycin lysate) phosphorylation is seen only when the medium on the cells was replaced with medium pre-warmed in a tube. Total JNK/SAPK1 (approximately 49 kD; positive control PC12 lysate) amounts stay approximately the same in all conditions.

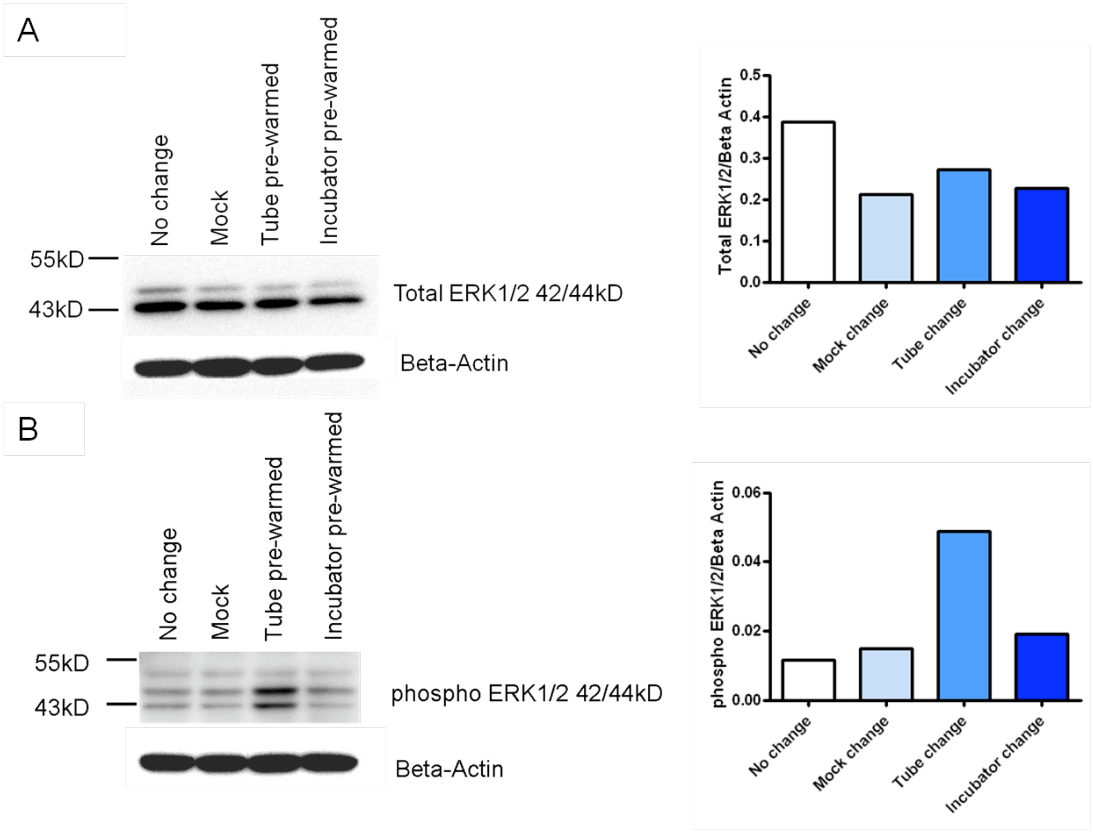

Figure 37: pERK1/2 phosphorylation is increased in mCCD$_{Cl6}$ cells upon the stress of medium change:mCCD$_{Cl6}$ cells were subjected to different medium changes: (1) A mock change, meaning the medium is aspirated and the same medium is added back to the cells immediately, (2) a medium change where the old medium is replaced by fresh minimal medium that was pre-warmed in a tube, (3) a medium change where the old medium is replaced by fresh medium that was CO_2-equilibrated and pre-warmed in the incubator, (4) a conditioned medium change where the medium is taken from one well of cells and put onto another. All cells were lysed seven min after the medium change took place. As a control, cells were lysed immediately, without a medium change. **A:** All conditions showed about equal amounts of total ERK1/2 protein (approximately 42/44 kD). **B:** An induction of ERK1/2 phosphorylation (approximately 42/44 kD) is seen only when the medium on the cells was replaced with medium pre-warmed in a tube and in none of the other conditions.

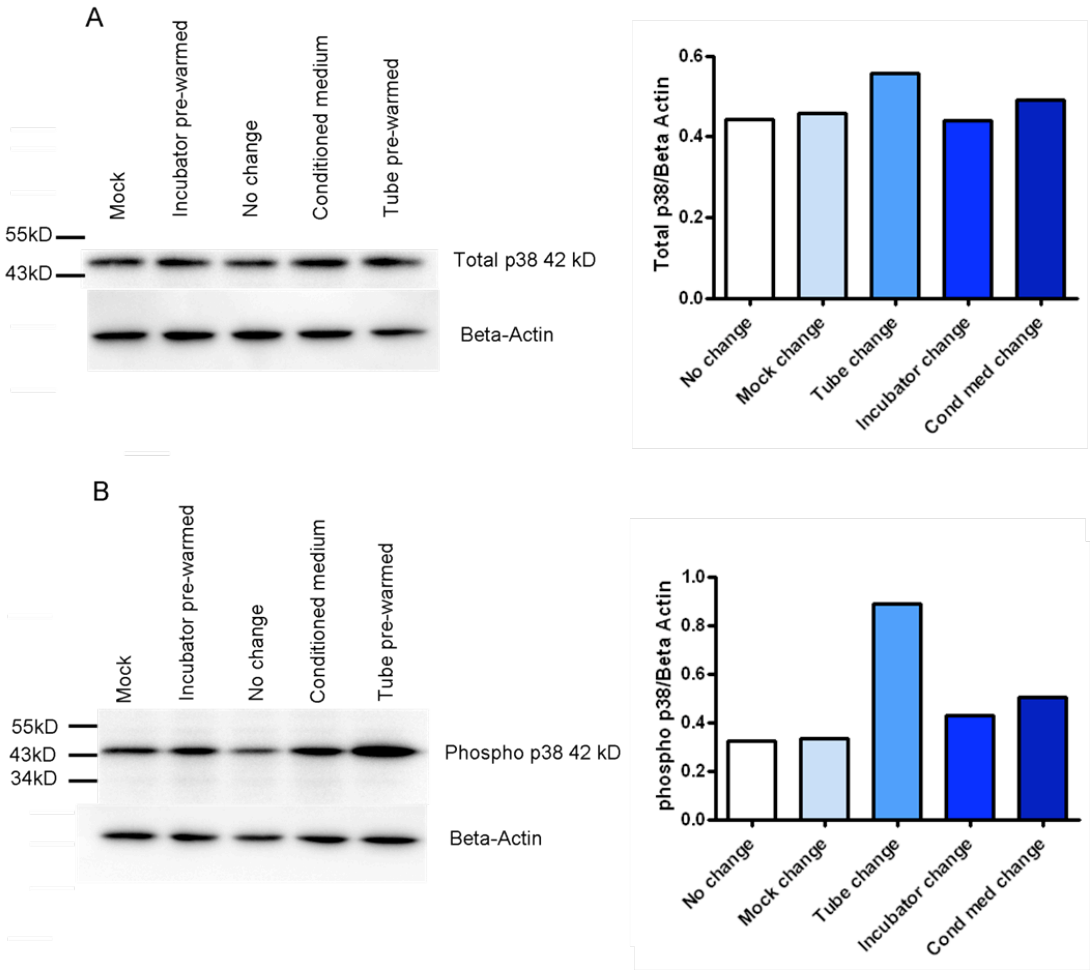

Figure 38: p38 phosphorylation is increased in $mCCD_{Cl6}$ cells upon the stress of medium change: $mCCD_{Cl6}$ cells were subjected to different medium changes: (1) A mock change, meaning the medium is aspirated and the same medium is added back to the cells immediately, (2) a medium change where the old medium is replaced by fresh minimal medium that was pre-warmed in a tube, (3) a medium change where the old medium is replaced by fresh medium that was CO_2-equilibrated and pre-warmed in the incubator, (4) a conditioned medium change where the medium is taken from one well of cells and put onto another. All cells were lysed seven min after the medium change took place. As a control, cells were lysed immediately, without a medium change. **A:** All conditions showed about equal amounts of total p38 protein (approximately 42 kD). **B:** The highest induction of p38 phosphorylation (approximately 42k D) was observed when the medium on the cells was replaced with medium pre-warmed in a tube.

5.2 Regulation and impact of ATF3 expression in mouse kidney (tubules)

5.2.1 NaCl-injection upregulates ATF3 expression but not SGK1 expression specifically in the kidney *in vivo*

The *in vitro* findings in $mCCD_{Cl6}$ cells shown in the previous section made us hypothesize that the induction of ATF3 could be due to stress as well *in vivo*. Since the control mice in the experiment that initially led to the conclusion that ATF3 is an early-aldosterone induced gene were not injected with a physiological saline solution, there was the possibility that the relative upregulation of ATF3 mRNA was due to the stress of the handling and injection, rather than the injected hormone itself. Thus, we hypothesized that a simple injection of a physiological saline solution might be enough to upregulate ATF3 mRNA expression in mice due to a stress reaction (see 3. general introduction). To test whether this reaction would be limited specifically to certain organs of the body, one group of WT C57BL/6 mice was injected with 0.9% NaCl / 0.3% ethanol (the vehicle used for the initial aldosterone-injection experiments) and sacrificed after 1 h while another group of mice was euthanized immediately. Total RNA was extracted from kidney, brain, colon mucosa and heart. qPCR analysis showed that 1 h after the mice were injected with 0.9% NaCl / 0.3% ethanol, the mRNA expression of ATF3 was upregulated specifically in the kidney, compared to non-injected mice (see Fig. 39). This effect was not observed in the other organs tested. In addition, the expression of SGK1 was not altered upon injection of saline solution after 1 h. This was expected since SGK1 has been shown repeatedly to be induced specifically by aldosterone and always served as a positive control in experiments where mice were treated with the hormone. In addition, this result is analogous to the observation made in the *in vitro* studies in $mCCD_{Cl6}$ cells. Thus, we conclude that the 4-fold upregulation of relative ATF3 mRNA expression (normalized to HPRT) *in vivo* is a specific immediate stress response and this effect is specific for the kidney.

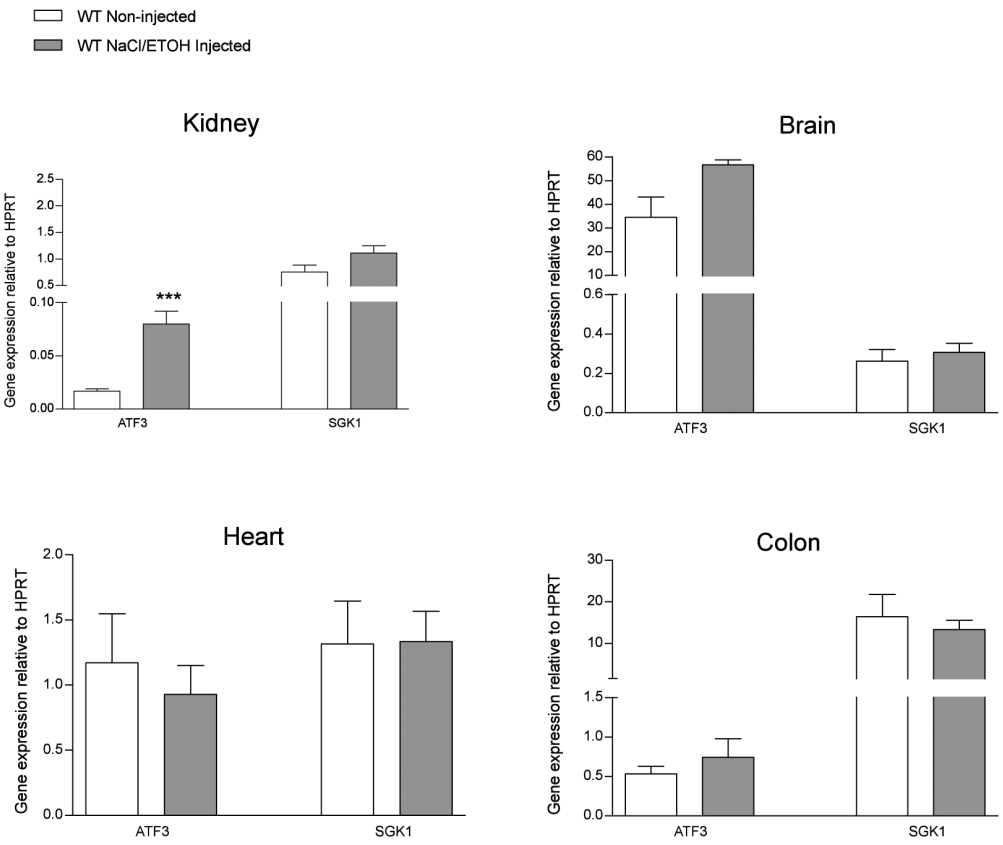

Figure 39: Expression of ATF3 and SGK1 in different mouse organs upon NaCl-Injection in WT C57BL/6 mice: 3 mice per group were either not treated or injected with 0.9% NaCl / 0.3% ethanol. All mice were sacrificed after 1 h. Subsequent total RNA extraction and qPCR shows upregulation of relative ATF3 mRNA expression in the kidney about 4-fold due to injection of saline as compared to mice that have not been injected until they were sacrificed. In brain this effect is only slightly seen as a tendency while in heart and mucosa scraped from the colon there was no difference in ATF3 expression observed. SGK1 mRNA expression is unaffected by injection of the saline solution in all the organs tested (kidney, heart, brain and colon mucosa, normalized to HPRT mRNA expression levels) *** = $p < 0.001$ with student t-test (unpaired) and 1-way-ANOVA. Error bars: SEM. The result represented relative to actin is shown in supplementary fig.1.

The effect of the injection of 0.9% NaCl / 0.3% ethanol was not only restricted to the mRNA level in mouse kidneys. Analyzing whole kidney protein lysates using a mouse polyclonal antibody against ATF3 in Western blots shows that ATF3 is also upregulated on the protein level upon injection when compared to WT mice (see Fig. 40).

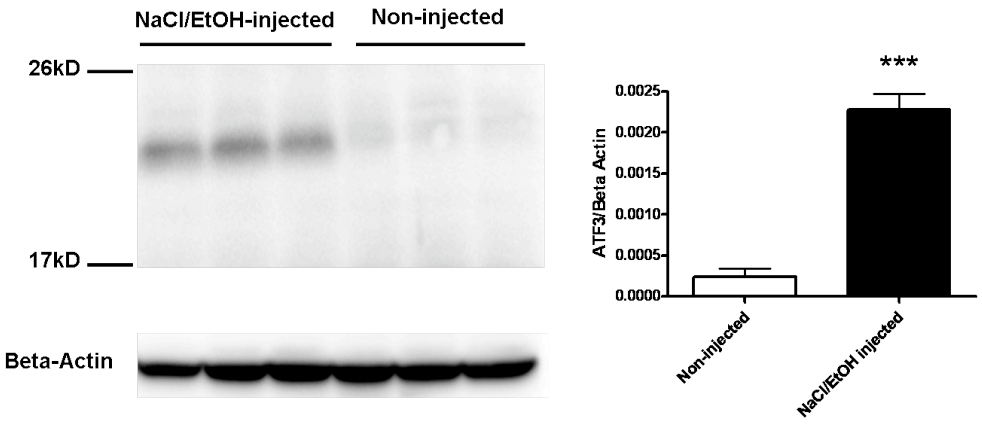

Figure 40: Injection of 0.9%NaCl / 0.3% EtOH induces ATF3 protein expression after 1 h in mouse kidney: 3 WT C57BL/6 mice per group were either not treated or injected with 0.9% NaCl / 0.3% ethanol. All mice were sacrificed after 1 h. In total kidney lysates of NaCl/EtOH injected WT mice ATF3 protein expression (approximately 23 kD, polyclonal antibody 1:500, 40µg of protein loaded per lane) was upregulated compared to the non-injected control group. *** = $p < 0.001$, student t-test (unpaired). Error bars: SEM.

5.2.2 Injection of NaCl/EtOH has no effect on ATF3 mRNA expression but increases protein expression in CNT/CCD

Sorting of kidney tubule segment by COPAS

The original experiment underlying this thesis was performed on micro-selected kidney tubules of the ASDN (CNT/CCD), to allow studying the effect of aldosterone injection on gene expression in this specific part of the kidney. Therefore the question was asked whether the upregulation of ATF3 mRNA as a response

to the stress of an injection was also present and possibly even more pronounced in the ASDN. Micro-selecting tubules is a time-consuming task and the yield of material is usually low. Therefore it was sought to use an automated technique to select more tubules of the ASDN in less time, so that there would be enough material to not only study changes in mRNA expression but also at the protein level. The complex object parametric analyzer and sorter (COPAS) is a machine originally constructed to sort fluorescent *C.elegans* worms but can also be used to sort kidney tubules. The B1GEFP mouse expresses EGFP under the control of the promoter for the B1 subunit of the V-ATPase. This promoter is especially activated in intercalated cells of the CNT/CCD which leads to a specific expression of the fluorescent protein in this kidney tubule segment. 3 groups of mice (11-14 weeks old) were used to select CNT/CCD from: 4 WT B1EGFP C57BL/6 mice that were not injected (control mice), 4 WT B1EGFP C57BL/6 mice that were injected with 0.9% NaCl / 0.3% EtOH and sacrificed after one hour, and 4 non-injected B1EGFP ATF3 KO C57BL/6 mice that do not express ATF3 protein. For all mice a GFP fraction was sorted, assuming to be constituted of CNT/CCD tubules. To get a means of the quality of the sort, also a GFP-negative fraction (whole kidney cortex without green fluorescent CNT/CCD) and the whole kidney cortex were sorted. Total mRNA was extracted from approximately 4000-5600 sorted tubules and analyzed with qPCR. To check for specificity of the GFP-sorted tubules, we looked at the water channel aquaporine 2 (AQP2) and ENaC which should be enriched in the CNT/CCD fraction as compared to the negative tubules and the whole kidney cortex fraction. Indeed this was the case (see Fig. 41). Furthermore the proximal tubule sodium/phosphate co-transporter NaPi2a was lower in the GFP-sorted fractions as opposed to the GFP-negative fraction or whole kidney cortex. The Na/Cl-co-transporter NCC is expressed in the DCT. It was also enriched in the GFP-negative fraction and the whole kidney cortex compared to GFP-sorted tubules on both injected and non-injected mice. We conclude that the GFP-positive sorted material in all three mouse groups shows the expected gene expression profile of CNT/CCD.

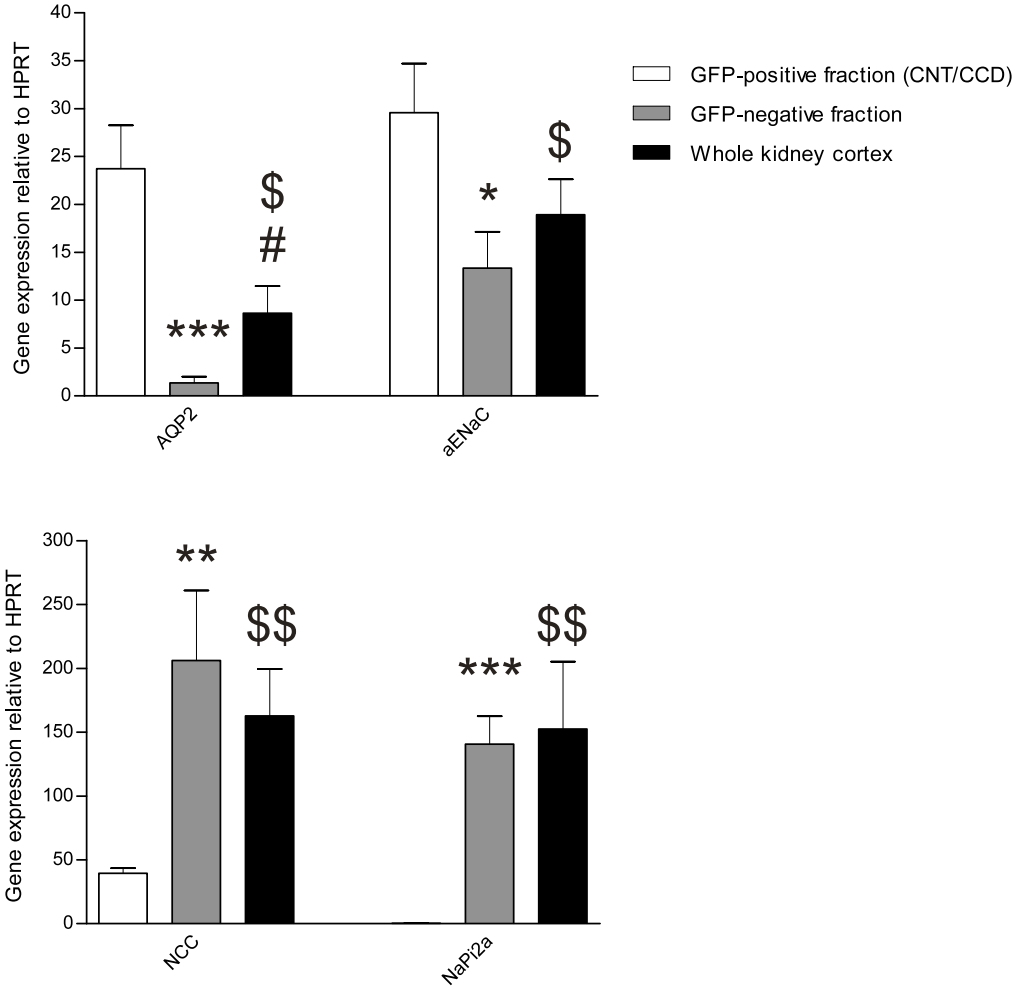

Figure 41: Characterization of COPAS-sorted tubule segment. Expression of specific genes was compared in the different tubule fractions: GFP positive (CNT/CCD) vs. GFP-negative tubules and total cortex tubules (pooled from 12 mice). Four mice per group (non-injected vs. 0.9% NaCl / 0.3% EtOH injected for 1 h) and ATF3 KO B1EGFP C57BL/6 mice) were sacrificed and kidney tubule suspensions were sorted with COPAS. Total RNA extraction and qPCR was performed. The CNT/CCD markers AQP2 and ENaC were enriched in the GFP-positive fractions compared to the negative fraction or whole kidney. This is accompanied by a lower expression of NaPi2a (proximal tubule) and NCC (DCT) in the GFP-sorted fraction compared to the other two fractions. All values of gene expression are relative to HPRT mRNA expression. * compares WT non-injected to WT injected mice; $ compares WT non-injected to ATF3 KO non-injected mice; # compares WT injected to ATF3 KO mice. *, $ and # = $p < 0.05$; **, $$ and ## = $p < 0.01$; *** = $p < 0.001$ with student t-test (unpaired). Error bars: SEM.

Three genes of interest were investigated whether they were regulated specifically in the COPAS sorted CNT/CCD fraction: ATF3, ATF4 and CHOP10. First, ATF3 mRNA expression was measured to test whether the injection of NaCl/EtOH has an even stronger effect on the relative mRNA expression of this transcription factor in this specific kidney segment than had been observed in whole kidney lysates beforehand. Second, the effect of the injection on ATF4 was examined, an upstream factor of ATF3 which is know to bind to the ATF3 promoter and to induce its transcription [110]. Last, the influence of the saline injection on expression of CHOP10, a target repressed by ATF3, was studied [49].

Effect of saline injection on mRNA expression in WT C57BL/6 WT mice and comparison with ATF3 KO mouse

Surprisingly the expected induction of relative ATF3 mRNA expression could not be observed in the CNT/CCD fraction when WT B1EGFP mice were injected with 0.9% NaCl / 0.3% EtOH for 1 h when compared to non-injected WT B1EGFP control mice (see Fig. 42). In the GFP-negative fraction and the whole kidney cortex the expected upregulation of ATF3 mRNA levels was seen as a tendency in injected WT B1EGFP mice compared to non-injected mice. As expected there was no expression of ATF3 in the ATF3 KO B1EGFP mice.

CHOP10 expression was not changed in WT B1EGFP mice in the CNT/CCD fraction; it was the same in all three groups of mice tested. Only in the GFP-negative sorted fraction CHOP10 mRNA levels showed a tendency to be decreased with the injection and even were lower in the ATF3 KO B1EGFP mouse.

ATF4 mRNA was equally expressed throughout all three fractions sorted by the COPAS. Also there was neither a difference observable between WT and ATF3 KO mice nor between the non-injected and injected mice.

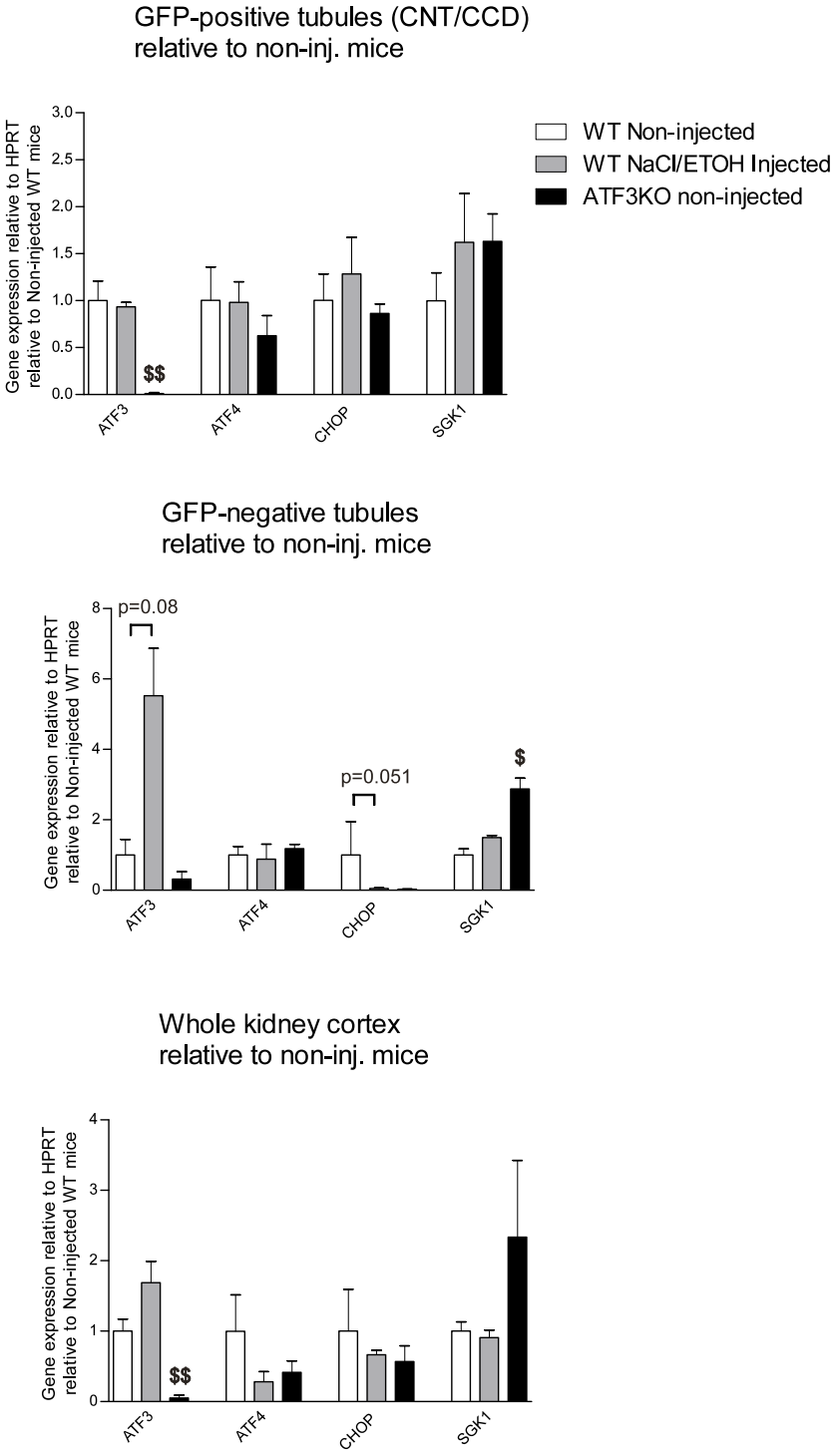
GFP-positive tubules (CNT/CCD)
relative to non-inj. mice
Gene expression relative to HPRT
relative to Non-injected WT mice
3.0
2.5
2.0
1.5
1.0
0.5
0.0
$$
ATF3
ATF4
CHOP
SGK1
WT Non-injected
WT NaCl/ETOH Injected
ATF3KO non-injected
GFP-negative tubules
relative to non-inj. mice
Gene expression relative to HPRT
relative to Non-injected WT mice
8
6
4
2
0
p=0.08
p=0.051
$
ATF3
ATF4
CHOP
SGK1
Whole kidney cortex
relative to non-inj. mice
Gene expression relative to HPRT
relative to Non-injected WT mice
4
3
2
1
0
$$
ATF3
ATF4
CHOP
SGK1

Figure 42: Effect of i.p. vehicle injection on gene expression in the different tubule fractions compared to non-injected and ATF3 KO mice. The GFP-sorted fraction (CNT/CCD), GFP-negative-sorted fraction and whole kidney cortex were sorted from WT B1EGFP (non-injected vs. 0.9% NaCl / 0.3% EtOH injected for 1 h) and ATF3 KO B1EGFP C57BL/6. Four mice per group were sacrificed and kidney tubule suspensions were sorted with COPAS. Total mRNA extraction and following qPCR was performed. Gene expression was normalized relative to HPRT expression in the different mouse groups and then normalized to the non-injected WT B1EGFP mice (= 1). Relative levels of ATF3 mRNA were not altered by the stress of NaCl/EtOH injection in the CNT/CCD (GFP-positive) sorted fraction in WT B1EGFP mice compared to non-injected WT B1EGFP mice. The injection only showed a tendency to increase in ATF3 mRNA levels in the GFP-negative sorted and the whole kidney cortex fraction of the injected WT B1EGFP mice compared to control. As expected, ATF3 expression was missing in the ATF3 KO B1EGFP mice. No effect of the injection or the lack of ATF3 in the KO mice was observed in relative mRNA expression levels of ATF4 throughout all the fractions. The expression of the ATF3 target protein CHOP10 mRNA is decreased in the negative sorted fraction of injected WT B1EGFP mice compared to the non-injected control and even lower in the ATF3 KO mice. In ATF3 KO mice, a trend of higher SGK1 levels compared to WT non-injected mice was observed in the GFP-negative and the whole kidney cortex fraction. N=4; except negative kidney fractions of WT non-injected and WT injected mice (N=2). * compares WT non-injected to WT injected mice; $ compares WT non-injected to ATF3 KO non-injected mice. $ = $p < 0.05$; ** and $$ = $p < 0.01$ with student t-test (unpaired). Error bars SEM.

The expected upregulation of ATF3 by the saline injection could not be observed on the mRNA level in CNT/CCD sorted tubules. However, when analyzing protein lysates of these tubules, a clear induction of ATF3 protein due to the injection was observed in B1EGFP WT mice compared to the endogenous ATF3 level in non-injected B1EGFP WT mice. Also CNT/CCD lysates from ATF3 KO mice do not show this band at the level of 23 kD where ATF3 protein is expected to migrate, confirming the antibody specificity (see. Fig 43 A). Furthermore, expression of AQP2 was unaffected by the injection of 0.9% NaCl / 0.3% EtOH in CNT/CCD of B1EGFP WT mice and B1EGFP ATF3 KO mice (see Fig 43 B).

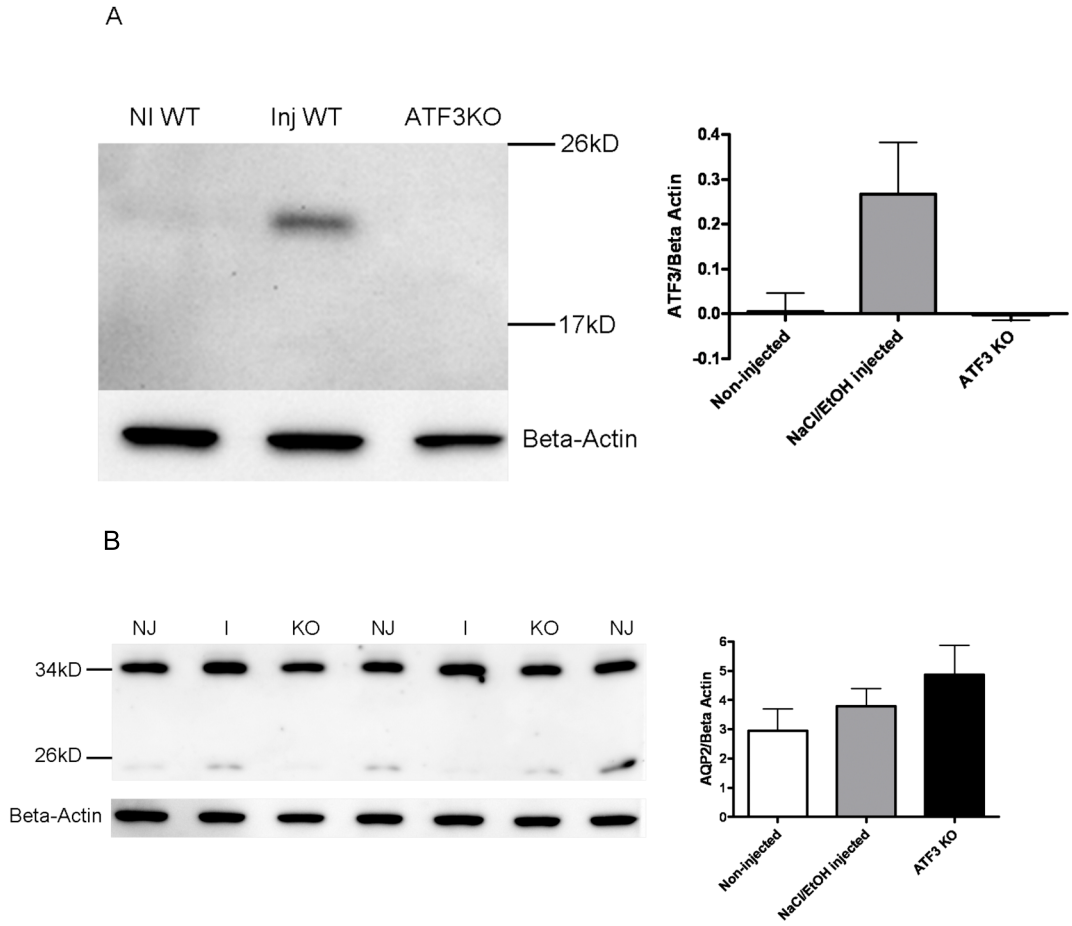

Figure 43: ATF3 protein expression is upregulated due to injection of NaCl/EtOH in CNT/CCD of B1EGFP WT mice: The GFP-sorted fraction (CNT/CCD) of WT B1EGFP mice (non-injected (NI WT) vs. 0.9% NaCl / 0.3% EtOH injected (Inj WT) for 1 h) and ATF3 KO B1EGFP mice were investigated for ATF3 protein expression. **A:** Western blot analysis shows a clear induction of a band migrating at the expected size for ATF3 protein (ca. 23 kD) in injected B1EGFP WT mice compared to non-injected littermates. Basal ATF3 expression in non-injected mice is almost not detectable in WT B1EGFP CNT/CCD tubule lysates. The band is absent in non-injected ATF3 KO mice. **B:** Western blot analysis using an antibody against AQP2 reveals a band running at 35 kD corresponding to the glycosylated form of the water channel, while the weaker band running at 25 kD represents unglycosylated AQP2. The injection of 0.9% NaCl / 0.3% EtOH did not significantly influence the expression of AQP2 in B1EGFP WT mice compared to non-injected B1EGFP WT mice and B1EGFP ATF3 KO mice. Approximately 400 tubules were loaded per lane, N=4. Error bars: SEM.

5.2.3 Characterization of ATF3 knockout mouse

Since there have only been a few studies using isolated cells from the ATF3 KO mouse[105] and no description of its phenotype has been published, it was decided to perform metabolic cage experiments to characterize parameters in comparison to WT C57BL/6 mice. Mice were placed into metabolic cages for an accommodation phase of two days with one day of resting phase in between. Then they were kept in the metabolic cage for the experimental period of four consecutive days (see Fig. 44) to determine water and food consumption, as well as urine and feces production and to follow the weight gain or loss. On the third day of the experiment, we challenged the mice with a 23-hour-water-deprivation. If ATF3 played an important role specifically in the kidney (that might be stress-related) the knockout mice might show different ability of coping with this insult.

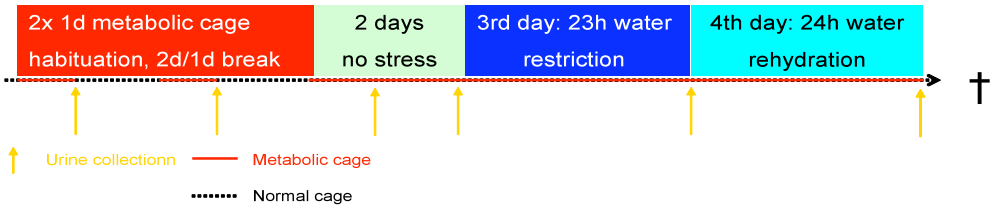

Figure 44: Timecourse of metabolic cage experiments to characterize WT C57BL/6 vs. ATF3 KO mice: First the mice were allowed to adapt to the metabolic cages two times for one day with a one- or a two-day break in normal cages in between. Then the animals were kept in metabolic cages for two days without any stress challenge. On the third day no water was supplied to the animals for 23 hours (water deprivation). On the 4th day of the experiment, mice were allowed to drink again (rehydration). After another day, the animals were sacrificed. During the whole experiment animals were weighed and food/water consumption as well as urine/feces production was determined.

Over the whole period of the experiment the ATF3 KO animals had a tendency to weigh slightly less (approximately 1 g) than the WT mice. The weight changes were paralleled over the timecourse of the experiment in both groups. Both ATF3 KO as well as WT mice showed a similar transient drop in weight upon

23-h-water-deprivation (see Fig. 45 A).

The food and water consumption was the same for WT or ATF3 KO animals over the whole period in the metabolic cage, including the water deprivation (see Fig. 45 B and C). On this day, along with the water restriction, there was a decrease in food consumption observed (see Fig 45 C). The ATF3 KO mice showed a tendency to produce less urine than the WT mice but this difference was not significant. There was a decrease in urine production after the water deprivation, while 24 h after the mice were rehydrated, urine levels were back to the former level in both groups of mice (see Fig. 45 D). Also the amount of feces produced by the mice was similar for WT and ATF3 KO mice, after the water deprivation, fewer feces were produced in both groups and the feces produced were much drier (see Fig. 45 E).

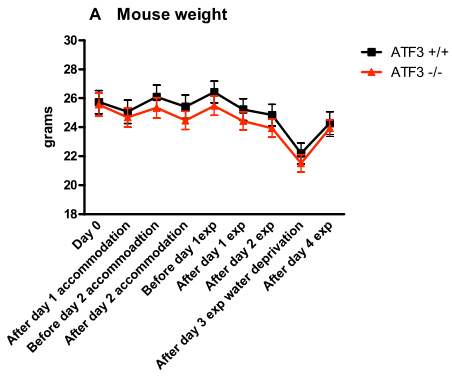
A Mouse weight
grams
30
28
26
24
22
20
18
Day 0
After day 1 accommodation
Before day 2 accommoadtion
After day 2 accommodation
Before day 1exp
After day 1 exp
After day 2 exp
After day 3 exp water deprivation
After day 4 exp
ATF3 +/+
ATF3 -/-

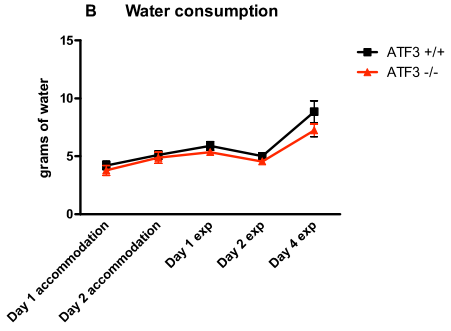
B Water consumption
grams of water
15
10
5
0
Day 1 accommodation
Day 2 accommodation
Day 1 exp
Day 2 exp
Day 4 exp
ATF3 +/+
ATF3 -/-

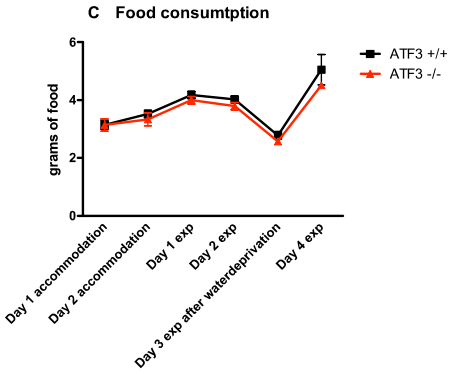
C Food consumtption
grams of food
6
4
2
0
Day 1 accommodation
Day 2 accommodation
Day 1 exp
Day 2 exp
Day 3 exp after waterdeprivation
Day 4 exp
ATF3 +/+
ATF3 -/-

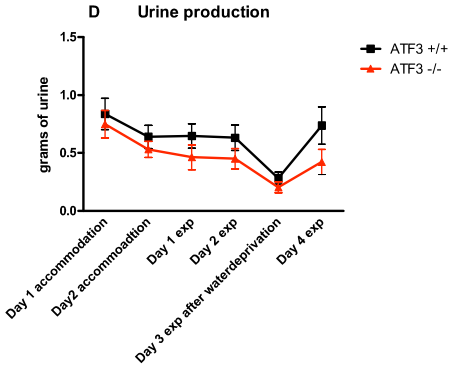
D Urine production
grams of urine
1.5
1.0
0.5
0.0
Day 1 accommodation
Day2 accommoadtion
Day 1 exp
Day 2 exp
Day 3 exp after waterdeprivation
Day 4 exp
ATF3 +/+
ATF3 -/-

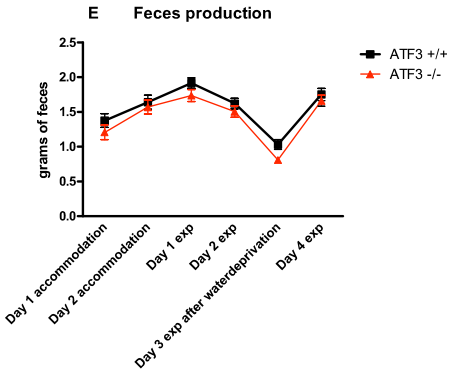
E Feces production
grams of feces
2.5
2.0
1.5
1.0
0.5
0.0
Day 1 accommodation
Day 2 accommodation
Day 1 exp
Day 2 exp
Day 3 exp after waterdeprivation
Day 4 exp
ATF3 +/+
ATF3 -/-

Figure 45: Characterization of WT C57BL/6 vs. ATF3 KO mice: A: The weight in both groups changed in parallel during the experiment. After water deprivation there is a clear loss in weight in both groups. **B:** Mice of both the WT or ATF3 KO group drank same amounts of water which increased after the water deprivation on the third day of the experiment. **C:** Food consumption was the same for both WT and ATF3 KO mice; it was almost reduced by half after the day of water deprivation and increased to even higher levels than in the beginning of the experiment when mice were rehydrated on day 4. **D:** Urinary excretion constantly decreased in both groups over the course of the experiment. It reached the minimum after the water deprivation phase and went back up to baseline levels after the rehydration. There was no significant difference between the two groups of mice. **E:** Feces production was parallel in WT and ATF3 KO mice. It first increased until the first day of the experiment. After water deprivation, on the third day of the experiment, there were the lowest amounts of feces excretion observed in both groups. Allowing the mice to drink water again restored feces production to similar levels as on the days before. N=19. Error bars: SEM.The separate results for males or females are represented in supplementary figure 3 and 4, respectively.

6 Discussion

6.1 Potential role of ATF3 as aldosterone-induced gene product in the kidney ASDN

The aim of this thesis was to gain more insight into the role of activating transcription factor 3 in the kidney. The underlying observation that motivated this aim was the fact that the ATF3 mRNA was 3.5-fold upregulated in the aldosterone sensitive part of the nephron in a previous study [7]. So far no other report has been published on a link between aldosterone and ATF3 in the kidney. We initially hypothesized that aldosterone-induced ATF3 might play a role in the action of aldosterone in the ASDN. Specifically the hypothesis was that ATF3 would regulate the expression of genes that are involved in the aldosterone-stimulated stabilization of ENaC in the apical membrane of epithelial cells in the ASDN, its increased recruitment to the membrane and function and/or the anabolic action of aldosterone, namely the increase of the energy providing machinery, of the membrane surface etc. So far the key players in these events are only partially known. Finding that a transcription factor is upregulated by aldosterone opened a lot of new room for speculation about what happens between the binding of aldosterone to its target gene promoters and the final increase in Na^+-transport via ENaC that is the outcome for the cell. ATF3 is a transcription factor that dimerizes with itself and also forms heterodimers with various other transcription factors, also from other transcription factor families. Depending on the combination of the dimerization partner, ATF3 might either repress or activate transcription of its target gene [29]. We wanted to find possible targets of ATF3 to reveal players further down the line towards Na^+-transport regulation by aldosterone. It was reported that aldosterone has short term effects as well as long term effects. A short term effect is represented in the upregulation of gene transcripts that immediately affect Na^+-transport via ENaC. The proteins formed from these transcripts might then cause long term effects on the cells, for example

by initiating differentiation, leading to formation of more mitochondria to meet the increased energy needs that results from increased Na^+- and K^+-ion transport rates. Furthermore during the differentiation the cells form many invaginations of the basolateral membrane to make sure that the excess Na^+ taken up by ENaC apically can be released into the blood stream on the basolateral side of the cell. Supporting this hypothesis, ATF3 regulates the expression of certain proteins that are involved in gene differentiation. One example is the inhibitor of differentiation (ID1). ATF3 binds to a target sequence in the ID1 promoter and therefore inhibits transcription of the gen [48]. This would contribute to the differentiation of the cell and rather inhibit it from proliferating further on. To investigate the role of ATF3 in long-term aldosterone effects *in vitro*, namely in the differentiation of the cell, we generated a mpkCCD$_{Cl14}$ cell model that shows Dox-inducible overexpression of ATF3. The aim was to functionally investigate this cell line in an Ussing chamber setup to test whether overexpressing ATF3 has an effect on transepithelial short circuit currents or transepithelial resistances, both markers of differentiated principal cells. Furthermore it was planned to investigate possible morphological effects of differentiation.

6.2 Cortical collecting duct cell lines to study the role of ATF3 in sodium transport

The mpkCCD$_{Cl14}$ KRABATF3 transduced cells originally generated to study ATF3 function on cell differentiation showed a considerable induction of expression of the transcription factor when treated with Dox for 3 days (see Fig. 24-26). However, when we performed functional tests in the Ussing chamber, neither the transduced cells nor the WT cells seemed to respond to aldosterone stimulation by increasing their transepithelial short circuit Na^+ -currents. The work could not be continued under these conditions, where the basic physiological response specific for this cell line was not reproducibly observed. Trying various optimization measures (change of FCS batch, media compositions, coating conditions of

transwell filter growth supports, cell number etc.) did not change this fact (see. Fig. 28). Contacting other laboratories working with the Ussing chamber and principal cell lines revealed that also other research groups faced similar problems, as well with another mouse cortical collecting duct cell line, the $mCCD_{Cl1}$. The group of Prof. Olivier Staub isolated a new clone of this cell line the clone 6, which reproducibly displayed the expected induction of transepithelial current upon addition of aldosterone in Ussing chamber, which could be blocked with amiloride, confirming that the induced current was a Na^+-current mediated via ENaC (see Fig. 29). Since the ability of the model cell line to respond to aldosterone by increasing ENaC-mediated current was an absolute prequisite for our study, we could therefore not use the ATF3KRAB overexpressing $mpkCCD_{Cl14}$ that had been a time consuming work. In particular, the $mpkCCD_{Cl14}$ cells turned out to be more resistant to lentiviral transduction than HEKT293 cells, HeLa cells or MDCK cells that were used for GFP controls of virus infectivity (data not shown). Since it was decided to use $mCCD_{Cl6}$ cells instead of the $mpkCCD_{Cl14}$ cells, we tried to transduce these cells with KRAB and ATF3 lentiviral constructs as had been done previously for the $mpkCCD_{Cl14}$ cells. All attempts were not successful. The GFP control construct revealed that the GFP expression was lost within a few days, the transduction rates were very low (approximately 10-20%, data not shown), suggesting that a stable insertion of the transduced gene did not take place. In the context of the Ussing chamber studies with $mpkCCD_{Cl14}$ cells, we also tested aldosterone induced ATF3 transcription *in vitro* in this cell line. Surprisingly it was found that aldosterone itself did not have the expected effect on the transcription factor and that it was rather the stress of a medium change performed when adding the aldosterone to the cells that led to this effect.

6.3 Stress induction of ATF3 in cultured CCD cells and in mouse kidney

Based on the observation that the induction of ATF3 mRNA levels in $mCCD_{Cl6}$ WT cells is due to the medium change rather than to aldosterone, it was decided

to adapt the focus of the project. The new focus was the characterization of the stress-related induction of the transcription factor ATF3 in kidney epithelial cells, how it is mediated and possibly its functional consequences. There are numerous reports in the literature about ATF3 being an immediate stress-induced gene and this has also been found to be true for the kidney. Mouse models of ischemia-reperfusion kidney injury showed that an overexpression of ATF3 protected the kidneys from the insult compared to mice that had normal ATF3 levels. Since ATF3 is also found in urinary exosomes it has been suggested that this transcription factor might be a marker for kidney injuries. We tested the possibility that the ATF3 induction observed following aldosterone injection in mice was analogous to the stress-induction of ATF3 observed in the *in vitro* studies. Mice were injected mice with a physiological saline solution to test whether the effect of restraining and injecting per se could have the same effect on kidney cells as the *in vitro* medium change did. Working with animals, there are at least two groups compared to eachother: a "non-treated" group vs. a treated group. When animals are injected with a certain substance to provoke a reaction of interest, there is always a second group that is injected with the vehicle. This group is then considered as a "not-treated negative control". The need of a similar treatment of the control animals is substantiated by the study of Rulter et al., who showed that injecting only saline i.p. into mice can have an effect on gene expression of specific genes in the brain [111]. This report clearly questions the reliability of results compared from two groups, a treated and an untreated group when looking at gene expression. From the initial experiment performed by Fakitsas et al. it had been concluded that ATF3 is upregulated by aldosterone. In this study the control group was indeed untreated and sacrificed without injection beforehand and the results of the more adequate control, namely the mice injected with a mineralocorticoid receptor antagonist (canrenoate) had not been used due to apparent technical problems. When the first evidence from our *in vitro* experiments pointed out that ATF3 is stress-regulated rather than aldosterone regulated, we decided to see if the injection of 0.9% NaCl / 0.3% EtOH (this being the solvent from the original study that revealed ATF3 to be

aldosterone related) per se could specifically upregulate ATF3. Like Rulter et al., we also found that the i.p. injection of saline was enough to induce specific mRNAs, in this case ATF3 mRNA in kidney. In contrast, this was not the case for SGK1, a gene product induced by glucocorticoids and thus stress-sensitive. The expression of a series of genes was measured not only in kidney but also in brain, colon and heart. ATF3 levels were upregulated only in kidney, indicating that this effect has a certain specificity.

6.4 Test of injection-stress induced ATF3 regulation in COPAS-sorted tubule segments

Since ATF3 upregulation had originally been observed after aldosterone-injection in the CNT/CCD micro-selected tubule material sorted by Fakitsas [7], it appeared meaningful to test whether the effect of saline injection was present in this tubule segment as well. To do so, green fluorescent CNT/CCD tubules from a mouse that expresses EGFP in intercalated cells only under the control of the B1 (V-ATPase subunit) promoter were sorted with a COPAS.

Unexpectedly the hypothesis that ATF3 mRNA levels might be strongest upregulated in the CNT/CCD due to the saline injection could not be confirmed. Furthermore, there is only a tendency seen for ATF3 mRNA induction in negative sorted fractions and whole kidney fractions. For these two fractions the RNA quality was quite low in two samples per group, so we could only include an N=2 in our data analysis. This is why we cannot say that the ATF3 upregulation seen in the two before mentioned fractions is significant; nevertheless, the tendency is clearly distinguishable.

Thus, one reason why we were possibly not able to see the predicted upregulation of ATF3 mRNA levels in the CNT/CCD sorted tubules by COPAS is rather technical than biological: the sorting process takes 8 h which is considerably long. The quality of the tubule preparation is crucial and depends mainly on the

perfusion quality and also on the digestion in the collagenase solution. Kidney tubules from mice where the perfusion failed to give nicely perfused kidneys had a lower green fluorescence to start off with and this fluorescence decreased with time, making the sorting process slower. Therefore the samples spent up to 8 h on ice. It is possible that during this time certain species of mRNA are more degraded than others. Moreover, since ATF3 is found in such low abundance in the kidney as well as in other organs in general, it is likely that degradation of mRNA soon reaches a level where ATF3 mRNA expression falls below the detectable limit. Most probably there was also mRNA degradation for the other candidates investigated, however mRNA levels e.g. for NaPi2a and NCC are much higher in the kidney. Thus, detecting these species was still possible, even if there might also have been less mRNA after 8h of sorting than at the time when the kidney was extracted from the mouse. Furthermore samples were not cooled during the sorting period of approximately 5 min. This might also be an explanation why the effect on ATF3 mRNA observed in the first injection experiment (where the whole kidney was lysed) was more pronounced than in the negative sorted and the whole cortex fraction from the COPAS sorted tubules: The process of sample preparation was indeed much faster for the initial experiment done with whole kidney extracts than with the sorted tubules. When preparing kidney lysates from whole kidneys, the organs were immediately snap-frozen after sacrificing the animal for later processing of the tissue.

Testing the ATF3 protein expression in the selected tubule fractions was thus not only crucial because the protein is the active product of a gene, but also in regard of the suspected mRNA degradation that had taken place during the tubule selection procedure. Importantly, Western blotting revealed indeed a strong upregulation of ATF3 protein in the CNT/CCD sorted tubules of all 4 mice injected with the saline solution (see Fig. 43 A) compared to the 4 non-injected littermates. The ATF3 band detected in Western blot was at the expected size of approximately 23 kD and was missing in the CNT/CCD tubules sorted from B1EGFP ATF3KO mice. Indeed, as shown in Supplementary Fig. 7,

a weak ATF3 band was seen in the non-injected B1EGFP WT mouse CNT/CDD samples, whereas in constrast this band was always completely absent in the B1EGFP ATF3 KO mice. As a control AQP2 protein expression was tested, which was, as expected, not regulated by the stress of a saline injection (see Suppl. Fig 6).

The goal of sorting CNT/CCD with COPAS was not only to test the effect of injection on ATF3 mRNA expression in these kidney segments, but to also test upstream and downstream factors of ATF3. Therefore the gene expression of two candidates was measured: First, ATF4 which is found upstream of ATF3, binding its promoter and increasing its transcription [110] [113]. ATF4 relative mRNA levels were not altered in any of the mice or fractions studied. This result suggests that the stress-induced activation of ATF3 in the saline injected mice is not mediated via ATF4. However, this result needs to be considered with caution in view of the probable mRNA degradation that took place during the sorting procedure. Second, we studied CHOP10 which lies downstream of ATF3. There is an ATF3 target site in the CHOP10 promoter, allowing it to bind and to repress the expression of CHOP10. Interestingly CHOP10 itself actually inhibits the function of ATF3 by forming a non-functional heterodimer with it [114]. CHOP10 is able to bind to ATF3 because it also contains a leucine zipper region, which allows the dimerization [115]. Thus, ATF3 represses the expression of its own inhibitor [49].Therefore the expectation was that the levels of CHOP10 mRNA would be higher in the ATF3 KO B1EGFP mouse than in the B1EGFP WT mice and possibly lower in mice that were injected with the saline solution, due to upregulated ATF3. CHOP10 relative mRNA levels were by trend lower in the negative sorted fractions of WT injected mice compared to negative sorted fractions from WT mice that were not injected with the saline solution. However, the ATF3 KO mice show the same low expression levels of CHOP10 as do the injected WT mice. This does not support the notion that ATF3 KO mice would have higher levels of CHOP10, due to the abundance of this repressor. Whether another transcription factor can take over the role of ATF3 in repressing CHOP10

transcription is not known. Also this result has to be considered with caution, since apparently mRNA degradation took place during the sorting process (see above for ATF3). Thus, additional experiments, in particular at the protein level would be necessary to confirm the results for ATF4 and CHOP10 and to draw reliable conclusions on how these two transcription factors are regulated by the NaCl/EtOH-injection.

6.5 Lack of gross metabolic phenotype in ATF3 KO mice

The ATF3 KO mouse was so far only used to study pathological conditions, such as different types of diabetes and involvement of the transcription factor in immune reactions. The group of Prof. T. Hai (Ohio, USA) that originally generated the mouse mostly takes interest in studying the effects of ATF3 in pancreatic beta cell islets in diabetic mice. It has been shown that transplanting pancreatic islets from healthy donors into diabetic rodents can normalize blood glucose levels. However, transplanting islets is a difficult task and recipients need to be immunosuppressed to do so. Hai et al. found ATF3 to contribute to apoptotic cell death in WT pancreatic beta cell islets. Apparently ATF3 KO islets show a better survival than the WT islets [116]. They also found ATF3 to be induced in mouse macrophages by lipopolysaccharide (LPS), a toxin that is released from bacteria. LPS binds to Toll-like receptor 4 (TLR4) which is a receptor on the endosome surface in macrophages. TLRs promote the formation of toxic cytokines to contribute to the immune reaction caused by the LPS, to help fight the infectious intruders. The role of ATF3 once induced by LPS via TLR4 is to constitute a negative feedback loop that regulates the TLR4 signalling, keeping the macrophages from producing an unattenuated immune reaction [117].

So far there was no characterization of ATF3 KO mice performed on the level of basic physiological body functions like water and food uptake going along with

urine and feces excretion. We hypothesized that since we found ATF3 to be regulated specifically in the kidney upon stress, there might be a kidney phenotype when knocking out the transcription factor compared to WT mice. Furthermore, there was the possibility that ATF3 KO mice might not be able to respond adequately to a stressor. Thus, we also performed a 23-h water deprivation in the course of a metabolic cage experiment designed to test the gross parameters mentioned above. No significant differences were observed between ATF3 KO and WT mice for urine and feces excretion, food and water uptake and handling the stress of a water deprivation (see Figs. 45 A-E). ATF3 KO mice showed a tendency to be slightly lighter than the WT mice. Both groups of mice drank about equal amounts of water and also increased their drinking similarly after being re-supplied with water following the water deprivation. Moreover, WT as well as ATF3 KO mice ate less during the time of water deprivation. This is most probably due to the fact that the food was supplied as a dry powder, which was less attractive when no water was provided in parallel. Urine and feces excretion both decreased during the water deprivation to similar extents in both groups, which paralleled the decrease in water and food intake. This is also why the mice lost weight during this period. After the water deprivation the mice returned to the baseline levels of urine and feces production as shown before the stress period. Due to the very strict animal laws in Switzerland, the mice could only be kept 4 days in the metabolic cages, preventing to further analyze how long it took for the mice for normalizing their food and water intake. Nevertheless we conclude that the kidneys of ATF3 KO mice seem to function normal and are also able to respond to the stress of water deprivation as the kidneys of WT mice do. Moreover, there was no difference between males and females found in this experimental setup (see supplementary material Figs. 3 and 4).

It is not very surprising that the KO mouse of the transcription factor ATF3 is viable and does not show any obvious phenotype. This is most probably due to the mode of action of ATF3. Since it heterodimerizes with so many other transcription factors, there might be for many of its actions redundant proteins,

meaning that other transcription factors could take over the role of ATF3 in the ATF3 KO mice. Other heterodimers might have similar effects on target genes of ATF3, since there are numerous proteins from different families (ATF, fos and jun) that form the so called AP-1 transcription factors of which ATF3 can form a part of. It is possible that ATF3 is replaced by other transcription factors, which still allow the formed AP-1 transcription factor to regulate in most cases gene expression similarly as when ATF3 constitutes one of the two heterodimer-partners.

6.6 Signalling pathways involved in stress-induced ATF3 regulation in cultured kidney cells

We were interested in which signalling pathways relay the stress-signal that induces the upregulation of ATF3 *in vitro* by the medium change. There are various reports about ATF3 being regulated mainly by the MAPK pathways, namely JNK/SAPK [59], p38 and ERK [118] pathways. When treating $mCCD_{Cl6}$ cells with different conditions of medium change, there was an increase in JNK/SAPK1, p38 and ERK1/2 phosphorylation only when the medium had been previously warmed in a tube in a 37 °C waterbath. For JNK/SAPK1, this phosphorylation was accompanied additionally by an upwards shift of the total protein band in the samples treated with the tube-pre-warmed medium change, suggesting that most JNK/SAPK1 is modified to a slower migrating phosphorylated form under this condition. We conclude that the upregulation of ATF3 due to the medium change (as it is also shown in Fig. 35) might be mediated by all three MAPK pathways studied herein, namely JNK/SAPK1, p38 and ERK1/2 signalling pathways.

Seven min after changing the medium (with medium pre-warmed in a tube), phosphorylation of p38, JNK/SAPK1 and ERK1/2 is induced, meaning the signalling pathways were activated by the stress of the medium change. Of course after seven min the ATF3 expression is not altered that rapidly. The earliest

time point at which ATF3 mRNA expression was studied after a medium change was 30 min (see Fig. 22) in the case of mpkCCD$_{Cl14}$ cells. At this time point its increase was already nearly maximal. The probable lag of ATF3 mRNA upregulation after MAPKs have been phosphorylated (see Fig. 35) is that these kinases per se do not act on ATF3 transcription directly, but that there are several steps in between. Activated MAPK first phosphorylate transcription factors which only then translocate to the nucleus and bind to target sequences in the ATF3 promoter to influence its transcription rate. We do not know which transcription factors are phosphorylated by the MAPK in this specific medium change experiment. In the case of JNK/SAPK1 for example, target factors that can be phosphorylated have been reported to include ATF2 [119], c-Jun [120] and c-Myc [121], which act positively on ATF3 transcription. Thus we hypothesize that p38, JNK/SAPK1 and ERK1/2 pathway are activated immediately by the medium change, they then act on ATF3 which is visible after 30 min on mRNA level (see Fig. 22 and 34) and after 1h at protein level (see Fig. 35). To find possible interplayers between the MAPK phosphorylation and the subsequent ATF3 mRNA upregulation, phospho-protein blots from cells treated with the different medium changes should be performed to test the mentioned upstream transcription factors. It would also be interesting to perform a timecourse experiment similar to the one made with aldosterone addition (see Fig. 22), so see after how much time a maximal induction of ATF3 protein by the medium change is observed.

In all studies carried out so far, ATF3 is reported to be upregulated when the p38 or JNK/SAPK pathways are activated. For the ERK pathway the results of the different studies are more opposing. ERK seems to have either a repressing or an inducing effect on ATF3 expression, depending on the stimulus that provoked the phosphorylation of the MAPK: While ERK repressed ATF3 transcription in vascular endothelial cells [19] when activated by TNFα, there is also evidence that when different cell types are exposed to UV-light, the activated MEKK1 phosphorylates ERK (and also p38) which leads to an increase in ATF3 mRNA

levels [122]. Thus, in the case of our medium change experiments it is possible that on one hand the activation of the ERK1/2 pathway contributes to the upregulation of ATF3 mRNA via phosphorylation of transcription factors that favor the induction of ATF3 transcription. On the other hand it is also possible that ATF3 levels would be even higher in the tube pre-warmed medium change condition, if ERK phosphorylation was prevented, since it might counteract the effect of p38 and JNK/SAPK1. To find out if this is the case, one would have to add specific inhibitors for ERK (e.g. PD98059) to the cell medium to test whether this would increase or decrease upregulation after the medium change. The reason that for one stimulus a MAPK pathway like the ERK pathway can stimulate ATF3 expression (e.g. UV-light) while its induction by another stimulus can inhibit ATF3 expression (e.g. TNFα) is that there are other mediators acting between phosphorylated ERK and ATF3 transcription and ATF3 protein accumulation. Depending on the protein that is phosphorylated by the MAPK, activation of the same signalling pathway might have dual effects on ATF3 expression. In the case of UV-light, it is p53 that mediates the positive effect on ATF3 expression [122]. Tolfenamic acid (Ta) a non-steroidal anti-inflammatory drug also upregulated ATF3 expression in cancer cells via the very same three MAPK that we investigated. This is mediated by ATF2 phosphorylation and subsequent binding of ATF2 to the ATF3 promoter [123]. It has also been shown that there is crosstalk between the different MAPK pathways going on [124] [125]. This makes the possibilities for regulation of gene transcription even more broad. The use of specific inhibitors helps elucidating how the interplay between the MAPK might influence the expression of a target gene like ATF3.

The before mentioned studies where ATF3 is reported to be induced by a certain MAPK are usually carried out with very specific stimuli like cytokines (TNFα), irradiation (UV-light) or cytotoxic agents (cis-platin, tolfenamic acid). Compared to these extracellular signals, the medium change in the approach we used is quite an unspecific stimulus. Several factors could actually mediate the MAPK phosphorylation. To test whether it is the mechanical stimulation of the cell, due

to the medium change we performed a mock change re-using the same medium. This did not induce a significant change in ATF3 mRNA levels (see Fig. 34) and had no effect on the protein level (see Fig. 35) as opposed to the medium change with the tube pre-warmed medium. Also none of the MAPK that we investigated was phosphorylated when cells were treated with a mock change only, as opposed to a real change with medium pre-warmed in a tube. Therefore we could exclude the mechanical stimulation to be the cause of ATF3 upregulation when changing the medium. These results are also not compatible with the hypothesis that ATF3 induction was due to the detachment of cells as demonstrated in experiments with keratinocytes anchored to the basement membrane via the glycoprotein laminin 5 [126].

The original experiments made to test the effect of a medium change on ATF3 expression in $mCCD_{Cl6}$ cells were performed using medium that was pre-warmed in a tube. We then realized that the medium might not have been equally CO_2 equilibrated compared to the medium used for the mock medium change control. Therefore we also tested the effect of medium that had been pre-warmed in the incubator for 3h in 10 cm petri dishes to have a large enough surface for efficient gas exchange. Apparently, it indeed made a difference on the phosphorylation of JNK/SAPK1, p38 and ERK1/2. After seven min, when the medium used for the change was pre-warmed in the tube, there was an increase in phosphorylation of the three MAPK compared to non-treated controls. This was not the case with the medium that had been pre-warmed in the incubator. Thus, we hypothesized that this might be due to a higher pH due to a lack of CO_2 equilibration. However, this possibility was ruled out by measuring the pH, that was exactly 7.37 (data not shown) for both media either pre-warmed in the incubator or in a tube. Therefore it appears that the observed MAPK phosphorylation was not due to the pH of the medium.

Furthermore, it can probably be excluded that the MAPK phosphorylation is due to specific fresh medium ingredients, since for both medium changes either pre-warmed in the tube or in the incubator, the same fresh medium was used. An

additional possibility that could be excluded Is that replacing the medium was actually removing an inhibitor. Indeed, in both cases the conditioned medium was replaced with the same fresh medium, removing potential inhibitors.

Taken together, we can apparently exclude pH, temperature, medium composition and mechanical stress as factors responsible for the phosphorylation of p38, JNK/SAPK1 and ERK1/2 induced by a medium change in $mCCD_{Cl6}$ cells, leading to an increase in ATF3 mRNA and protein levels after 1 h. The current hypothesis is that this is due to the lack of CO_2 in the medium. However, it still remains to be positively demonstrated what factor is the cause of this effect.

6.7 Conclusion

From the present study we conclude that $mpkCCD_{Cl14}$ cells can be transduced with lentiviral constructs to give stable and inducible cell lines for the gene of interest, in this case ATF3. It is the first time that this has been possible for this special cortical collecting duct kidney cell line. Achieving the same for the mCCD cell line still remains an unreached goal. Our investigations show that ATF3 is an early-induced stress response gene in the cortical collecting duct cell line $mCCD_{Cl6}$ *in vitro* and also in mouse kidney *in vivo*. This stress-induction of ATF3 is apparently mediated by the JNK/SAPK1, ERK1/2 and p38 MAPK signalling cascades*in vitro*. ATF3 stress-induction by NaCl/EtOH injection is specific for the kidney and not for other organs tested. Moreover, the upregulation of ATF3 by the injection-stress is also seen on the protein level in CNT/CCD segments of the kidney. Furthermore ATF3 KO mice are not different from WT littermates in terms of food and water consumption as well as feces and urine excretion.

6.8 Outlook

Further investigations on the nature of ATF3 upregulation in the whole kidney, CNT/CCD tubules and $mCCD_{Cl6}$ cells due to stress of either injection or medium change should be made. For instance, it still remains to be further confirmed that the induction of ATF3 due to medium change is truly due to activation of the investigated MAPK pathways. To do so medium change studies using specific MAPK inhibitors against p38, ERK1/2 and JNK/SAPK1 should be performed. This would also allow drawing conclusions about how the single pathways contribute to the cellular response to the medium change. It is possible that also other signalling pathways not involving MAPK phosphorylation are involved in the upregulation of ATF3 expression in response to the medium change. Possible candidates are the nuclear factor kappa B (NF?B)-signalling-pathway [127], Akt-kinase signalling pathway and also transforming growth factor beta (TGFβ) [64] signalling pathway, since they were all found to be involved in the regulation of ATF3 expression. Furthermore, as mentioned in the discussion the different mediators in the signalling pathways (e.g. ATF2, p53) that are phosphorylated by the MAPK should be investigated. To obtain conclusive results concerning the main factor responsible for the phosphorylation of MAPKs upon medium change, the role of CO_2 equilibration of the medium should be clarified.

To really discern the role of injection-stress from that of aldosterone for the upregulation of ATF3 in the CNT/CCD tubules, B1EGFP mice should be either non-injected, saline-injected or aldosterone-injected for one hour and green fluorescent tubules sorted with COPAS for subsequent qPCR analysis. In order to perform this experiment there are several technical limitations that need to be overcome, one being the breeding of the mice which had not been very efficient. On the one hand the B1EGFP female mice show lower fertility than WT mice. On the other hand the females also tend to eat their litters. Thus, breeding enough mice of the same age and sex to obtain enough animals for additional COPAS

experiments is a long process. Furthermore, at the moment the mice do not have a complete C57BL/6 background. When the B1EGFP mice were shipped to Prof. Carsten A. Wagner (University of Zurich, Switzerland) the mothers were pregnant and had some pups that were brown, indicating that the transgenic mice created with C57BL/6 x CBA F1 embryos were not backcrossed into C57BL/6 background over an appropriate number of generations [106]. To obtain more reliable results the mice would first need to be backcrossed into C57BL/6 background. Moreover the sorting procedure when using the COPAS needs to be optimized, the sample should be cooled at all times and the sorting time reduced drastically in order to prevent RNA degradation. Furthermore, it seems crucial to analyze the genes investigated with qPCR for their protein expression as well. Thus, for the COPAS experiment shown in this study, ATF4 and CHOP10 expression should be analyzed on the protein level to draw conclusions about the effect of the saline injection on their expression.

7 Supplementary figures

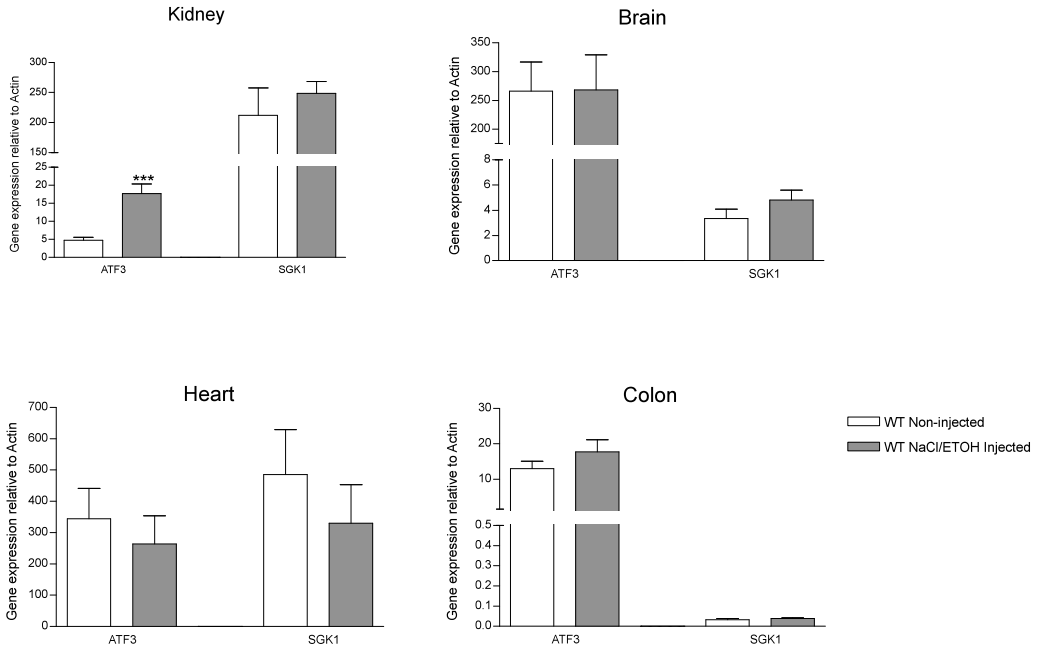

Supplentary figure 1: Expression of ATF3 and SGK1 mRNA in different organs upon NaCl-Injection in WT C57BL/6 mice expressed relative to β-actin mRNA:: 3 mice per group were either not treated or injected with 0.9% NaCl / 0.3% ethanol. All mice were sacrificed after 1 hour. Subsequent total RNA extraction and qPCR shows upregulation of relative ATF3 mRNA expression in the kidney about 4-fold due to injection of saline as compared to mice that have not been injected until they were sacrificed. In brain heart and mucosa scraped from the colon there was no difference in ATF3 expression observed between the two groups. SGK1 mRNA expression is unaffected by injection of saline solution in all the organs tested (kidney, heart, brain and colon mucosa, normalized to mouse β-Actin) *** = $p < 0.001$ student t-test (unpaired), error bars: SEM. Fig. 39 of the main text shows the same data relative expressed relative to HPRT mRNA.

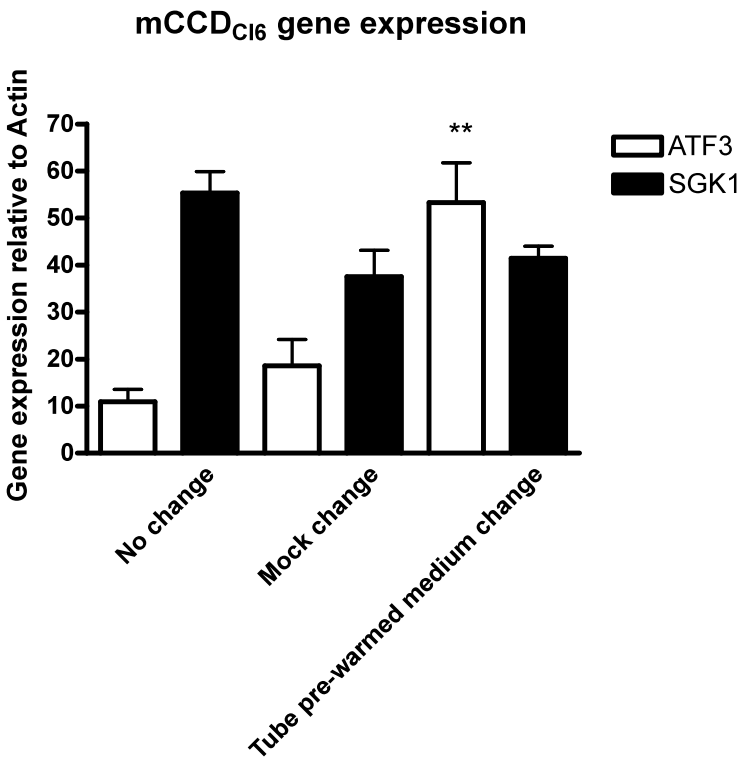

Supplentary figure 2: Relative ATF3 mRNA expression is induced due to medium change in mCCD$_{Cl6}$ cells expressed relative to β-actin mRNA: mCCD$_{Cl6}$ cells were serum and growth factor starved for 24 h. Cells either underwent no medium change, a mock change where the medium on the cells was sucked up and put back on the cells immediately or a change of medium replacing the old medium with fresh pre-warmed medium. The mock change of the medium lead to an approximately 2-fold upregulation of relative ATF3 mRNA expression, while a real medium change showed an approximately 5-fold increase of ATF3 mRNA expression (normalized to mouse β-Actin).This was not observed for SGK1 expression. N=4; ** = $p < 0.01$ student-test and 1-way ANOVA, error bars: SEM. Data expressed relative to HPRT mRNA are shown in the main text in Fig. 34.

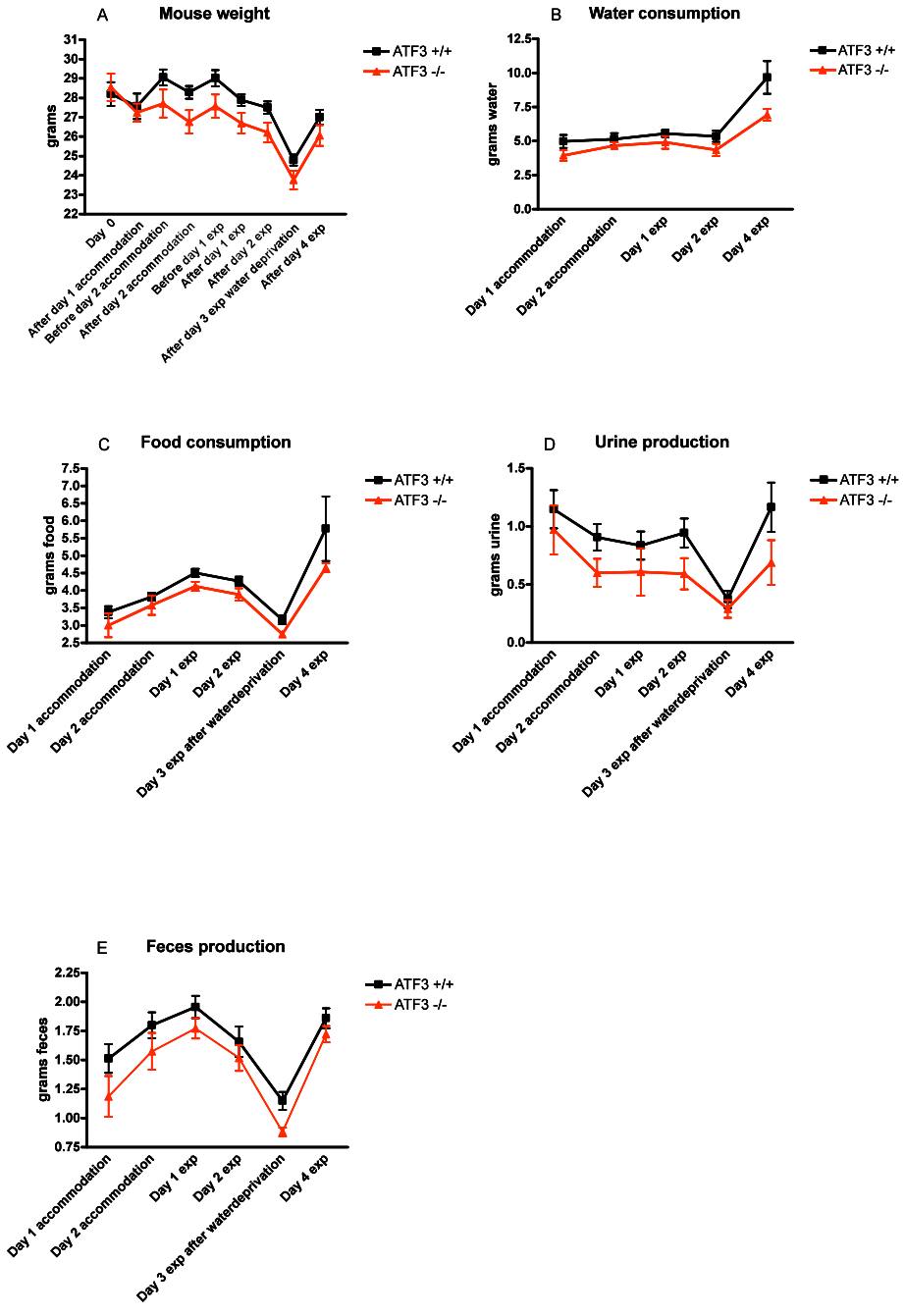
A
Mouse weight
grams
ATF3 +/+
ATF3 -/-
Day 0
After day 1 accommodation
Before day 2 accommodation
After day 2 accommodation
Before day 1 exp
After day 1 exp
After day 2 exp
After day 3 exp water deprivation
After day 4 exp
B
Water consumption
grams water
Day 1 accommodation
Day 2 accommodation
Day 1 exp
Day 2 exp
Day 4 exp
C
Food consumption
grams food
Day 3 exp after waterdeprivation
D
Urine production
grams urine
E
Feces production
grams feces

Supplentary figure 3: Characterization of WT vs. ATF3 KO male mice: A: The weight in both groups changed in parallel during the experiment. After day 2 of accommodation, the ATF3 KO mice were lighter than the WT mice. After water deprivation there is a similar loss in weight in both groups. **B:** Male mice of either the WT or ATF3 KO group drank same amounts of water which increased after the water deprivation on the third day of the experiment. **C:** Food consumption was the same for both WT and ATF3 KO male mice; it was reduced after the day of water deprivation and increased back to normal levels when mice were rehydrated on day 4. **D:** Urine excretion constantly decreased in both groups over the course of the experiment. It reached the minimum after the water deprivation phase and went back up to normal baseline levels after the rehydration. There was no significant difference between the two groups of male mice. E: Feces production was parallel in WT and ATF3 KO male mice, it first increased until the first day of the experiment. After water deprivation, on the third day of the experiment, there were the lowest amounts of feces excretion observed in both groups. Allowing the mice to drink water again restored feces production to similar levels as on the days before. N=10 for WT males, N=9 for ATF3 KO males. Data pooled from males and females are shown in the main text in Fig. 45.

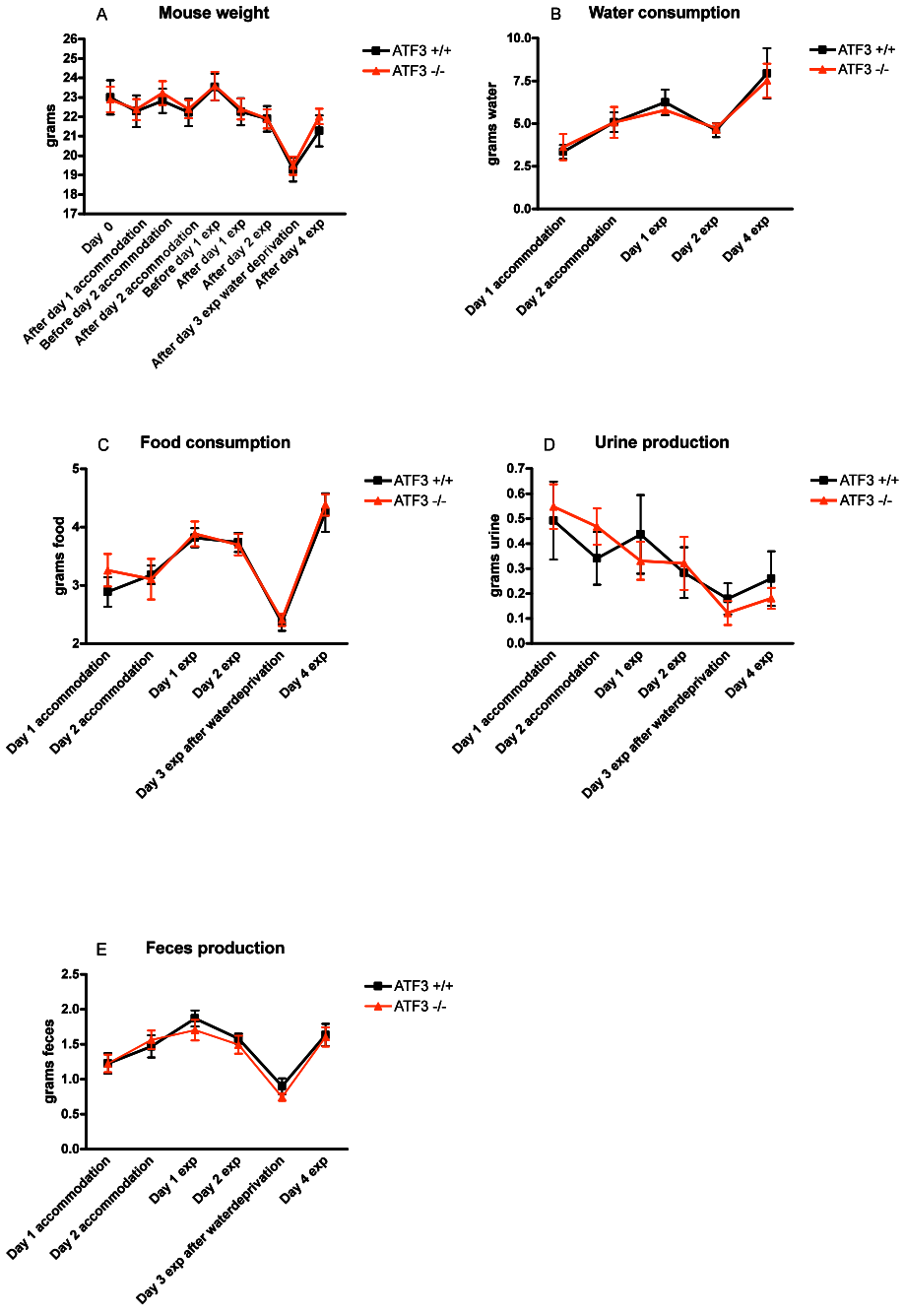
A
Mouse weight
grams
ATF3 +/+
ATF3 -/-
Day 0
After day 1 accommodation
Before day 2 accommodation
After day 2 accommodation
Before day 1 exp
After day 1 exp
After day 2 exp
After day 3 exp water deprivation
After day 4 exp
B
Water consumption
grams water
Day 1 accommodation
Day 2 accommodation
Day 1 exp
Day 2 exp
Day 4 exp
C
Food consumption
grams food
Day 3 exp after waterdeprivation
D
Urine production
grams urine
E
Feces production
grams feces

Supplentary figure 4: Characterization of WT vs. ATF3 KO female mice: A: The weight of females in both groups changed in parallel during the experiment. After water deprivation there is a similar loss in weight in both groups. **B:** Female mice of either the WT or ATF3 KO group drank same amounts of water. The mice on both groups did not drink a lot more than usual to compensate for the water deprivation on the fourth day of the experiment. **C:** Food consumption was the same for both WT and ATF3 KO female mice with a big drop on the day of the water deprivation. **D:** Urine excretion constantly decreased in both groups over the course of the experiment. It reached the minimum after the water deprivation phase. There was no significant difference between the two groups of female mice. **E:** Feces production was parallel in WT and ATF3 KO female mice, it first increased until the first day of the experiment. After water deprivation, on the third day of the experiment, there were the lowest amounts of feces excretion observed in both groups. Allowing the mice to drink water again restored feces production to similar levels as on the days before. N=10 for WT females, N=9 for ATF3 KO females. Data pooled from males and females are shown in the main text in Fig. 45.

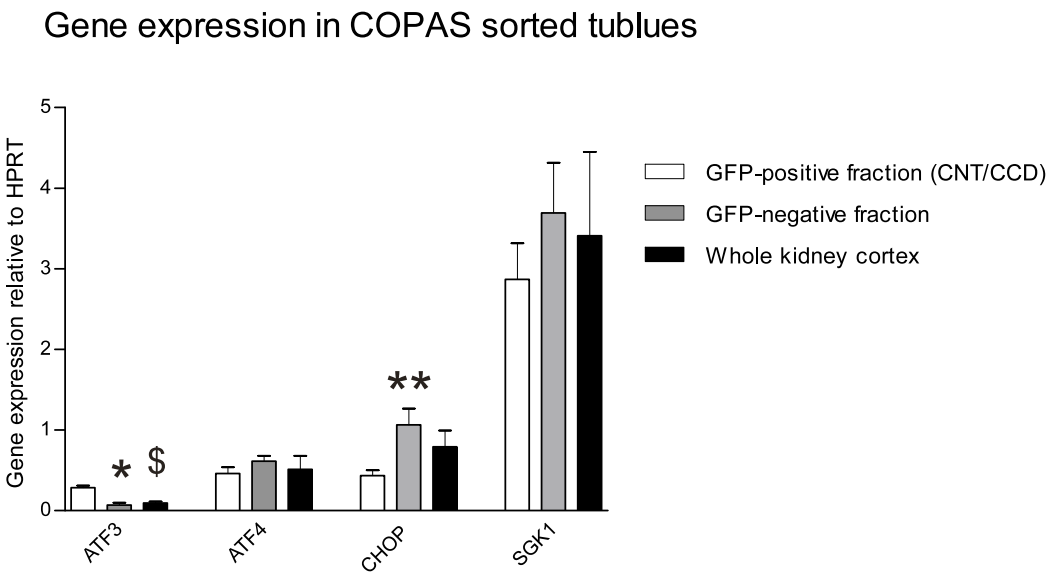

Supplentary figure 5: Characterization of COPAS-sorted tubule segment. Expression of specific genes was compared in the different tubule fractions: GFP positive (CNT/CCD) vs. GFP-negative tubules and total cortex tubules (N=12, except for ATF3 KO mice, where values for ATF3 expression were excluded, N=8). Four mice per group (non-injected vs. 0.9% NaCl / 0.3% EtOH injected for 1 h) and ATF3 KO B1EGFP C57BL/6 mice) were sacrificed and kidney tubule suspensions were sorted with COPAS. Total RNA extraction and qPCR was performed. ATF3 expression was highest in the CNT/CCD (GFP-positive fraction). ATF4 and SGK1 expression were similar in all fractions while CHOP expression was observed to be lowest in the CNT/CCD. All values of gene expression are relative to HPRT mRNA expression. * compares WT non-injected to WT injected mice; $ compares WT non-injected to ATF3 KO non-injected mice; # compares WT injected to ATF3 KO mice. *and $ = $p < 0.05$; ** = $p < 0.01$ with student t-test (unpaired), error bars: SEM.

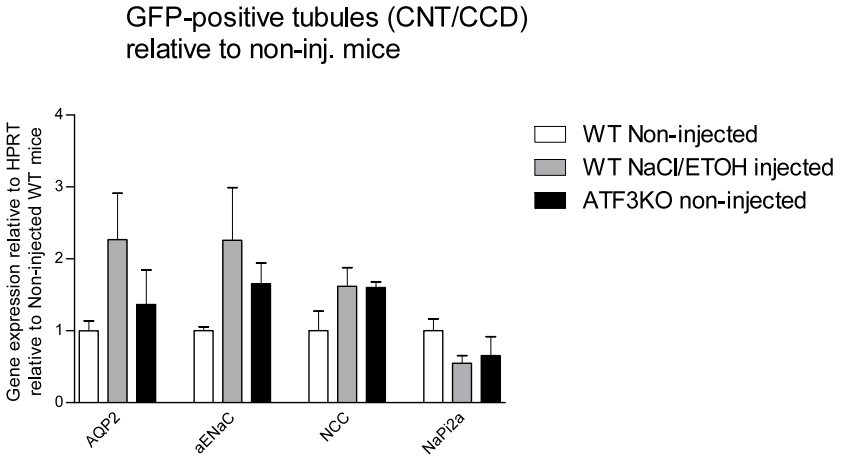
GFP-positive tubules (CNT/CCD)
relative to non-inj. mice
Gene expression relative to HPRT
relative to Non-injected WT mice
WT Non-injected
WT NaCl/ETOH injected
ATF3KO non-injected
AQP2
aENaC
NCC
NaPi2a

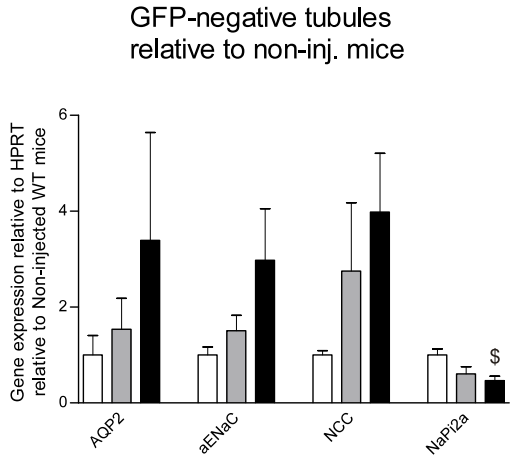
GFP-negative tubules
relative to non-inj. mice
Gene expression relative to HPRT
relative to Non-injected WT mice
$
AQP2
aENaC
NCC
NaPi2a

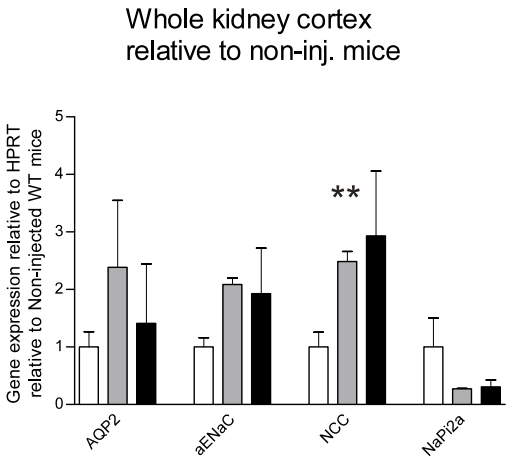
Whole kidney cortex
relative to non-inj. mice
Gene expression relative to HPRT
relative to Non-injected WT mice
**
AQP2
aENaC
NCC
NaPi2a

Supplentary figure 6: Effect of i.p. vehicle injection on gene expression in the different tubule fractions compared to non-injected and ATF3 KO mice. The GFP-sorted fraction (CNT/CCD), GFP-negative-sorted fraction and whole kidney cortex were sorted from WT B1EGFP (non-injected vs. 0.9% NaCl / 0.3% EtOH injected for 1 h) and ATF3 KO B1EGFP C57BL/6. Four mice per group were sacrificed and kidney tubule suspensions were sorted with COPAS. Total mRNA extraction and following qPCR was performed. Gene expression was normalized relative to HPRT expression in the different mouse groups and then normalized to the non-injected mice (= 1). Relative levels of ATF3 mRNA were not altered by the stress of NaCl/EtOH injection in the CNT/CCD (GFP positive) sorted fraction in WT B1EGFP mice compared to non-injected WT B1EGFP mice (see main text Fig. 42). AQP2 and ENaC expression were similar for all the groups tested within the different sorted fractions. The saline injection lead to an apparent increase in NCC expression in the whole kidney fraction of WT mice compared to non-injected WT mice. Also NaPi2a expression was lower in ATF3 KO mice than in WT injected mice in the GFP-negative fraction. It is interpreted that the large variation and apparent effects of the injection are probably due to uneven mRNA degradation during the sorting procedure (see main text) N=4; except negative kidney fractions of WT non-injected and WT injected mice (N=2). * compares WT non-injected to WT injected mice; $ compares WT non-injected to ATF3 KO non-injected mice. $ = $p < 0.05$; ** and $$ = $p < 0.01$ with student t-test (unpaired), error bars: SEM.

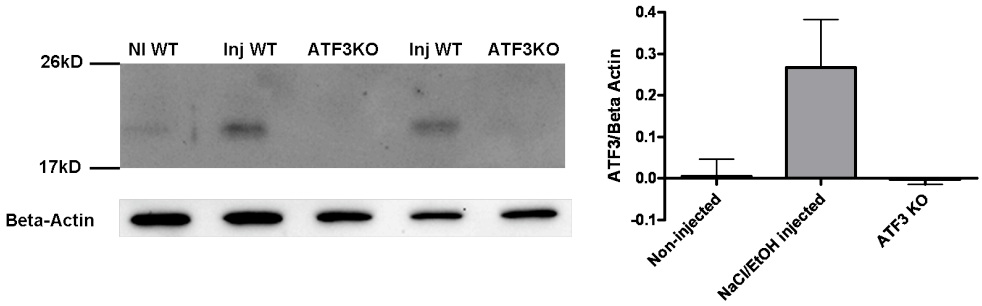

Supplentary figure 7: ATF3 protein expression is upregulated due to injection of NaCl/EtOH in CNT/CCD of B1EGFP WT mice: The GFP-sorted fraction (CNT/CCD) of WT B1EGFP mice (non-injected (NI WT) vs. 0.9% NaCl / 0.3% EtOH injected (Inj WT) for 1 h) and ATF3 KO B1EGFP mice were investigated for ATF3 protein expression. Western blot analysis shows a clear induction of a band migrating at the expected size for ATF3 protein (ca. 23 kD) in injected B1EGFP WT mice compared to non-injected littermates. Basal ATF3 expression in non-injected mice is almost not detectable in WT B1EGFP CNT/CCD tubule lysates. The band is absent in non-injected ATF3 KO mice. Approximately 400 tubules were loaded per lane, N=4, error bars: SEM.

8 List of Figures

9 References

[1] Boulpaep, B.., 2005. *Medical Physiology*. Updated edition.

[2] Williams, G.H., 2005. *Aldosterone biosynthesis, regulation, and classical mechanism of action*. Heart Fail Rev, 10(1): 7–13.

[3] Hamming, I. et al., 2007. *The emerging role of ACE2 in physiology and disease*. J Pathol, 212(1): 1–11.

[4] Rad, A., 2006, *Available from: http://fr.academic.ru/dic.nsf/frwiki/1591792*.

[5] Subramanya, A.R. et al., 2006. *WNK kinases regulate sodium chloride and potassium transport by the aldosterone-sensitive distal nephron*. Kidney Int, 70(4): 630–4.

[6] Winter, C. et al., 2004. *Nongenomic stimulation of vacuolar H+-ATPases in intercalated renal tubule cells by aldosterone*. Proc Natl Acad Sci U S A, 101(8): 2636–41.

[7] Fakitsas, P. et al., 2007. *Early aldosterone-induced gene product regulates the epithelial sodium channel by deubiquitylation*. J Am Soc Nephrol, 18(4): 1084–92.

[8] Landschulz, W.H. et al., 1988. *The leucine zipper: a hypothetical structure common to a new class of DNA binding proteins*. Science, 240(4860): 1759–64.

[9] Kehat, I. et al., 2006. *The role of basic leucine zipper protein-mediated transcription in physiological and pathological myocardial hypertrophy*. Ann N Y Acad Sci, 1080: 97–109.

[10] Nantel, F. et al., 1996. *Spermiogenesis deficiency and germ-cell apoptosis in CREM-mutant mice*. Nature, 380(6570): 159–62.

[11] Meyer, T.E. and Habener, J.F., 1993. *Cyclic adenosine 3',5'-monophosphate response element binding protein (CREB) and related transcription-activating deoxyribonucleic acid-binding proteins*. Endocr Rev, 14(3): 269–90.

[12] Deppmann, C.D. et al., 2004. *Dimerization specificity of all 67 B-ZIP motifs in Arabidopsis thaliana: a comparison to Homo sapiens B-ZIP motifs*. Nucleic Acids Res, 32(11): 3435–45.

[13] Poels, J. and Vanden Broeck, J., 2004. *Insect basic leucine zipper proteins and their role in cyclic AMP-dependent regulation of gene expression*. Int Rev Cytol, 241: 277–309.

[14] Vinson, C. et al., 2006. *Deciphering B-ZIP transcription factor interactions in vitro and in vivo*. Biochim Biophys Acta, 1759(1-2): 4–12.

[15] Kool, J. et al., 2003. *Induction of ATF3 by ionizing radiation is mediated via a signaling pathway that includes ATM, Nibrin1, stress-induced MAPkinases and ATF-2*. Oncogene, 22(27): 4235–42.

[16] Bakin, A.V. et al., 2005. *Smad3-ATF3 signaling mediates TGF-beta suppression of genes encoding Phase II detoxifying proteins*. Free Radic Biol Med, 38(3): 375–87.

[17] Chrivia, J.C. et al., 1993. *Phosphorylated CREB binds specifically to the nuclear protein CBP*. Nature, 365(6449): 855–9.

[18] Shaulian, E. and Karin, M., 2001. *AP-1 in cell proliferation and survival*. Oncogene, 20(19): 2390–400.

[19] Inoue, K. et al., 2004. *TNFalpha-induced ATF3 expression is bidirectionally regulated by the JNK and ERK pathways in vascular endothelial cells.* Genes Cells, 9(1): 59–70.

[20] Manna, P.R. et al., 2009. *Role of basic leucine zipper proteins in transcriptional regulation of the steroidogenic acute regulatory protein gene.* Mol Cell Endocrinol, 302(1): 1–11.

[21] Roesler, W.J. et al., 1988. *Cyclic AMP and the induction of eukaryotic gene transcription.* J Biol Chem, 263(19): 9063–6.

[22] Hai, T.W. et al., 1989. *Transcription factor ATF cDNA clones: an extensive family of leucine zipper proteins able to selectively form DNA-binding heterodimers.* Genes Dev, 3(12B): 2083–90.

[23] Chinenov, Y. and Kerppola, T.K., 2001. *Close encounters of many kinds: Fos-Jun interactions that mediate transcription regulatory specificity.* Oncogene, 20(19): 2438–52.

[24] Hai, T. and Hartman, M.G., 2001. *The molecular biology and nomenclature of the activating transcription factor/cAMP responsive element binding family of transcription factors: activating transcription factor proteins and homeostasis.* Gene, 273(1): 1–11.

[25] Park, E.A. et al., 1993. *Relative roles of CCAAT/enhancer-binding protein beta and cAMP regulatory element-binding protein in controlling transcription of the gene for phosphoenolpyruvate carboxykinase (GTP).* J Biol Chem, 268(1): 613–9.

[26] Mohn, K.L. et al., 1991. *The immediate-early growth response in regenerating liver and insulin-stimulated H-35 cells: comparison with serum-*

stimulated 3T3 cells and identification of 41 novel immediate-early genes. Mol Cell Biol, 11(1): 381–90.

[27] Amundson, S.A. et al., 1999. *Fluorescent cDNA microarray hybridization reveals complexity and heterogeneity of cellular genotoxic stress responses.* Oncogene, 18(24): 3666–72.

[28] Hai, T. et al., 1999. *ATF3 and stress responses.* Gene Expr, 7(4-6): 321–35.

[29] Hai, T. and Curran, T., 1991. *Cross-family dimerization of transcription factors Fos/Jun and ATF/CREB alters DNA binding specificity.* Proc Natl Acad Sci U S A, 88(9): 3720–4.

[30] Hsu, J.C. et al., 1992. *Interactions among LRF-1, JunB, c-Jun, and c-Fos define a regulatory program in the G1 phase of liver regeneration.* Mol Cell Biol, 12(10): 4654–65.

[31] Chu, H.M. et al., 1994. *Activating transcription factor-3 stimulates 3',5'-cyclic adenosine monophosphate-dependent gene expression.* Mol Endocrinol, 8(1): 59–68.

[32] Liang, G. et al., 1996. *ATF3 gene. Genomic organization, promoter, and regulation.* J Biol Chem, 271(3): 1695–701.

[33] Chen, B.P. et al., 1994. *ATF3 and ATF3 delta Zip. Transcriptional repression versus activation by alternatively spliced isoforms.* J Biol Chem, 269(22): 15819–26.

[34] Kitajima S, Tanaka Y, K.J.., June 2009, *ATF3 (activating transcription factor 3).*

[35] Thiaville, M.M. et al., 2008. *Deprivation of protein or amino acid induces C/EBPbeta synthesis and binding to amino acid response elements, but its*

action is not an absolute requirement for enhanced transcription. Biochem J, 410(3): 473–84.

[36] Lopez, A.B. et al., 2007. *A feedback transcriptional mechanism controls the level of the arginine/lysine transporter cat-1 during amino acid starvation.* Biochem J, 402(1): 163–73.

[37] Pan, Y.X. et al., 2007. *Activation of the ATF3 gene through a co-ordinated amino acid-sensing response programme that controls transcriptional regulation of responsive genes following amino acid limitation.* Biochem J, 401(1): 299–307.

[38] Turchi, L. et al., 2008. *Hif-2alpha mediates UV-induced apoptosis through a novel ATF3-dependent death pathway.* Cell Death Differ, 15(9): 1472–80.

[39] Koike, M. et al., 2005. *Characterization of ATF3 induction after ionizing radiation in human skin cells.* J Radiat Res (Tokyo), 46(4): 379–85.

[40] Chen, S.C. et al., 2008. *Acute hypoxia to endothelial cells induces activating transcription factor 3 (ATF3) expression that is mediated via nitric oxide.* Atherosclerosis, 201(2): 281–8.

[41] Ameri, K. et al., 2007. *Induction of activating transcription factor 3 by anoxia is independent of p53 and the hypoxic HIF signalling pathway.* Oncogene, 26(2): 284–9.

[42] Yoshida, T. et al., 2008. *ATF3 protects against renal ischemia-reperfusion injury.* J Am Soc Nephrol, 19(2): 217–24.

[43] Whitmore, M.M. et al., 2007. *Negative regulation of TLR-signaling pathways by activating transcription factor-3.* J Immunol, 179(6): 3622–30.

[44] Drysdale, B.E. et al., 1996. *Identification of a lipopolysaccharide inducible*

transcription factor in murine macrophages. Mol Immunol, 33(11-12): 989–98.

[45] Farber, J.M., 1992. *A collection of mRNA species that are inducible in the RAW 264.7 mouse macrophage cell line by gamma interferon and other agents.* Mol Cell Biol, 12(4): 1535–45.

[46] Yin, T. et al., 1997. *Tissue-specific pattern of stress kinase activation in ischemic/reperfused heart and kidney.* J Biol Chem, 272(32): 19943–50.

[47] Wolfgang, C.D. et al., 2000. *Transcriptional autorepression of the stress-inducible gene ATF3.* J Biol Chem, 275(22): 16865–70.

[48] Kang, Y. et al., 2003. *A self-enabling TGFbeta response coupled to stress signaling: Smad engages stress response factor ATF3 for Id1 repression in epithelial cells.* Mol Cell, 11(4): 915–26.

[49] Wolfgang, C.D. et al., 1997. *gadd153/Chop10, a potential target gene of the transcriptional repressor ATF3.* Mol Cell Biol, 17(11): 6700–7.

[50] Fawcett, T.W. et al., 1999. *Complexes containing activating transcription factor (ATF)/cAMP-responsive-element-binding protein (CREB) interact with the CCAAT/enhancer-binding protein (C/EBP)-ATF composite site to regulate Gadd153 expression during the stress response.* Biochem J, 339 (Pt 1): 135–41.

[51] Allen-Jennings, A.E. et al., 2001. *The roles of ATF3 in glucose homeostasis. A transgenic mouse model with liver dysfunction and defects in endocrine pancreas.* J Biol Chem, 276(31): 29507–14.

[52] Sassone-Corsi, P. et al., 1988. *Transcriptional autoregulation of the proto-oncogene fos.* Nature, 334(6180): 314–9.

[53] Molina, C.A. et al., 1993. *Inducibility and negative autoregulation of CREM: an alternative promoter directs the expression of ICER, an early response repressor.* Cell, 75(5): 875–86.

[54] Roberts, P.J. and Der, C.J., 2007. *Targeting the Raf-MEK-ERK mitogen-activated protein kinase cascade for the treatment of cancer.* Oncogene, 26(22): 3291–310.

[55] Hartman, M.G. et al., 2004. *Role for activating transcription factor 3 in stress-induced beta-cell apoptosis.* Mol Cell Biol, 24(13): 5721–32.

[56] Ishiguro, T. et al., 1996. *Identification of genes differentially expressed in B16 murine melanoma sublines with different metastatic potentials.* Cancer Res, 56(4): 875–9.

[57] Taub, R., 1996. *Liver regeneration 4: transcriptional control of liver regeneration.* FASEB J, 10(4): 413–27.

[58] Francis, J.S. et al., 2004. *Over expression of ATF-3 protects rat hippocampal neurons from in vivo injection of kainic acid.* Brain Res Mol Brain Res, 124(2): 199–203.

[59] Mei, Y. et al., 2008. *Activating transcription factor 3 up-regulated by c-Jun NH(2)-terminal kinase/c-Jun contributes to apoptosis induced by potassium deprivation in cerebellar granule neurons.* Neuroscience, 151(3): 771–9.

[60] Li, D. et al., 2008. *The repression of IRS2 gene by ATF3, a stress-inducible gene, contributes to pancreatic beta-cell apoptosis.* Diabetes, 57(3): 635–44.

[61] Yin, X. et al., 2008. *A potential dichotomous role of ATF3, an adaptive-response gene, in cancer development.* Oncogene, 27(15): 2118–27.

[62] Zhou, H. et al., 2008. *Urinary exosomal transcription factors, a new class of biomarkers for renal disease.* Kidney Int, 74(5): 613–21.

[63] Yuen, P.S. et al., 2006. *Ischemic and nephrotoxic acute renal failure are distinguished by their broad transcriptomic responses.* Physiol Genomics, 25(3): 375–86.

[64] Hu, G. et al., 2005. *Revealing transforming growth factor-beta signaling transduction in human kidney by gene expression data mining.* OMICS, 9(3): 266–80.

[65] Yan, C. et al., 2002. *ATF3 represses 72-kDa type IV collagenase (MMP-2) expression by antagonizing p53-dependent trans-activation of the collagenase promoter.* J Biol Chem, 277(13): 10804–12.

[66] Wang, J. et al., 2003. *Regulation of proglucagon transcription by activated transcription factor (ATF) 3 and a novel isoform, ATF3b, through the cAMP-response element/ATF site of the proglucagon gene promoter.* J Biol Chem, 278(35): 32899–904.

[67] James, C.G. et al., 2006. *The transcription factor ATF3 is upregulated during chondrocyte differentiation and represses cyclin D1 and A gene transcription.* BMC Mol Biol, 7: 30.

[68] Li, H.F. et al. *ATF3-mediated epigenetic regulation protects against acute kidney injury.* J Am Soc Nephrol, 21(6): 1003–13.

[69] Pluta, K. and Kacprzak, M.M., 2009. *Use of HIV as a gene transfer vector.* Acta Biochim Pol, 56(4): 531–95.

[70] Temin, H.M. and Mizutani, S., 1970. *RNA-dependent DNA polymerase in virions of Rous sarcoma virus.* Nature, 226(5252): 1211–3.

[71] Poeschla EM, Buchschacher GL, J.W.S.F., 2000. *Etiology of cancer: RNA viruses*. In H.S.R.S. DeVita VT Jr. (editor), *Principal and Practice of Oncology. 6th Edition*, Lippincott, Williams & Wilkins, Philadelphia, pp. 149–158.

[72] Nermut, M.V. and Hockley, D.J., 1996. *Comparative morphology and structural classification of retroviruses*. Curr Top Microbiol Immunol, 214: 1–24.

[73] Amado, R.G. and Chen, I.S., 1999. *Lentiviral vectors–the promise of gene therapy within reach?* Science, 285(5428): 674–6.

[74] Hemminki, T.H. and Akseli, 2005. *Enhancement of cancer gene therapy with modified viral vectors and fusion genes*. Gene Ther Mol Bio, 9: 153–168.

[75] Kootstra, N.A. and Verma, I.M., 2003. *Gene therapy with viral vectors*. Annu Rev Pharmacol Toxicol, 43: 413–39.

[76] Page, K.A. et al., 1990. *Construction and use of a human immunodeficiency virus vector for analysis of virus infectivity*. J Virol, 64(11): 5270–6.

[77] Landau, N.R. et al., 1988. *The envelope glycoprotein of the human immunodeficiency virus binds to the immunoglobulin-like domain of CD4*. Nature, 334(6178): 159–62.

[78] Landau, N.R. et al., 1991. *Pseudotyping with human T-cell leukemia virus type I broadens the human immunodeficiency virus host range*. J Virol, 65(1): 162–9.

[79] Naldini, L. et al., 1996. *In vivo gene delivery and stable transduction of nondividing cells by a lentiviral vector*. Science, 272(5259): 263–7.

[80] Dull, T. et al., 1998. *A third-generation lentivirus vector with a conditional packaging system*. J Virol, 72(11): 8463–71.

[81] Kim, V.N. et al., 1998. *Minimal requirement for a lentivirus vector based on human immunodeficiency virus type 1.* J Virol, 72(1): 811–6.

[82] Miyoshi, H. et al., 1998. *Development of a self-inactivating lentivirus vector.* J Virol, 72(10): 8150–7.

[83] Zufferey, R. et al., 1998. *Self-inactivating lentivirus vector for safe and efficient in vivo gene delivery.* J Virol, 72(12): 9873–80.

[84] Iwakuma, T. et al., 1999. *Self-inactivating lentiviral vectors with U3 and U5 modifications.* Virology, 261(1): 120–32.

[85] Bukovsky, A.A. et al., 1999. *Interaction of human immunodeficiency virus-derived vectors with wild-type virus in transduced cells.* J Virol, 73(8): 7087–92.

[86] Aiken, C., 1997. *Pseudotyping human immunodeficiency virus type 1 (HIV-1) by the glycoprotein of vesicular stomatitis virus targets HIV-1 entry to an endocytic pathway and suppresses both the requirement for Nef and the sensitivity to cyclosporin A.* J Virol, 71(8): 5871–7.

[87] Chazal, N. et al., 2001. *Human immunodeficiency virus type 1 particles pseudotyped with envelope proteins that fuse at low pH no longer require Nef for optimal infectivity.* J Virol, 75(8): 4014–8.

[88] Burns, J.C. et al., 1993. *Vesicular stomatitis virus G glycoprotein pseudotyped retroviral vectors: concentration to very high titer and efficient gene transfer into mammalian and nonmammalian cells.* Proc Natl Acad Sci U S A, 90(17): 8033–7.

[89] Corbel, S.Y. and Rossi, F.M., 2002. *Latest developments and in vivo use of the Tet system: ex vivo and in vivo delivery of tetracycline-regulated genes.* Curr Opin Biotechnol, 13(5): 448–52.

[90] Baron, U. and Bujard, H., 2000. *Tet repressor-based system for regulated gene expression in eukaryotic cells: principles and advances*. Methods Enzymol, 327: 401–21.

[91] Gossen, M. and Bujard, H., 1992. *Tight control of gene expression in mammalian cells by tetracycline-responsive promoters*. Proc Natl Acad Sci U S A, 89(12): 5547–51.

[92] Gossen, M. et al., 1995. *Transcriptional activation by tetracyclines in mammalian cells*. Science, 268(5218): 1766–9.

[93] Kohan, D.E., 2008. *Progress in gene targeting: using mutant mice to study renal function and disease*. Kidney Int, 74(4): 427–37.

[94] Kafri, T. et al., 2000. *Lentiviral vectors: regulated gene expression*. Mol Ther, 1(6): 516–21.

[95] Vigna, E. et al., 2002. *Robust and efficient regulation of transgene expression in vivo by improved tetracycline-dependent lentiviral vectors*. Mol Ther, 5(3): 252–61.

[96] Regulier, E. et al., 2003. *Early and reversible neuropathology induced by tetracycline-regulated lentiviral overexpression of mutant huntingtin in rat striatum*. Hum Mol Genet, 12(21): 2827–36.

[97] Deuschle, U. et al., 1995. *Tetracycline-reversible silencing of eukaryotic promoters*. Mol Cell Biol, 15(4): 1907–14.

[98] Margolin, J.F. et al., 1994. *Kruppel-associated boxes are potent transcriptional repression domains*. Proc Natl Acad Sci U S A, 91(10): 4509–13.

[99] Wiznerowicz, M. and Trono, D., 2003. *Conditional suppression of cellular*

genes: lentivirus vector-mediated drug-inducible RNA interference. J Virol, 77(16): 8957–61.

[100] Bens, M. et al., 1999. *Corticosteroid-dependent sodium transport in a novel immortalized mouse collecting duct principal cell line*. J Am Soc Nephrol, 10(5): 923–34.

[101] Gaeggeler, H.P. et al., 2005. *Mineralocorticoid versus glucocorticoid receptor occupancy mediating aldosterone-stimulated sodium transport in a novel renal cell line*. J Am Soc Nephrol, 16(4): 878–91.

[102] Hug, M.J., 2002, *Transepithelial measurements using the Ussing chamber*.

[103] Ussing HH, Z.K., 1950. *Active transport of sodium as the source of electric current in the short-circuited isolated frog skin*. Acta. Physiol. Scand., 23:11: 0–27.

[104] Adam, G., 2008. *Functional role of New Aldosterone Regulated Gene Products*. Ph.D. thesis, Zurich.

[105] Lu, D. et al., 2006. *Activating transcription factor 3, a stress-inducible gene, suppresses Ras-stimulated tumorigenesis*. J Biol Chem, 281(15): 10473–81.

[106] Miller, R.L. et al., 2005. *V-ATPase B1-subunit promoter drives expression of EGFP in intercalated cells of kidney, clear cells of epididymis and airway cells of lung in transgenic mice*. Am J Physiol Cell Physiol, 288(5): C1134–44.

[107] Paunescu, T.G. et al., 2004. *Expression of the 56-kDa B2 subunit isoform of the vacuolar H(+)-ATPase in proton-secreting cells of the kidney and epididymis*. Am J Physiol Cell Physiol, 287(1): C149–62.

[108] Hellal-Levy, C. et al., 1999. *Specific hydroxylations determine selective*

corticosteroid recognition by human glucocorticoid and mineralocorticoid receptors. FEBS Lett, 464(1-2): 9–13.

[109] Gauer, S. et al., 2007. *Aldosterone induces CTGF in mesangial cells by activation of the glucocorticoid receptor*. Nephrol Dial Transplant, 22(11): 3154–9.

[110] Wek, R.C. et al., 2006. *Coping with stress: eIF2 kinases and translational control*. Biochem Soc Trans, 34(Pt 1): 7–11.

[111] Rulten, S.L. et al., 2006. *Ethanol modifies the effect of handling stress on gene expression: problems in the analysis of two-way gene expression studies in mouse brain*. Brain Res, 1102(1): 39–43.

[112] Cai, Y. et al., 2000. *Homocysteine-responsive ATF3 gene expression in human vascular endothelial cells: activation of c-Jun NH(2)-terminal kinase and promoter response element*. Blood, 96(6): 2140–8.

[113] Kilberg, M.S. et al., 2009. *ATF4-dependent transcription mediates signaling of amino acid limitation*. Trends Endocrinol Metab, 20(9): 436–43.

[114] Chen, B.P. et al., 1996. *Analysis of ATF3, a transcription factor induced by physiological stresses and modulated by gadd153/Chop10*. Mol Cell Biol, 16(3): 1157–68.

[115] Weidenfeld-Baranboim, K. et al., 2008. *TRE-dependent transcription activation by JDP2-CHOP10 association*. Nucleic Acids Res, 36(11): 3608–19.

[116] Zmuda, E.J. et al. *Deficiency of Atf3, an adaptive-response gene, protects islets and ameliorates inflammation in a syngeneic mouse transplantation model*. Diabetologia, 53(7): 1438–50.

[117] Gilchrist, M. et al., 2006. *Systems biology approaches identify ATF3 as a negative regulator of Toll-like receptor 4.* Nature, 441(7090): 173–8.

[118] St Germain, C. et al. *Cisplatin induces cytotoxicity through the mitogen-activated protein kinase pathways and activating transcription factor 3.* Neoplasia, 12(7): 527–38.

[119] Gupta, S. et al., 1995. *Transcription factor ATF2 regulation by the JNK signal transduction pathway.* Science, 267(5196): 389–93.

[120] Fuchs, S.Y. et al., 1997. *c-Jun NH2-terminal kinases target the ubiquitination of their associated transcription factors.* J Biol Chem, 272(51): 32163–8.

[121] Tamura, K. et al., 2005. *Stress response gene ATF3 is a target of c-myc in serum-induced cell proliferation.* EMBO J, 24(14): 2590–601.

[122] Fan, F. et al., 2002. *ATF3 induction following DNA damage is regulated by distinct signaling pathways and over-expression of ATF3 protein suppresses cells growth.* Oncogene, 21(49): 7488–96.

[123] Lee, S.H. et al. *Activating transcription factor 2 (ATF2) controls tolfenamic acid-induced ATF3 expression via MAP kinase pathways.* Oncogene, 29(37): 5182–92.

[124] Whitmarsh, A.J. et al., 1997. *Role of p38 and JNK mitogen-activated protein kinases in the activation of ternary complex factors.* Mol Cell Biol, 17(5): 2360–71.

[125] Derijard, B. et al., 1994. *JNK1: a protein kinase stimulated by UV light and Ha-Ras that binds and phosphorylates the c-Jun activation domain.* Cell, 76(6): 1025–37.

[126] Harper, E.G. et al., 2005. *Wounding activates p38 map kinase and activation transcription factor 3 in leading keratinocytes.* J Cell Sci, 118(Pt 15): 3471–85.

[127] Suzuki, M. et al., 2009. *Nuclear factor-kappa B decoy suppresses nerve injury and improves mechanical allodynia and thermal hyperalgesia in a rat lumbar disc herniation model.* Eur Spine J, 18(7): 1001–7.

10 Acknowledgements

I would like to thank all the people who have helped me during the last 4 years, especially:

François Verrey, who gave me the opportunity to work in is lab. I learned many new techniques and he gave me the chance to interact with other collaborators. Thanks to him I also made the experience to travel to international congresses and meet members of the scientific community from all over the world.

The other members of my thesis committee: Prof. Dr. Sabine Werner and Prof. Dr. Johannes Loffing for the great input with which they helped to complete my project and to view things with a bit more distance.

Dr. Gabriele Adam for supervising me during my first year. Dr. Kathrin Meyer, who beat me in terms of finishing our PhDs and was always a good friend during our Biology studies at the University of Berne She was of great help with creating lentiviral ATF3-overexpressing cells. Thanks also to Dr. Julien Marquis who supervised us in doing so.

Nikolay Gresko for the help with the Ussing Chamber. It's good to share the fun.

Nadine Ruderisch, for not only scientific help but also for being a friend throughout all natural catastrophes.

Dr. Dustin Singer for helping me with the mice and for all the philosophical conversations (douche lampe).

Marta Torrente for coming all the way from Monopoli to brighten up my day.

Dr.med. Raphael Vuille-dit-Bille: Morgengruss! The best Doctor of the other

kind there will ever be (Du bist Du!).

Nicola Schäfer for always lending me an ear in any situation and creating head Zen gardens with me.

Lorenz Brandstätter for his patience and great sense of humour.

Alok Kumar Behara Baby for all the chips in all kinds of funky flavors.

My family for always believing in me.

Tom for all the support, interest and love I could wish for. Mercischön!